AN ABSTRACT OF THE THESIS OF

SAUL ALVAREZ-BORREGO for the DOCTOR OF PHILOSOPHY degree

in CHEMICAL OCEANOGRAPHY presented on September 25, 1972

OXYGEN-CARBON DIOXIDE-NUTRIENTS RELATIONSHIPS

IN THE NORTHEASTERN PACIFIC OCEAN AND

SOUTHEASTERN BERING SEA

Redacted for Privacy

Abstract approved: _____

The vertical distribution of density, salinity, temperature, dissolved oxygen, apparent oxygen utilization, nutrients, preformed phosphate, pH, alkalinity, alkalinity:chlorinity ratio, "in situ" partial pressure of carbon dioxide, and percent saturation of calcite and aragonite, for the Southeastern Bering Sea, is studied and explained in terms of biological and physical processes. Some hydrological interactions between the Bering Sea and the North Pacific Ocean are explained.

In the Northeastern Pacific Ocean the oxygen-phosphate and oxygen-nitrate relationships for the region of the water column above the oxygen minimum zone vary systematically with latitude. A similar but less pronounced variation is found below the oxygen minimum zone. The slopes of these relationships, in general, increase with increasing

latitude. In the entire water column, these slopes vary with depth. An effect on the slopes of the oxygen-phosphate and oxygen-nitrate relationships, similar to that observed when decreasing latitude, is observed when comparing winter versus summer data. The winter slopes are higher than the summer slopes. Multiple regression analysis was applied to the oxygen, phosphate, nitrate, and potential temperature data from stations at different geographic locations in the Pacific and Atlantic Oceans. Confidence intervals for the regression coefficients are consistent with the values predicted by the Redfield model for the $\Delta O_2 : \Delta PO_4$ and $\Delta O_2 : \Delta NO_3$ ratios for biological processes. Thus, the variation of the oxygen-phosphate and oxygen-nitrate slopes with depth, with latitude, and with time of the year is due to mixing between different water types with different preformed portions of oxygen, phosphate and nitrate. After the field oxygen, phosphate and nitrate data were found consistent with Redfield's model, preformed phosphates were calculated by using the model, and potential temperature versus preformed phosphate diagrams were constructed for different stations in the Pacific and Indian Oceans to study their water masses.

In the Northeastern Pacific Ocean the total inorganic carbon dioxide-oxygen relationship varies with depth. For the region of the water column above the oxygen minimum zone it varies systematically with latitude. The slope of this relationship in general decreases with

increasing latitude. Multiple linear regression analysis was applied to express total inorganic carbon dioxide, normalized to constant S‰, as a function of potential temperature and total alkalinity and oxygen normalized to constant S‰. Results of the regression are in agreement with the assumption that total alkalinity changes in the open ocean are only due to S‰ changes and calcium carbonate dissolution or precipitation, and with Redfield's model for the prediction of the total inorganic carbon dioxide-oxygen ratio for the biochemical oxidation. Thus, the variation of the total inorganic carbon dioxide-oxygen slope with depth and with latitude is due to mixing between different water types with different preformed portions of total inorganic carbon dioxide and oxygen, and to total alkalinity varying with depth as a function of S‰ and carbonate reaction.

Oxygen-Carbon Dioxide-Nutrients Relationships in the Northeastern Pacific Ocean and Southeastern Bering Sea

by

Saúl Alvarez-Borrego

A THESIS

submitted to

Oregon State University

in partial fulfillment of
the requirements for the
degree of

Doctor of Philosophy

June 1973

APPROVED:

Redacted for Privacy

Professor of Oceanography in Charge of Major

Redacted for Privacy

Dean of the School of Oceanography

Redacted for Privacy

Dean of Graduate School

Date thesis is presented September 25, 1972

Typed by Suelynn Williams for Saúl Alvarez-Borrego

With love and infinite gratitude to my parents

Pedro Alvarez-Ortega and

Dolores Borrego-De-Alvarez

With love to those that every day bring so much meaning and joy to my life: my wife, my daughter and my son

Esthela Elsie Millán-De-Alvarez

Yazae Alvarez-Millán

Dantenoc Alvarez-Millán

With great affection to my teacher and friend

Prof. Ricardo Suárez-Isla

ACKNOWLEDGMENTS

I thank my major professor Dr. P. Kilho Park for his guidance and suggestions throughout my graduate academic work. I also express my thanks to the "Consejo Nacional de Ciencia y Tecnologia" of Mexico for their support while working on my Ph. D. program.

The second chapter of this thesis comprises a paper of which, besides myself, Louis I. Gordon, Lynn B. Jones, Dr. P. Kilho Park and Dr. Ricardo M. Pytkowicz are coauthors. The third chapter comprises a paper of which Dr. Donald Guthrie, Dr. Charles H. Culberson and Dr. P. Kilho Park are coauthors. The fourth chapter comprises a paper of which Dr. P. Kilho Park is coauthor. I thank all these persons for their invaluable collaboration. Working with them has been a great learning experience.

I also like to extend my thanks to Suelynn Williams for typing all the drafts of the different chapters and the final version of this thesis.

This work was supported by the National Science Foundation grants GA-1281, GA-12113, GA-17011, and GX-28167; the Office of Naval Research through contract N00014-67-A-0369 under project NR083-102.

TABLE OF CONTENTS

LIST OF FIGURES

LIST OF FIGURES CONTINUED

LIST OF FIGURES CONTINUED

LIST OF FIGURES CONTINUED

LIST OF FIGURES CONTINUED

LIST OF FIGURES CONTINUED

LIST OF TABLES

OXYGEN-CARBON DIOXIDE-NUTRIENTS RELATIONSHIPS IN THE NORTHEASTERN PACIFIC OCEAN AND SOUTHEASTERN BERING SEA

I. INTRODUCTION

During the summer of 1966 Oregon State University's R/V YAQUINA undertook the first cruise of the YALOC series (Barstow, Gilbert, Park, Still and Wyatt, 1968). A very good set of hydrochemical data was obtained that has proved to be internally consistent through its utilization in several studies (Park, 1966ab, 1967ab, 1968; Park, Curl and Glooschenko, 1967; Pytkowicz and Fowler, 1967; Culberson and Pytkowicz, 1968; Hawley and Pytkowicz, 1969). Stations were occupied in seven hydrographic lines in the Northeastern Pacific Ocean and Southeastern Bering Sea. Data from this cruise have been used in this work to study the oxygen-carbon dioxide-nutrients relationships in the Northeastern Pacific Ocean and Southeastern Bering Sea. In some cases, when necessary, data from other cruises were also used.

It is a characteristic of our times to exchange scientific information as fast as possible. Because of this, different parts of this dissertation have been sent to journals for publication as they were completed. Three manuscripts have resulted that are complete works in themselves. They are put here as chapters. They deal with

different aspects of the same subject. As one would expect, some ideas developed as the different manuscripts were being generated, so that, sometimes what appears to be an incomplete answer to a certain question in the first chapter is more completely expressed in the subsequent chapters.

While arrangements were being made for the "International Symposium for Bering Sea Study," held in Hakodate, Japan, from 31 January to 4 February 1972, my major professor, Dr. P. Kilho Park, suggested to me to make a detailed study of the vertical distribution of the physical and chemical properties in the Southeastern Bering Sea, giving special emphasis to the oxygen-carbon dioxide-nutrients relationships. The results of that work are comprised in Chapter II.

A very important piece of our knowledge of the oxygen-carbon dioxide-nutrients relationships in the ocean is the model proposed originally by Redfield (1934), and revised and more completely described by Redfield, Ketchum and Richards (1963). The model explains the effects of the biological processes on the concentration of dissolved oxygen, total inorganic carbon dioxide and nutrients.

The application of Redfield's model to the description of the oxygen-nutrients relationships was questioned by Riley (1951) and Postma (1964). Redfield, Ketchum and Richards (1963) explained the reason of the discrepancy between the model and Riley's (1951)

results, but they did not give a definite independent proof that the model applies correctly to the whole open ocean world. A method to prove, independently of the model, that data from different regions of the ocean are consistent with the model was needed. In Chapter III a statistical method for this purpose is presented. By using multiple linear regression analysis it is shown that data from the Pacific and Northwestern Atlantic Oceans are consistent with Redfield's model.

The application of Redfield's model to the description of the oxygen-total inorganic carbon dioxide relationship was questioned by Postma (1964) and Craig (1969). But Culberson and Pytkowicz (1970) and Culberson (1972) have shown, based on theoretical considerations, that, when the data are corrected for changes due to all the processes other than the biological, the data are consistent with the model. Ben-Yaakov (1971, 1972) has applied multiple linear regression analysis to express total inorganic carbon dioxide as a function of dissolved oxygen, total alkalinity and temperature. Ben-Yaakov's (1971) results disagree with the assumptions made by Culberson and Pytkowicz (1970) and Culberson (1972) with regard to the processes that affect total alkalinity. And the results presented by Ben-Yaakov (1972) as his best estimate are in disagreement with Redfield's model. In Chapter IV regression analysis is applied to data, corrected according to well accepted theoretical considerations, to test the hypotheses that Redfield's model is correct and that total alkalinity changes in the open

ocean are only due to S‰ changes and carbonate reaction. The results are in agreement with Redfield's model and with the assumptions that Culberson and Pytkowicz (1970) and Culberson (1972) made regarding the processes that affect total alkalinity.

Many problems related to the oxygen-carbon dioxide-nutrients relationships in the ocean still are to be solved. Some suggestions for future work on the subject are given in Chapter V.

Chapter II is already in press to be published in the Journal of the Oceanographical Society of Japan. Chapter III has been submitted to "Limnology and Oceanography." And Chapter IV is to be submitted to "Deep-Sea Research."

II. OXYGEN-CARBON DIOXIDE-NUTRIENTS RELATIONSHIPS IN THE SOUTHEASTERN REGION OF THE BERING SEA

In his book entitled Hydrochemistry of the Bering Sea Ivanenkov (1964) discusses the vertical and horizontal distributions of dissolved oxygen (O_2), pH, alkalinity, alkalinity:chlorinity ratio, partial pressure of carbon dioxide, phosphate (PO_4), nitrite (NO_2), ammonia (NH_3), silicate (SiO_2) oxidizability and organic primary production, for different seasons. He explained the distribution of these parameters in terms of physical and biological processes.

Kelley and Hood (1971a) have studied the CO_2-system in the surface waters of the ice-covered Bering Sea, and Kelley and Hood (1971b) Kelley, Longerich and Hood (1971) and Gordon, Kelley, Hood and Park (1972) have studied the CO_2-system in the surface waters of the Bering Sea and North Pacific Ocean.

In the Bering Sea, according to Muromtsev (1958) (cited by Ivanenkov, 1964), the deep Pacific water is gradually transformed, rising into cyclonic gyres toward the surface, and returns to the Pacific Ocean in the form of surface water. Thus, the significance of the Bering Sea in the hydrochemical regime of the North Pacific Ocean is very great because it drains its deep water and disposes it as surface water.

Arsen'ev (1967) studied the non-periodical currents and water

masses of the Bering Sea based upon hydrological observations for many years. His work provides a very good framework for any type of study that has to take into account the physical processes that occur in the Bering Sea.

The purposes of the present work are: 1) to study the hydrochemical structure of the Southeastern Bering Sea; 2) to study the relationships of this hydrochemical structure to biological activity and to physical processes. We also consider some of the physical processes that link the Bering Sea to the North Pacific Ocean.

Field observations

During the YALOC-66 cruise seven hydrographic stations were taken in the Bering Sea, near the Aleutian Islands (Figure 1), during the period 24 June-4 July, 1966. In six of the stations water was sampled from near the sea bottom. Teflon-coated Nansen bottles were used. Temperature was measured and analyses were made at sea for salinity, O_2, pH, total alkalinity and PO_4. The samples for NO_3 and SiO_2 were frozen at sea for later analyses ashore. NO_3 was not determined for the two most eastern stations and SiO_2 was not determined for the easternmost station.

Although analyses were made for dissolved nitrogen and total carbon dioxide by gas chromatography, they are not included here owing to uncertainties in the data.

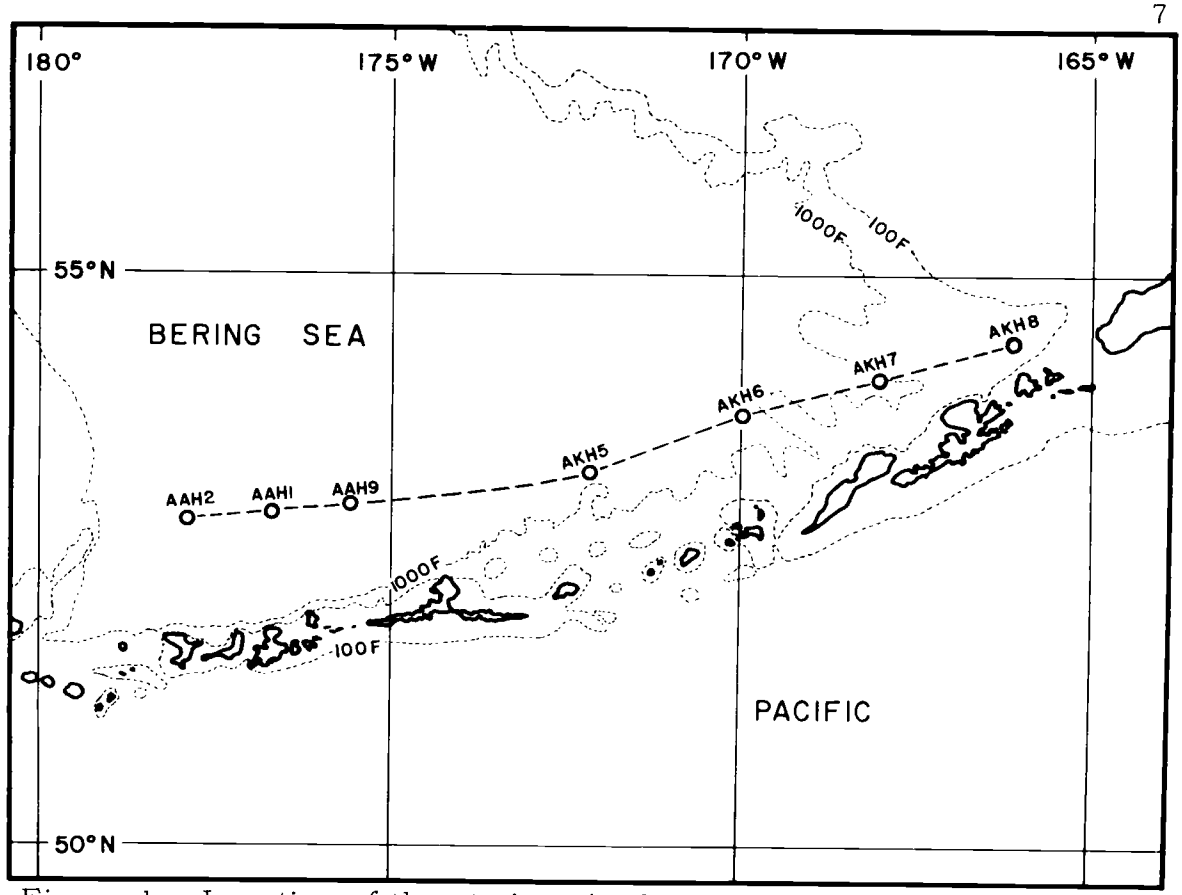

Figure 1. Location of the stations in the Bering Sea that were used in this study.

O_2, pH, total alkalinity, PO_4 and SiO_2 were determined according to the manual of Strickland and Parsons (1965). For further details on the method of pH determination, the reader is referred to Park (1966b). Salinity was measured by an inductive salinometer manufactured by Industria Manufacturing Engineers Pty. Ltd., Sydney, Australia (Brown and Hamon, 1961). NO_3 was determined by the method of Mullin and Riley (1955). Additional sigma-t data were used from Boreas cruise (Scripps Institution of Oceanography, 1966) to study the density distribution at the Kamchatka Strait.

Salinity increases monotonically with depth (Figure 2). At the upper 200 m it is lower at the eastern part than at the western. Temperature (Figure 3) shows a core of cold water at about 150 m with values less than 3.0°C. Below it there is a core of warm water, at about 400 m, with temperatures above 3.7°C. Below the warm core, temperature decreases monotonically. Figure 4 shows the T-S diagram for stations AAH9, in the Bering Sea, and HAH52 and HAH54, in the North Pacific Ocean. The temperature minimum and maximum are present in both the Bering Sea and North Pacific Ocean.

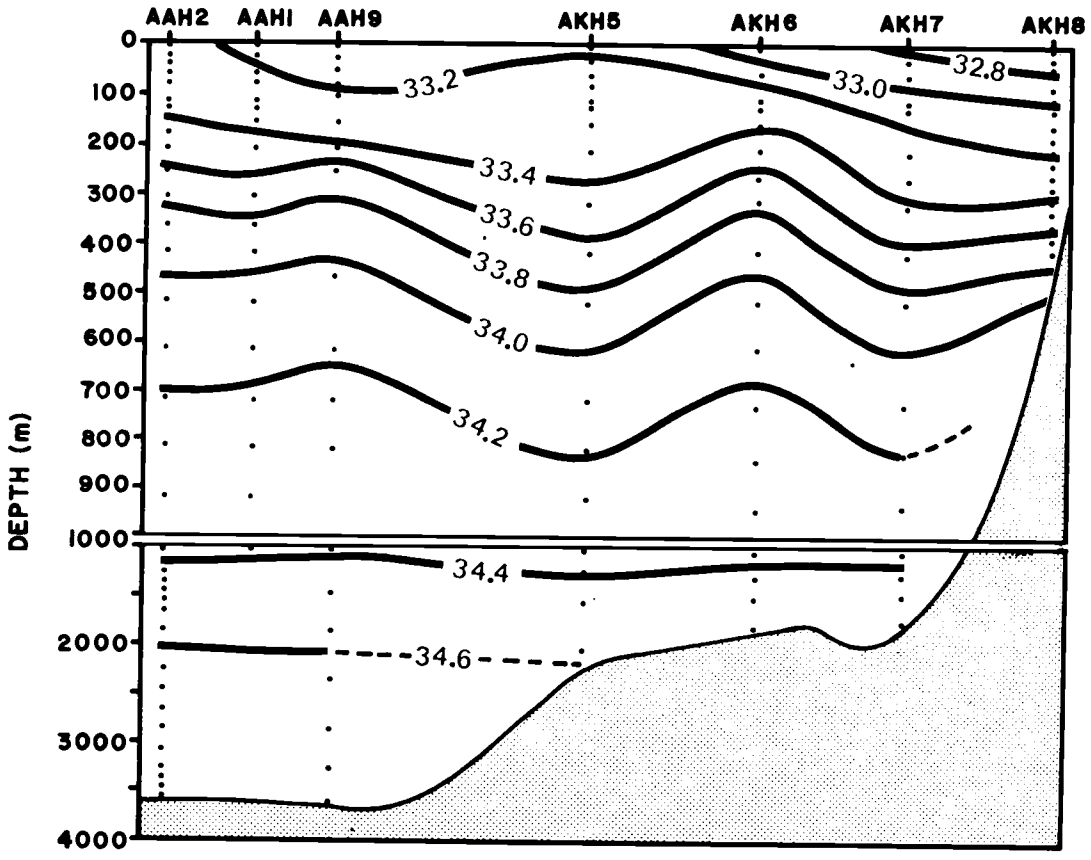

Figure 2. Vertical distribution of salinity (‰). The dots represent the sampling depths.

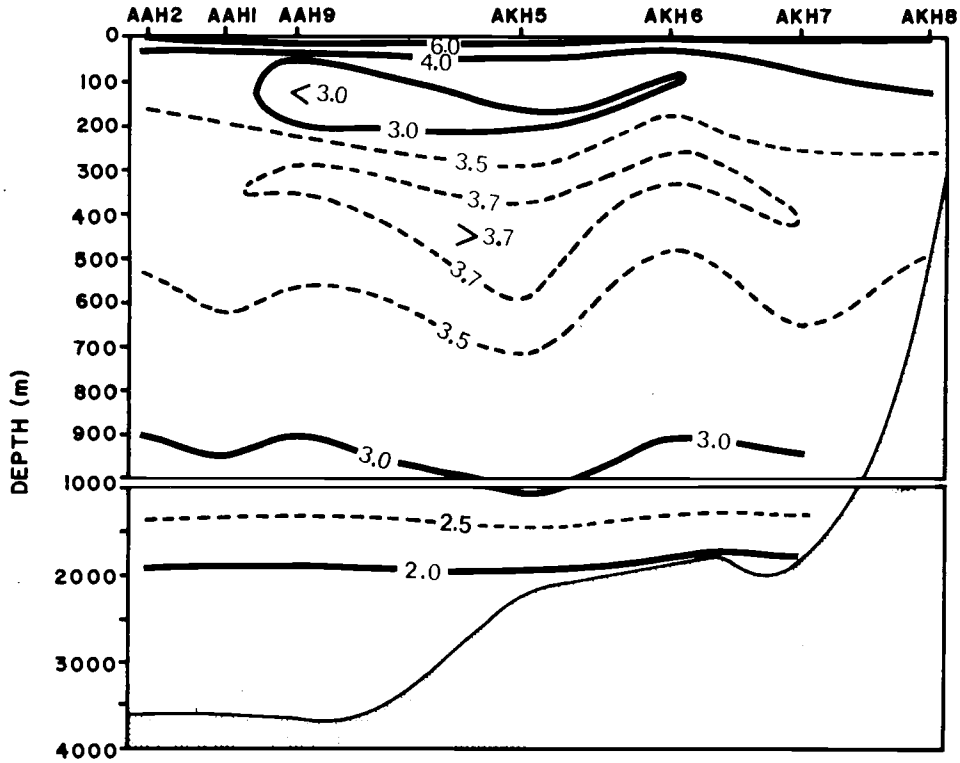

Figure 3. Vertical distribution of temperature (°C).

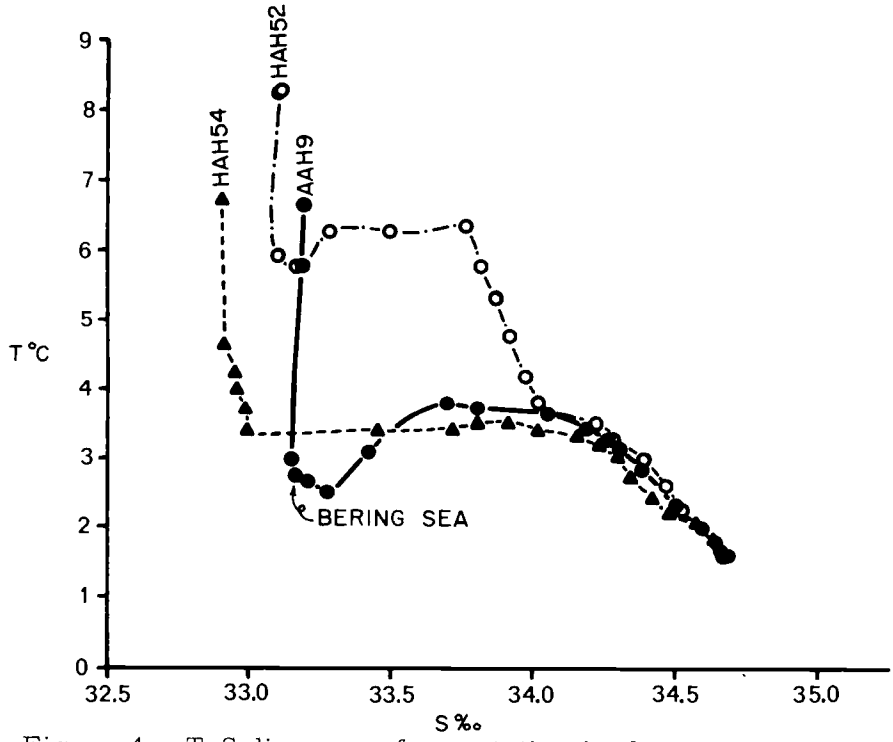

Figure 4. T-S diagrams for a station in the Bering Sea (AAH9) and two stations in the North Pacific Ocean (HAH52, 45°52.8'N, 174°02.3'W, and HAH54, 48°05.1'N, 175°21.8'W, both from YALOC-66 cruise also).

In the upper layer there is an O_2 maximum (Figure 5) with values of more than 7.5 ml/l. This maximum is at the sea surface at AAH1 and sinks eastward to about 50 m depth in AAH9 to ascend and reach the sea surface at AKH6. The O_2 minimum is near 900 m depth at the west and near 1000 m depth at the east, with values of less than 0.5 ml/l.

PO_4, NO_3 and SiO_2 (Figures 6, 7 and 8) show lower values at the east than at the west in the surface waters. The PO_4 and NO_3 maxima occur at about 1000 m depth, with values of more than 3.2 μM for PO_4, and more than 45 μM for NO_3 (Figures 6 and 7). SiO_2 increases monotonically with depth (Figure 8).

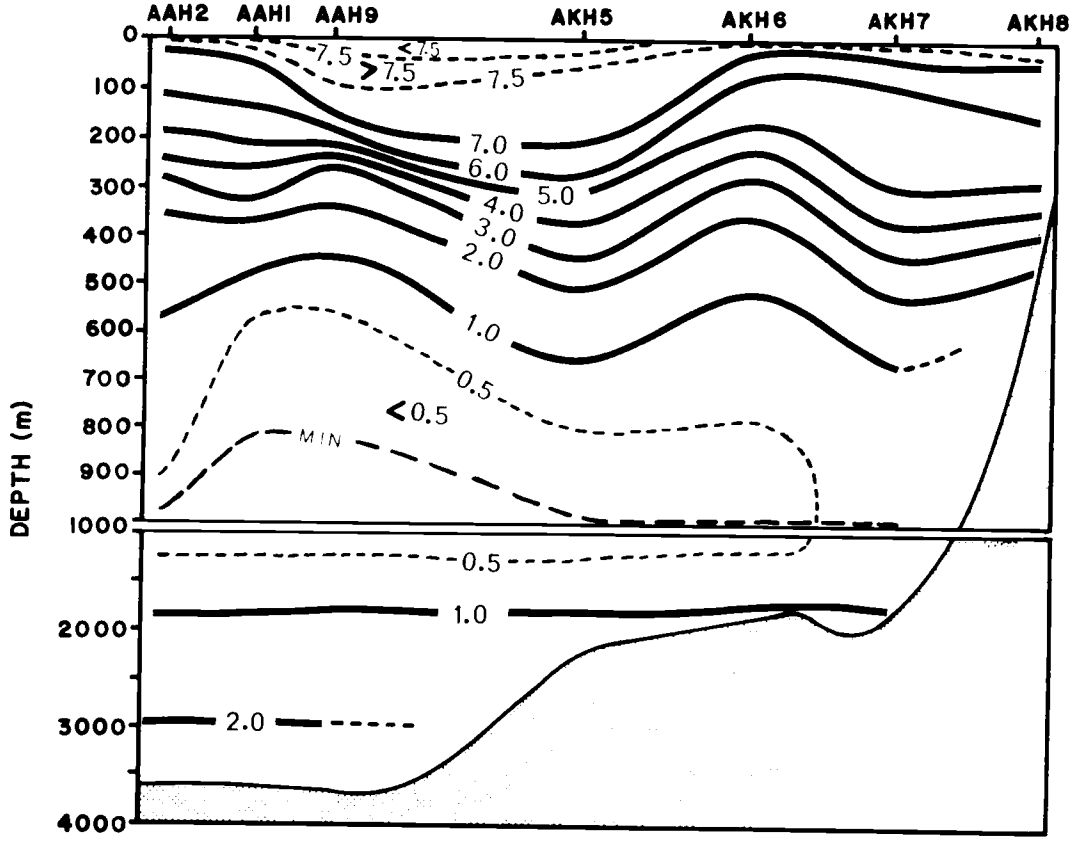

Figure 5. Vertical distribution of dissolved oxygen (ml/l).

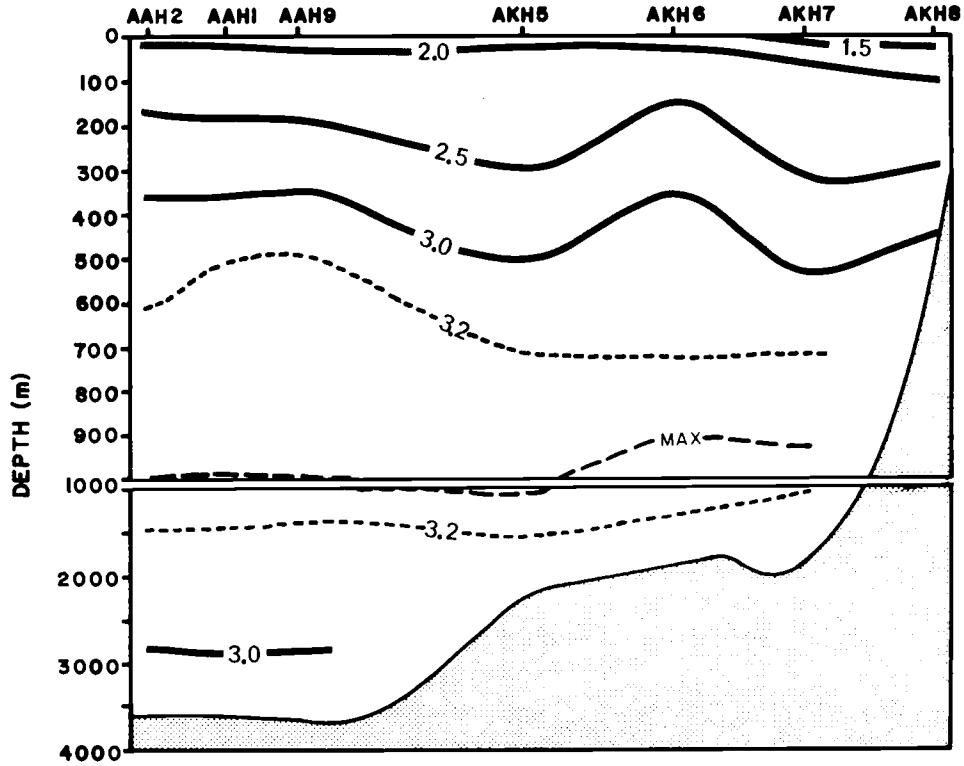

Figure 6. Vertical distribution of phosphate (μM).

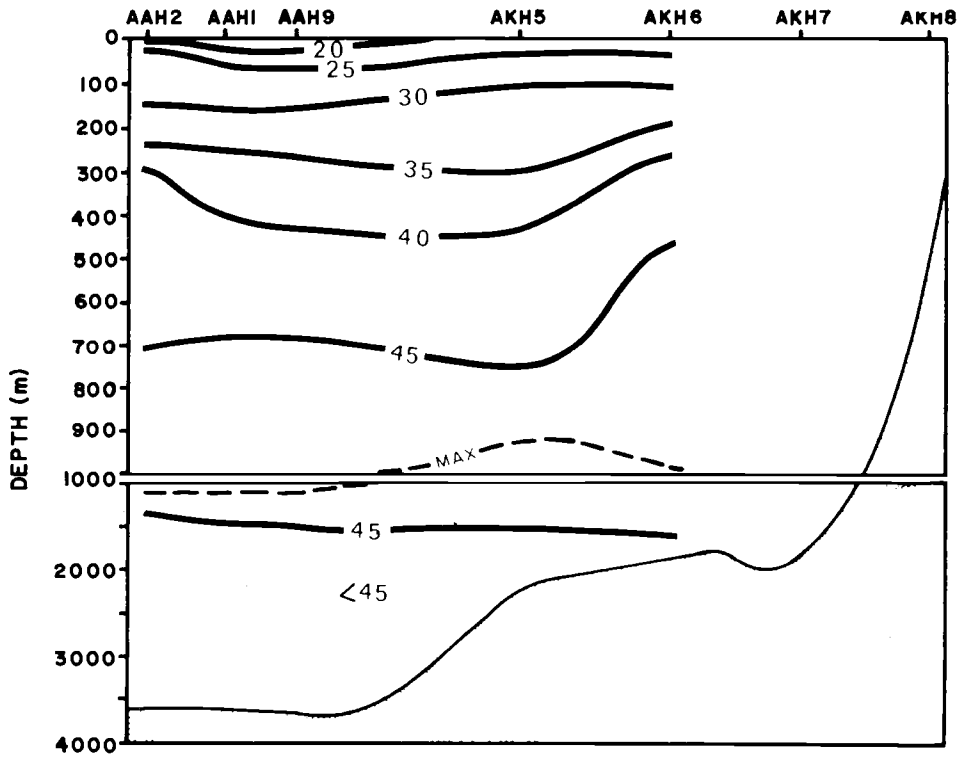

Figure 7. Vertical distribution of nitrate (μM).

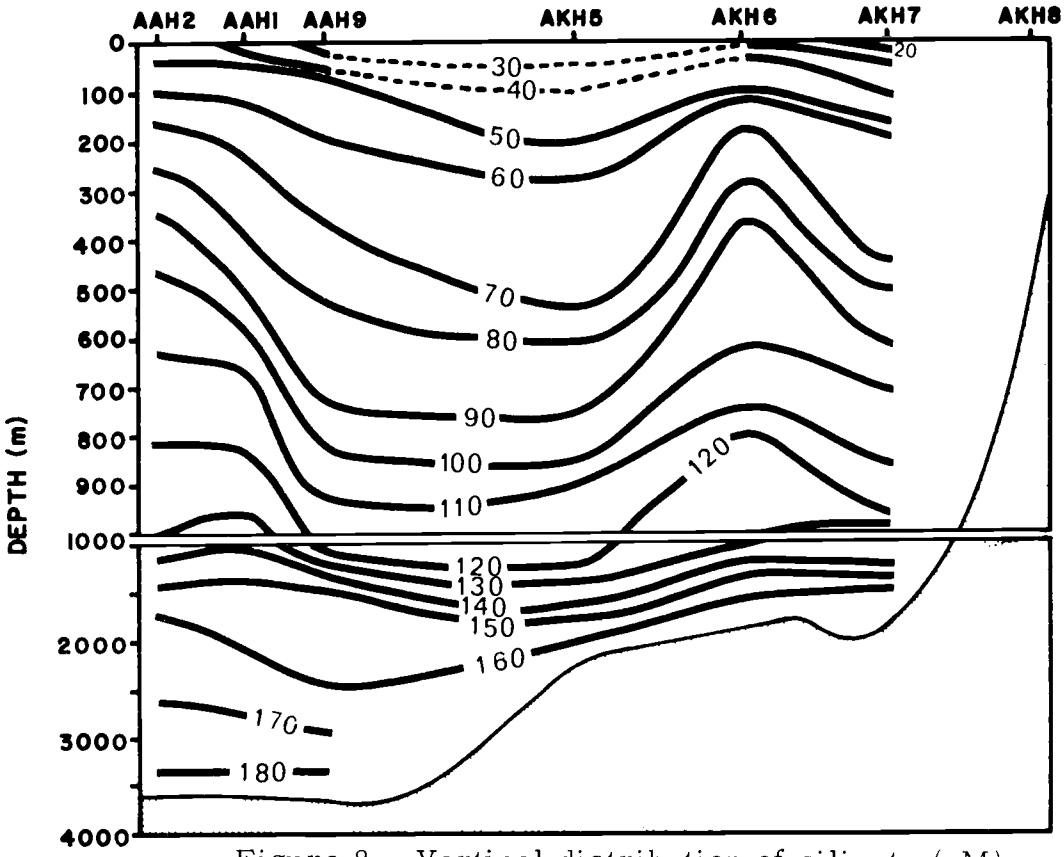

Figure 8. Vertical distribution of silicate (μM).

pH is higher and alkalinity is lower (Figures 9 and 10) at the eastern part of the section than at the western in the surface waters. The pH minimum (Figure 9) is at about the same depth of the O_2 minimum, with values of less than 7.45. Alkalinity (Figure 10) increases monotonically with depth, from about 2.35 at the sea surface to more than 2.50 in the deep waters.

Data analysis

The pH was measured aboard the R/V YAQUINA at 25°C and at atmospheric pressure during YALOC-66 cruise. To obtain the "in situ" pH the raw data was corrected for temperature and pressure by means of the following equation given by Culberson and Pytkowicz (1968):

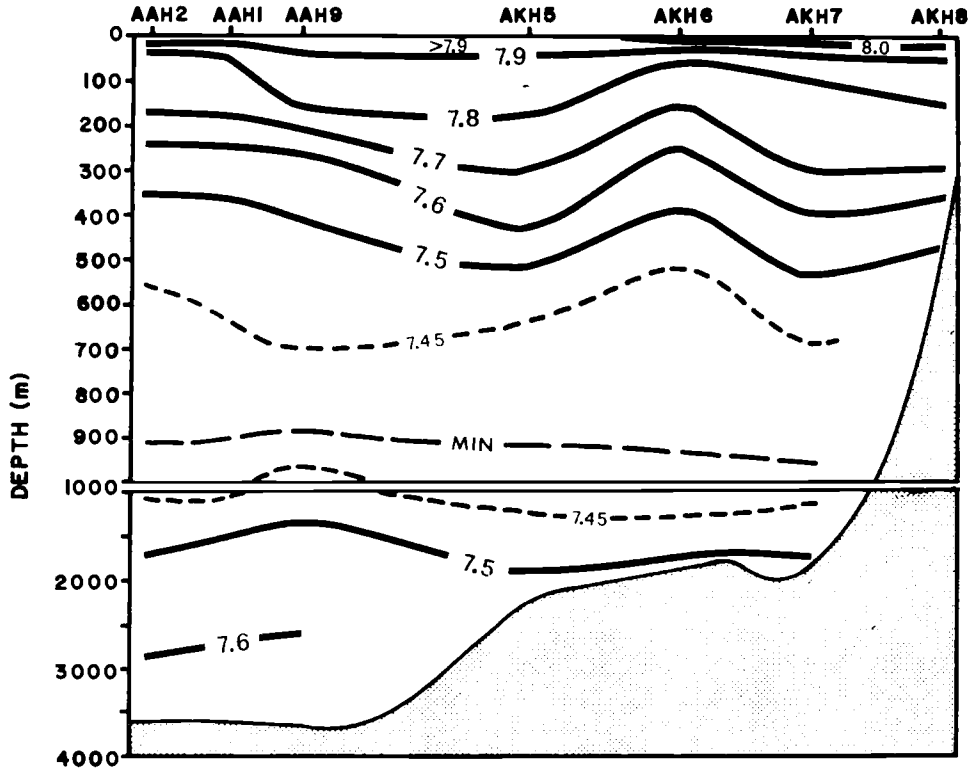

Figure 9. Vertical distribution of pH at 25° C and one atmosphere pressure.

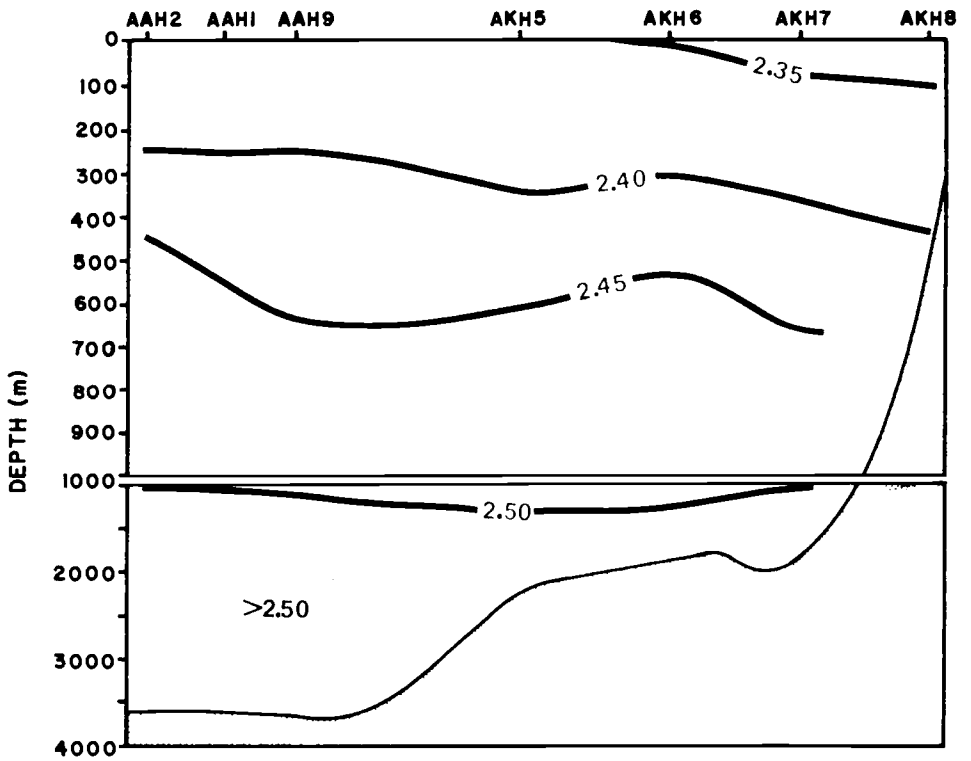

Figure 10. Vertical distribution of alkalinity (meq/l).

$$\frac{T_{(CO_2)}}{T_B} = \left[\frac{TA}{T_B} - \frac{K'_{Bp}}{a_{Hp}+K'_{Bp}} \right] \left[\frac{(a_{Hp})^2 + a_{Hp}K'_{1p} + K'_{1p}K'_{2p}}{a_{Hp}K'_{1p} + 2K'_{1p}K'_{2p}} \right] \quad (1)$$

where: $T(CO_2)$ is the total concentration of carbon dioxide, T_B is the total concentration of boron, TA is the total alkalinity, a_{Hp} is the hydrogen ion activity, K'_{Bp} is the apparent dissociation constant of boric acid and K'_{1p} and K'_{2p} respectively, the first and second apparent dissociation constants of carbonic acid. The subscript p indicates pressure conditions. TA, $T_{(CO_2)}$ and T_B are not functions of temperature and pressure, they can be calculated for one atmosphere pressure and 25° C and then used in equation (1) for "in situ" conditions. K'_{Bp}, K'_{1p}, and K'_{2p} are known for any given temperature and pressure using Lyman's (1956) values and Culberson's (1968) pressure coefficients. An iteration procedure suggested by Ben-Yaakov (1970) was used to solve for a_{Hp}, and thus for pH.

"In situ" partial pressure of carbon dioxide, P_{CO_2}, is defined and calculated by means of the following equation:

$$P_{CO_2} = \left[TA - \frac{K'_{Bp} \cdot T_B}{(K'_{Bp} + a_{Hp})} \right] \left[\frac{(a_{Hp})^2}{K'_{1p} \cdot \alpha_s \cdot (a_{Hp} + 2K'_{2p})} \right] \quad (2)$$

where α_s is the solubility coefficient of carbon dioxide in seawater at one atmosphere pressure. This is the partial pressure that carbon dioxide dissolved in seawater at certain depth would exert if that parcel of seawater would be brought to the sea surface without

changing the "in situ" equilibria of carbonic and boric acids. This concept is analogous to the potential temperature concept in oceanography. To give an idea of what the effect of the pressure correction is, if we compare the P_{CO_2} corrected only for temperature against the "in situ" P_{CO_2}, at the P_{CO_2} maximum level, the "in situ" P_{CO_2} is lower by 12 ppm, and at the deepest part of our section under study (3600 m) "in situ" P_{CO_2} is lower by 32 ppm.

The "in situ" percent saturation of calcium carbonate with respect to calcite and aragonite was calculated from pH, total alkalinity, temperature, salinity and depth data. The percent saturation of calcium carbonate in a solution is expressed as the ratio of the ionic product of calcium and carbonate to the equilibrium solubility product of calcium carbonate, multiplied by one hundred, i.e.,

$$(\%\ \text{Saturation}) = \left[Ca^{++}\right] \cdot \left[CO_3^{=}\right]_p \times 100/K'_{SP_p} \qquad (3)$$

where $\left[Ca^{++}\right]$ and $\left[CO_3^{=}\right]_p$ are the total concentration of calcium and carbonate ions, respectively, including both free ion and ion-pair forms, and K'_{SP_p} is the apparent solubility product of calcium carbonate at pressure P.

To calculate $\left[Ca^{++}\right]$ the following Wattenberg's (1936) relationship was used:

$$\left[Ca^{++}\right] = 1/2\ CA + 477 \times 10^{-3}\ Cl‰ \quad (\text{mmoles/liter}) \qquad (4)$$

The term CA, carbonate alkalinity, is calculated from the following expression:

$$CA = TA - (T_B \cdot K'_{Bp})/(K'_{Bp} + a_{Hp}) \quad (5)$$

By the use of equation (5) we calculate $\left[CO_3^{=}\right]_p$ as follows:

$$\left[CO_3^{=}\right]_p = CA \cdot K'_{2p}/(a_{Hp} + 2K'_{2p}) \quad (6)$$

Li, Takahashi and Broecker (1969), using the values of the apparent solubility product of calcium carbonate that MacIntyre (1965) measured for calcite and aragonite over a temperature range of 0° to 40°C and estimating the effect of chlorinity on the basis of measurements by Wattenberg (1936), derived the equations for K'_{SP} which is the apparent solubility product at one atmosphere.

$$K'_{SP}(\text{calcite}) = (0.69 - 0.0063T_p) \cdot 10^{-6} \cdot (Cl‰/19) \quad (7)$$

$$K'_{SP}(\text{aragonite}) = (1.09 - 0.0078T_p) \cdot 10^{-6} \cdot (Cl‰/19) \quad (8)$$

where the unit of K'_{SP} is in $\text{mole}^2/\text{liter}^2$ and T_p is the "in situ" temperature in degrees centigrade.

Knowing K'_{SP} we can calculate K'_{SPp} as follows:

$$K'_{SPp} = (10^{-\overline{\Delta V} \cdot Z/23RT_k})K'_{SP} \quad (9)$$

where $\overline{\Delta V}$ is the change in partial molar volume for calcium carbonate for the reaction of dissociation in sea water, Z is the depth in meters,

R is the gas constant and T_k is the "in situ" temperature in °K.

Values of $\Delta\overline{V}$ are available in the literature only for temperatures of 25°C, 22°C and 2°C. Hawley and Pytkowicz (1969) calculated the pressure coefficient of K'_{SP} for aragonite at 2°C and, by assuming the temperature dependence of calcite to be the same as that of aragonite, they calculated the values of the pressure coefficient of K'_{SP} for calcite at 2°C and 500 and 1000 atmospheres. Using those values in equation (9) $\Delta\overline{V}$ was found to be equal to -35.8 cubic centimeters per mole for calcite and -34.5 cubic centimeters per mole for aragonite.

The temperature range for our data is 1.5° to 6.9°C with most of the data around 2°C. The higher temperature values are near or at the sea surface where the pressure effect is very small. Therefore, we used the values of $\Delta\overline{V}$ for 2°C as constants in the calculations of the pressure coefficients of K'_{SP}.

The apparent oxygen utilization (AOU) has been defined by Redfield (1942) as the amount of O_2 that has disappeared from the water owing to metabolic processes. It is defined mathematically by

$$AOU = O'_2 - O_2 \qquad (10)$$

where O'_2 is the calculated concentration of dissolved oxygen at saturation and O_2 is the measured dissolved oxygen concentration. To calculate O'_2, Carpenter's oxygen solubility data were used

(Gilbert, Pawley and Park, 1968). Recently Harmon Craig of Scripps Institution of Oceanography and Bruce Benson of Amherst College have advocated the concurrent use of conservative argon concentration in sea water to estimate reliable AOU values. Since no argon data are available from YALOC-66 cruise, we used equation (10) to calculate AOU in this work.

Preformed phosphate ($P.PO_4$) was defined by Redfield (1942) as the phosphate that was present in the parcel of water before it left the sea surface. It is defined mathematically by

$$P.PO_4 = PO_4 - AOU/138 \qquad (11)$$

where PO_4 is the measured total dissolved inorganic phosphate and AOU is as defined above and expressed in μM.

For a detailed discussion of the AOU and $P.PO_4$ concepts, the reader is referred to Pytkowicz (1971).

Discussion

General considerations

Arsen'ev (1967) presents a schematic pattern of the Bering Sea surface circulation showing a complex set of gyres with a general cyclonic character, and the strong southward flowing Kamchatka current. He calculated surface geostrophic currents with respect to the 1000 decibars (db) surface. Reid (1966) reports a geostrophic

speed, relative to 1500 db, of 60 cm/sec and flow of 23 x 10^6 m^3/sec--"or about three times as much"--near Cape Africa for the Kamchatka current during winter 1966, compared to a summer flow of about 8 x 10^6 m^3/sec. Taking a mean value of about 15 x 10^6 m^3/sec we calculated that roughly 473, 000 km^3/year of sea water flows from the Bering Sea into the Pacific Ocean by the Kamchatka current. According to Yankina (1963) (cited by Ivanenkov, 1964) the mean, annual flow of water through the Bering Strait to the Arctic Ocean is 30, 000 km^3. All this water from the Bering Sea is mainly balanced by surface and intermediate water flowing from the Pacific Ocean through the Aleutian chain passes, and by deep Pacific water flowing through the Kamchatka Strait and Near Pass. Favorite (1967) concluded that the Alaskan Stream is continuous as far westward as 170° E where it divides sending one branch into the Bering Sea. A very small portion of the balance is achieved by a net precipitation and river input of 1600 km^3/ year, with the Yukon river being the main contributor, and 85% of the precipitation being in summer (Ivanenkov, 1964). This has a measurable effect on the hydrochemical characteristics of the surface waters during summer.

To infer the direction of motion in the deep waters of the Bering Sea (i.e. more than 2000 m depth) we could plot AOU values on sigma-t surfaces (Pytkowicz and Kester, 1966; Alvarez-Borrego and Park, 1971). But, since the horizontal distribution of salinity and

temperature is relatively uniform in deep waters (Arsen'ev, 1967), as an approximation we can use the O_2 distribution for that purpose, assuming that a gradient of O_2 along a depth surface is due, to some extent, to biological consumption and, thus, that lower values of O_2 means older water, with the direction of flow being from higher to lower values. Ivanenkov (1964) presents two contour charts of the O_2 distribution at 2000 and 2500 m respectively, we have reproduced them here and have drawn arrows to indicate the direction of motion (Figure 11). Of course, our analysis only gives a very rough idea of the direction of motion. According to Ivanenkov (1964) the high O_2 values at the eastern part of the basin, at 2000 m (Figure 11), near the continental slope, can be explained in terms of turbulent mixing with the overlying layers richer in O_2. The flow at both 2000 and 2500 m is indicated to be from the Pacific Ocean into the Bering Sea through the Kamchatka Strait, and then northward and eastward in the basin.

This is in disagreement with the results obtained by Arsen'ev (1967) who calculated geostrophic flow at the 2000 db surface relative to the 3000 db surface. His results show that water is flowing from the Bering Sea to the Pacific Ocean at the 2000 db surface through the Kamchatka Strait and at the most western part the Kamchatka current, with a relatively high velocity, is continuously preserved. However, he indicates that the study of the deep circulation of the Bering Sea is still in an early stage. There remains the possibility that the water

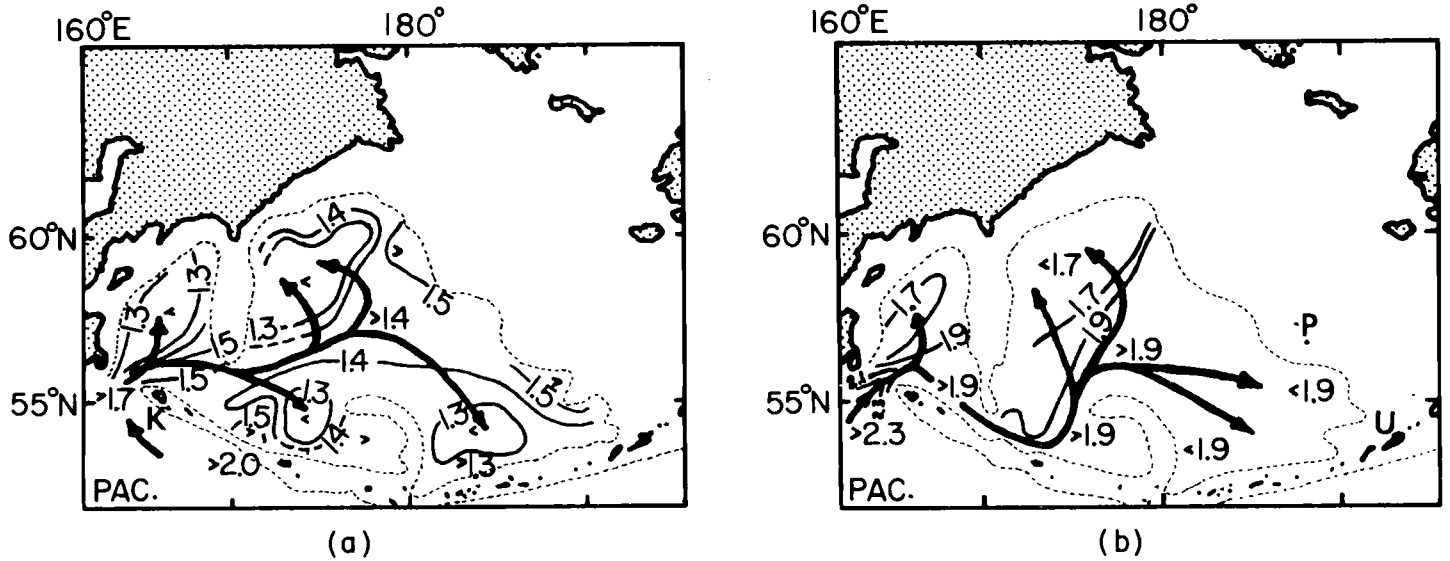

Figure 11. Distribution of oxygen (ml/l) at 2000 m (a) and at 2500 m (b) depths (the 2000 m and 2500 m isobaths respectively, are shown by dotted lines) (after Ivanenkov, 1964). We have drawn arrows to indicate the direction of water motion. K in (a) shows the location of the Komandorskiye Islands, and P and U, in (b) show the location of the Pribilof and Unalaska Islands respectively.

at the 3000 db level is moving with higher velocity than the water at the 2000 db level, both into the Bering Sea. So that, when the 3000 db surface is taken as the level of no motion the results show a water motion at the 2000 db surface from the Bering Sea into the Pacific Ocean when the real direction of motion is the opposite. According to Favorite (1972) there are still questions concerning not only how well the averaged data that Arsen'ev (1967) used denote actual conditions, but also whether or not geostrophic flow is a good indicator of actual circulation. According to him, recent oceanographic surveys in the central and eastern Bering Sea indicate that present interpretations of flow in the Bering Sea are still inaccurate. Further studies are needed to solve this problem.

In the Northern Hemisphere currents flow in such a direction that the water of low density is on the right-hand side of the currents, and the water of high density is on the left-hand side (Sverdrup, Johnson and Fleming, 1942) By plotting sigma-t on a vertical section at the Kamchatka Strait, using Boreas data (Scripps Institution of Oceanography, 1966) (Figure 12) we can see that the Kamchatka current is deeper than 1500 m and at that depth is becoming much weaker than at the layers above, and a flow into the Bering Sea begins to become apparent near the Komandorskiye islands (the location of these islands is shown in Figure 11a). This supports the direction of flow inferred from the O_2 distribution as stated above.

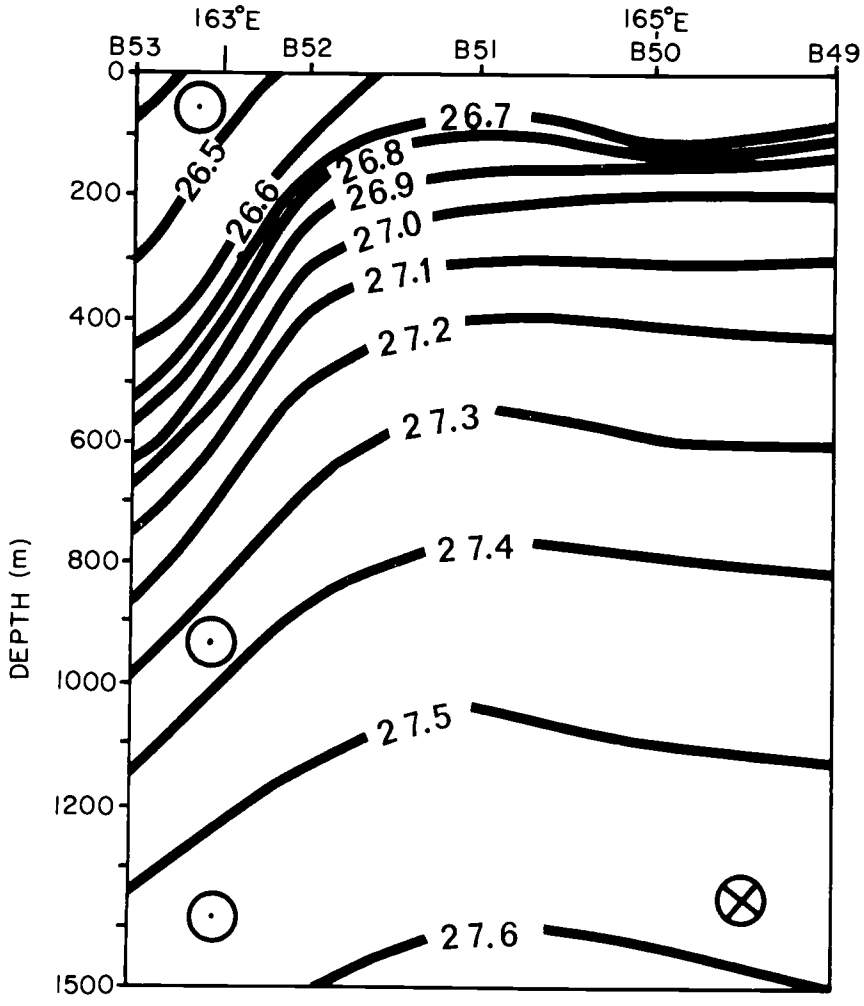

Figure 12. Vertical distribution of density (σ_t) in the Kamchatka Strait. The symbols ⊙ and ⊗ denote flux out and flux in respectively.

Packard, Healy and Richards (1971) have estimated the rate of O_2 consumption in sea water by measuring the activity of the respiratory electron transport system in plankton in the waters of the eastern tropical Pacific Ocean (off Peru). Their average value for depths below 1000 m is 3.8×10^{-4} mg-at/l per year. Their value agrees very well with that obtained by Culberson (personal communication) of 3.6×10^{-4} mg-at/l per year. Culberson applied the vertical

diffusion model to the distribution of O_2 in a station off San Francisco, California, during YALOC-69 cruise. To further check the validity of applying Packard, Healy and Richards' (1971) values to the North Pacific Ocean we have calculated the time that is required for the water to move from 180° to 170°W at about 45°N by using Alvarez-Borrego and Park's (1971) AOU distribution on the 26.8 sigma-t surface (~ 350 m depth) and Packard, Healy and Richards' (1971) O_2 consumption rate values; and by using the geostrophic velocities as calculated by Dodimead, Favorite and Hirano (1963). By using the AOU distribution the result is about 2.5 years, and by using the geostrophic method it is about 1.2 years. This may mean that the O_2 consumption rate in the shallow waters (i.e. less than 500 m depth) of the North Pacific Ocean is higher than that of the tropical Pacific Ocean by about a factor of two.

Thus, although direct measurements of the O_2 consumption rate have not yet been carried out for the North Pacific Ocean and the Bering Sea, it seems that at least the results for the deep waters (i.e. below 1000 m depth) obtained from the tropical Pacific Ocean by Packard, Healy and Richards (1971) are applicable to the Northeast Pacific Ocean. Since the deep water of the Bering Sea is coming from the North Pacific Ocean, we will extend the use of Packard, Healy and Richards' (1971) data, to the Bering Sea.

By using Packard, Healy and Richards' (1971) O_2 consumption

rate values and Ivanenkov's (1964) O_2 distribution at 2000 m and 2500 m in the Bering Sea (Figure 11) we estimate that it takes roughly 20 years for the water to move from the Kamchatka Strait to the farthest parts of the basins, at 2000 m depth; and, at 2500 m depth, it takes about 20 years for the water to move from the Kamchatka Strait to the southeastern part of the eastern basin, and about 30 years to move from the Kamchatka Strait to the northern part of the eastern basin and to the northern part of the western basin. These results agree very well with Arsen'ev's (1967) conclusions that the Bering Sea exchanges water rather rapidly with the North Pacific Ocean. According to Arsen'ev (1967) a complete rejuvenation of the Bering Sea occurs on the average of 35 years. This has a profound effect on the hydrochemical structure of the Bering Sea.

Sigma-t, salinity, temperature

In the vertical section studied during YALOC-66 (Figure 1), at the upper 200 m, salinity and sigma-t (Figures 2 and 13) are lower at the eastern part than at the western. This is probably the result of continental runoff. This type of effect, as we will see, is also shown by the distribution of other chemical parameters.

In the upper 1000 m sigma-t shows a wavy distribution (Figure 13). In general the isograms of the different chemical parameters follow the same pattern as the sigma-t isograms (Figures 2 through

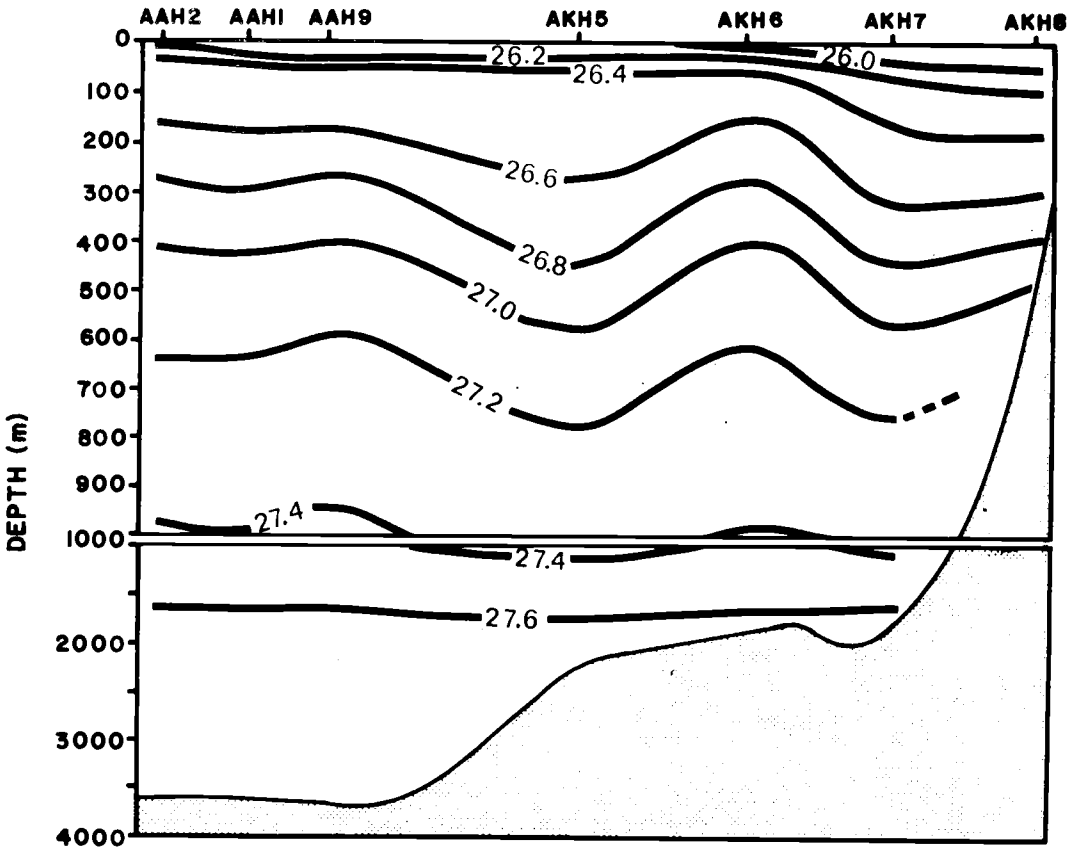

Figure 13. Vertical distribution of density (σ_t).

10). According to Smetanin (1956) (cited by Ivanenkov, 1964) the wave-like curves of the isograms for the physical and chemical characteristics in the vertical sections are produced by meandering currents.

The T-S diagrams for stations AAH9, HAH52 and HAH54 (Figure 4) show that a temperature minimum and maximum are present in both the Bering Sea and North Pacific Ocean. For the North Pacific Ocean, they have been referred to as Dicothermal and Mesothermal Water (Uda, 1935). The Dicothermal water, which has

also been called Inter-Cooled Water (Hirano, 1961), is formed as a consequence of the seasonal cycle of heating and cooling (Uda, 1963). The Mesothermal Water is not a product of the seasonal cycle of heating and cooling but it is formed by advective processes. According to Reid (1966) it is apparent that this warm subsurface water, which at the North Pacific Ocean is flowing westward with the Alaskan Stream, does not come directly from the warm water of lower latitudes but comes from the Gulf of Alaska. It flows into the Bering Sea through the Aleutian passes.

O_2, AOU, nutrients

In the upper layer there is an O_2 maximum (Figure 5) with values of more than 7.5 ml/l. This maximum is at the sea surface in AAH1 and sinks eastward to about 50 m depth in AAH9 to ascend and reach the sea surface in AKH6. Strong photosynthetic activity at about 50 m depth plus heating of the surface waters may cause this O_2 maximum near the sea surface.

Pytkowicz (1964) concluded that the subsurface O_2 maximum that forms in summer off the Oregon coast is due to the increase of temperature in the near surface waters. According to him deviations of the O_2-PO_4 correlations from linearity suggest that, as the near surface water warms up and becomes supersaturated with O_2, O_2 diffuses to the atmosphere. A similar mechanism may be responsible

for the O_2 maximum shown in Figure 5.

The fact that the O_2 maximum is not present along the whole section but only between AAH1 and AKH6 was due to the surface temperature being highest between AAH1 and AKH6 (Figure 3), and possibly the patchiness of phytoplankton populations was such that photosynthetic activity, at about 50 m, was greater between those two stations. AOU distribution (Figure 14) indicates that the waters were supersaturated with O_2 to greater depths between AAH1 and AKH6 than everywhere else. SiO_2 distribution (Figure 8) in the upper layers shows a good correlation with the O_2 distribution.

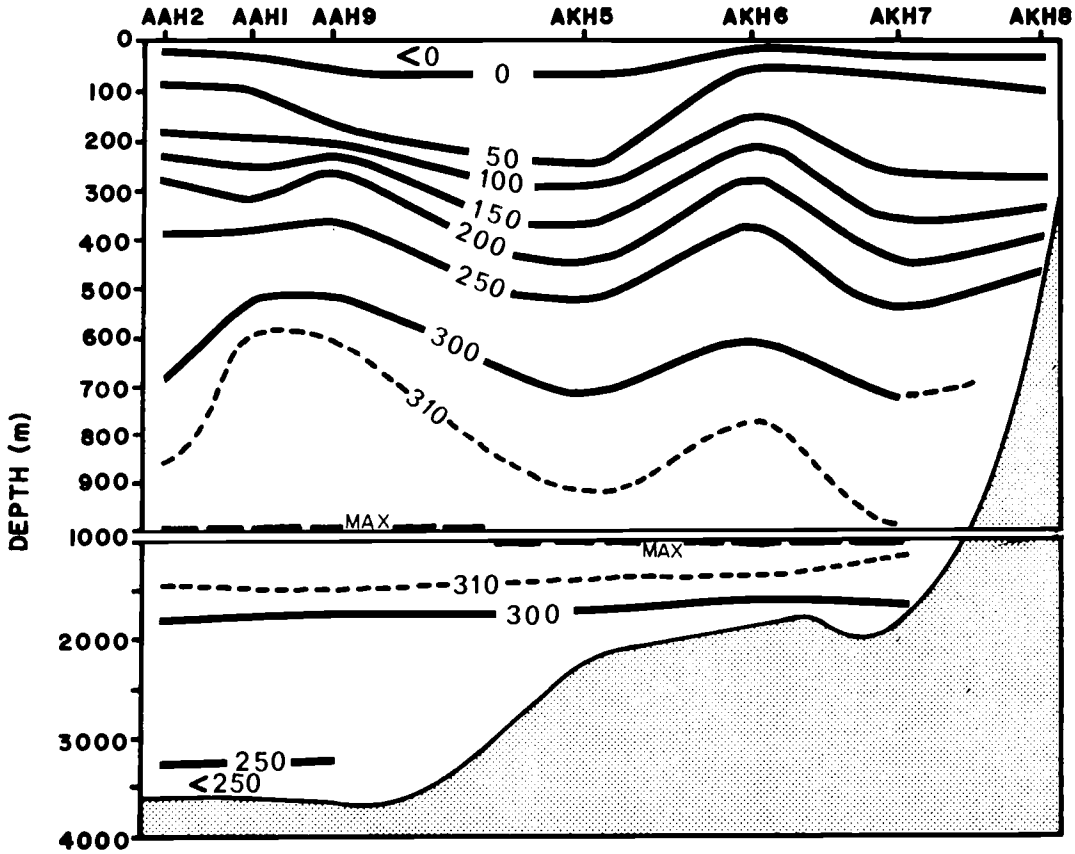

Figure 14. Vertical distribution of apparent oxygen utilization (μM).

PO_4, NO_3 and SiO_2 (Figures 6, 7 and 8) show lower values at the east than at the west in the surface waters. This probably is the result of the continental runoff having low nutrient concentrations.

PO_4, NO_3 and SiO_2 concentrations at the sea surface are higher in the Bering Sea (Figures 6, 7 and 8) than in the North Pacific Ocean. PO_4 values of 1.8 μM, NO_3 values of 22 μM, and SiO_2 values of 30 μM were measured in the surface waters of the Bering Sea. Park (1967b) reported PO_4 values of less than 0.5 μM, NO_3 values of less than 2 μM, and SiO_2 values of less than 5 μM, in the surface waters of the North Pacific Ocean, at about 40°N measured during YALOC-66. According to Muromtsev (1953) (cited by Ivanenkov, 1964) the deep waters of the Bering Sea upwell in the cyclonic gyres. This may be the main reason for the high surface concentration of nutrients. Evidence for upwelling near the margin of the continental shelf extending along the 200 fathom line from Unalaska Island to the Pribilof Islands (the locations of these islands are shown in Figure 11b) was indicated by Dugdale and Goering (1966), who found sharp surface gradients of NO_3 concentrations. Kelley, Longerich and Hood (1971) suggest that this may be inertial type of upwelling caused by deep eastward currents sliding up the continental slope with sufficient velocity to cause surface outcropping. They supported this statement by the fact that random wind direction measured in June and September of 1970 over an area of consistent upwelling showed that wind-driven upwelling

does not appear to be a major factor here.

The vertical distribution of nutrients in the deep waters of the Southeastern Bering Sea is very near the same as in the deep waters of the North Pacific, with similar levels of concentration. The location of the PO_4 and NO_3 maxima (Figures 6 and 7) correlates well with that of the AOU maximum (Figure 14) in the Bering Sea.

The P. PO_4 vertical distribution (Figure 15) shows a near surface maximum, at about 100 m; and a minimum between 1000 m and 1500 m. Values are higher than 1.0 μM near the bottom in deep waters. The P. PO_4 minimum has also been found in the North Pacific Ocean (Park,

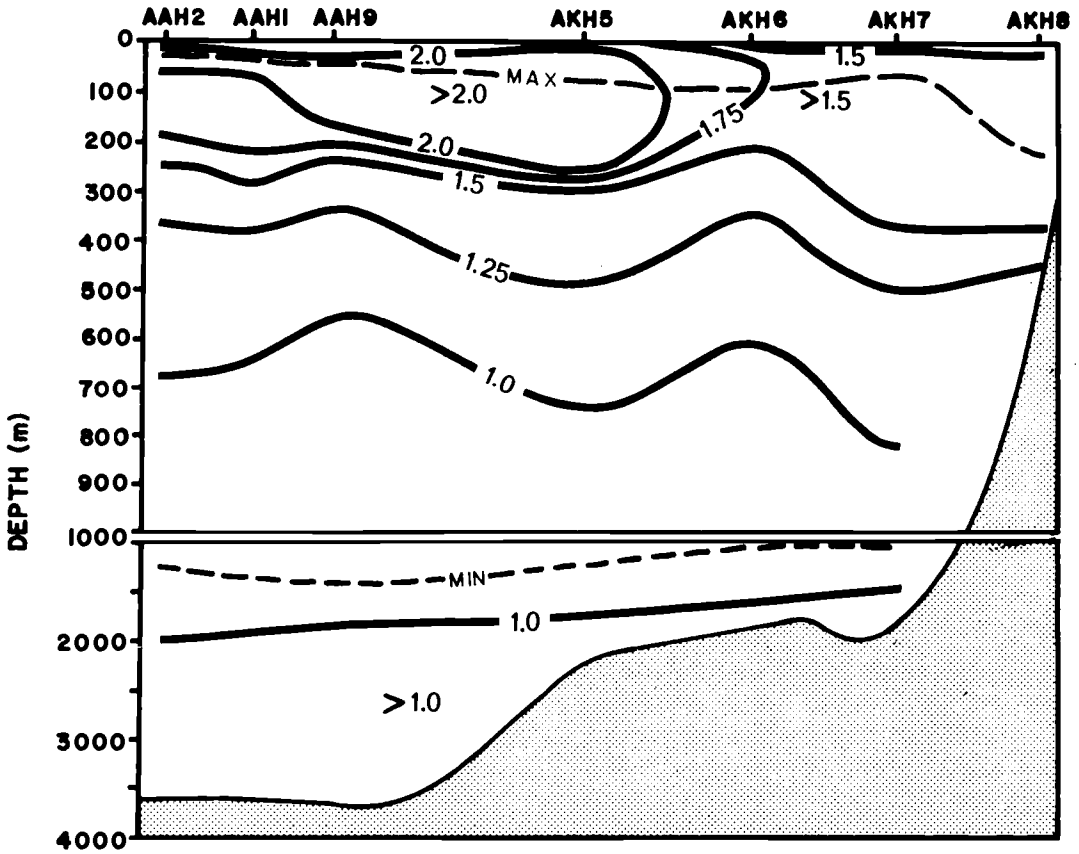

Figure 15. Vertical distribution of preformed phosphate (μM).

1967b) and in the Antarctic waters (Pytkowicz, 1968). One possible explanation for the P. PO_4 minimum is that it is the core of a water mass which when at the sea surface had undergone intense photosynthesis with depletion of PO_4 concentration to very low values.

The P. PO_4 maximum near the sea surface (Figure 15) does not have much hydrological significance since O_2 air-sea exchange at the sea surface diminishes the meaning of calculated values of P. PO_4. The AOU distribution (Figure 14) indicates that the surface waters are supersaturated with O_2. This causes the O_2 to escape from the water to the air. So, when the AOU is calculated by equation (10), the magnitudes of the negative values at the sea surface are smaller than they would be if there were no air-sea O_2 exchange. These smaller negative AOU values give lower P. PO_4 values calculated by equation (11), at the sea surface. Probably the P. PO_4 maximum near the sea surface is due to this.

Figure 16 shows the relationship between nutrients and AOU, and between P. PO_4 and AOU.

According to Postma (1964) the advantage of the use of the PO_4-O_2 diagram is similar to that of the temperature-salinity diagram, in that mixing between two water "masses" with different PO_4 and O_2 concentrations results in a straight line between the two points which represent the two water "masses." (The term "water mass" Postma (1964) uses can be interpreted as water types.) And in the case of the

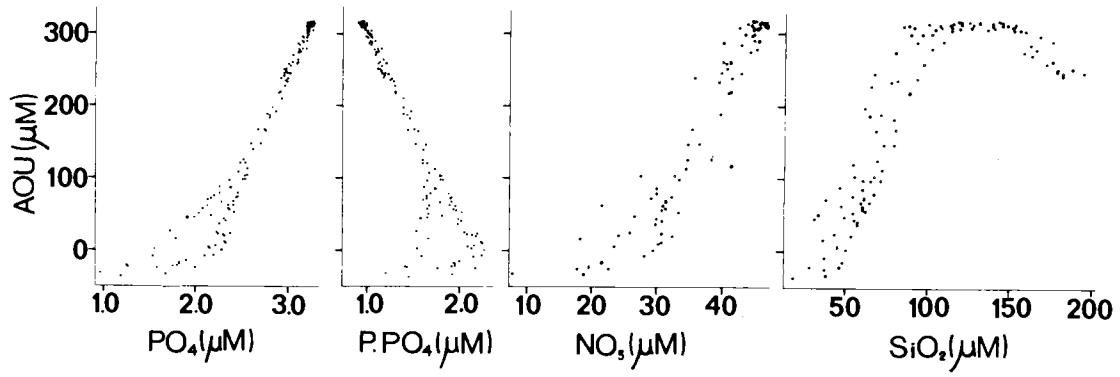

Figure 16. Nutrients-apparent oxygen utilization and preformed phosphate-apparent oxygen utilization relationships.

PO_4-O_2 relationship an additional advantage is that changes in a water type by biochemical processes develop a straight line, the direction of which is defined by the biochemical ratio of liberation and consumption of O_2 and PO_4.

However, when mixing between two water types occurs, where biochemical processes are concurrently occurring, both linear and non-linear relationships between PO_4 and O_2 can be found. To avoid the effect of air-sea exchange, we confine ourselves to the PO_4-O_2 relationship for depths below the euphotic zone, and consider here only oxidation; we further assume that the ratio of consumption of O_2 to liberation of PO_4 is constant when oxidation occurs at any depth. Either of the two effects, mixing or oxidation, separately generates a straight PO_4-O_2 line, but the sum of the two is only linear when, by chance, the slope of the two lines is the same. A detailed explanation

of this conclusion follows.

The initial concentrations of PO_4 and O_2 before mixing begins depend on the history of the two water types and on the extent of the biochemical processes. PO_4 depends on the $P.PO_4$ values, and the O_2 saturation values depend on temperature and salinity. Thus, the mixing line generally has a slope different than the oxidation line. The sum of the two effects is shown in Figure 17. The points A and B represent the two water types. Since we are only considering the effect of the oxidation while mixing occurs and not before, the two points, A and B, have the same (0, 0) position in the oxidation line. To facilitate the illustration a third point C is considered to represent the maximum oxidation level. In Figure 17 $\Delta O_2 = -\Delta AOU$.

To sum the two lines, a direct algebraic summation using the equations that represent the two lines is not correct since there is no direct correspondence of the points through the coordinates used in the diagram (Figures 17a, b). The correspondence exists through a third coordinate, i.e.: depth (Figure 17c). Figure 17c shows that the straight line of the PO_4-O_2 oxidation line is the projection of a curve on the PO_4-O_2 plane. Thus, the summation has to be made by adding the abscissas and ordinates of the corresponding points (Figures 17a, b).

According to Redfield (1942) PO_4 has two components: $P.PO_4$ and PO_4 of biological origin ($PO_{4_{ox}}$). $PO_{4_{ox}}$ can be expressed as a function of AOU, thus:

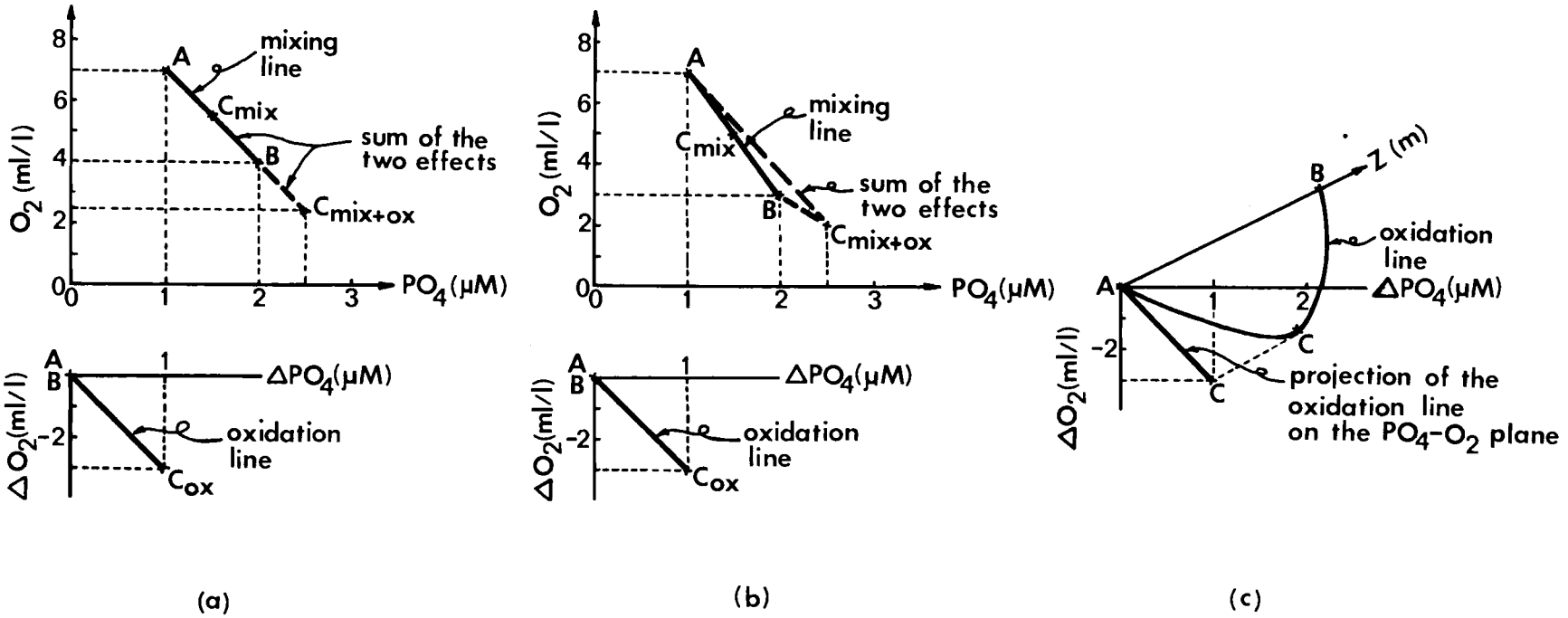

Figure 17. Two water types phosphate-oxygen hypothetic oxidation and mixing lines, plus the sum of the two effects, for the case where the slope of the mixing and oxidation lines is the same (a), and for the case where the slopes are different (b). The point C does not show a third water type, but the point of maximum oxidation. (c) shows the projection of the phosphate-oxygen line on the PO_4-O_2 plane.

$$PO_4 = P.PO_4 + a_R AOU \tag{12}$$

where a_R is the liberation of PO_4 to consumption of O_2 ratio. From equations (10) and (12)

$$PO_4 = P.PO_4 + a_R(O'_2 - O_2) \tag{13}$$

$$PO_4 = -a_R O_2 + P.PO_4 + a_R O'_2 = -a_R O_2 + b \tag{14}$$

$P.PO_4$ and O'_2 are source properties. b is a function of $P.PO_4$, temperature and salinity. If two water types A and B undergo mixing, we can express PO_4 as follows:

$$(PO_4)_A = -a_R(O_2)_A + b_A \tag{15}$$

$$(PO_4)_B = -a_R(O_2)_B + b_B \tag{16}$$

$$(PO_4)_M = -a_R f_A(O_2)_A + f_A b_A - a_R f_B(O_2)_B + f_B b_B \tag{17}$$

where $(PO_4)_M$ is the PO_4 of the water mass M, M has a fraction f_A of water type A and a fraction $f_B = 1 - f_A$ of water type B. From equation (17):

$$(PO_4)_M = -a_R\left[f_A(O_2)_A + f_B(O_2)_B\right] + f_A b_A + f_B b_B \tag{18}$$

$$(PO_4)_M = -a_R O_{2_M} + f_A b_A + b_B - f_A b_B \tag{19}$$

Thus, for the PO_4-O_2 relationship to be linear, either f_A and f_B are essentially constant with depth, i.e.: there is a constant proportion of two water types with depth (the PO_4-O_2 mixing line is a point), or $b_A = b_B$ (the PO_4-O_2 mixing line has the same slope as the oxidation line).

The second case is more likely.

Let us now consider the PO_4-AOU diagram. Again, when mixing occurs at the same time oxidation is going on, we expect to have a linear PO_4-AOU diagram only when the mixing and oxidation lines have the same slope. But, since AOU is not a function of temperature and salinity, for the mixing line to have the same slope as the oxidation line the only necessary and sufficient condition is that the two water types have the same $P.PO_4$ concentration. From equation (12) if two water types undergo mixing, we have:

$$(PO_4)_A = a_R AOU_A + (P.PO_4)_A \tag{20}$$

$$(PO_4)_B = a_R AOU_B + (P.PO_4)_B \tag{21}$$

Therefore:

$$(PO_4)_M = a_R f_A AOU_A + f_A(P.PO_4)_A + a_R f_B AOU_B + f_B(P.PO_4)_B \tag{22}$$

$$(PO_4)_M = a_R(f_A AOU_A + f_B AOU_B) + f_A(P.PO_4)_A + \\ + (1 - f_A)(P.PO_4)_B \tag{23}$$

$$(PO_4)_M = a_R AOU_M + f_A(P.PO_4)_A + (P.PO_4)_B - f_A(P.PO_4)_B \tag{24}$$

Then for the PO_4-AOU relationship to be linear, $(P.PO_4)_A = (P.PO_4)_B$ has to hold.

This algebraic treatment can be extended to the general case of n water types being mixed to show that the PO_4-AOU relationship, of the water mass formed, is linear when the $P.PO_4$ values are the same

for all the n water types. From equation (12), if n water types undergo mixing, we have:

$$(PO_4)_1 = a_R AOU_1 + (P.PO_4)_1 \tag{25}$$

$$(PO_4)_2 = a_R AOU_2 + (P.PO_4)_2 \tag{26}$$

$$\vdots$$

$$(PO_4)_n = a_R AOU_n + (P.PO_4)_n \tag{27}$$

Therefore:

$$(PO_4)_M = a_R f_1 AOU_1 + f_1(P.PO_4)_1 + a_R f_2 AOU_2 + \\ + f_2(P.PO_4)_2 + \ldots + a_R f_n AOU_n + f_n(P.PO_4)_n \tag{28}$$

$$(PO_4)_M = a_R(f_1 AOU_1 + f_2 AOU_2 + \ldots + f_n AOU_n) + \\ + f_1(P.PO_4)_1 + f_2(P.PO_4)_2 + \ldots + \\ + f_{n-1}(P.PO_4)_{n-1} + (1 - f_1 - f_2 + \ldots + \\ - f_{n-1})(P.PO_4)_n \tag{29}$$

$$(PO_4)_M = a_R AOU_M + f_1(P.PO_4)_1 + f_2(P.PO_4)_2 + \ldots + \\ + f_{n-1}(P.PO_4)_{n-1} + (P.PO_4)_n - f_1(P.PO_4)_n - \\ - f_2(P.PO_4)_n + \ldots - f_{n-1}(P.PO_4)_n \tag{30}$$

Then for the PO_4-AOU relationship to be linear, $(P.PO_4)_1 = (P.PO_4)_2 = \ldots = (P.PO_4)_{n-1} = (P.PO_4)_n$ has to hold.

One exceptional case where we would have a PO_4-AOU straight diagram without $P.PO_4$ being constant, would be when, by chance,

there is a linear relationship between $P.PO_4$ and AOU. $P.PO_4$ and AOU are independent parameters, but if, by chance, there is a linear relationship between them we can obtain an empirical expression of the type:

$$P.PO_4 = k_1 + k_2 AOU \tag{31}$$

where k_1 and k_2 are empirical constants. From equations (12) and (31) we have:

$$PO_4 = k_1 + k_2 AOU + a_R AOU = k_1 + (k_2 + a_R) AOU \tag{32}$$

In this case the slope of the PO_4-AOU diagram is not equal to the liberation of PO_4 to consumption of O_2 ratio. This seems to be the case for the Southeastern Bering Sea. Figure 16 shows a linear relationship between $P.PO_4$ and AOU for the region where AOU is higher than 100 μM (deeper than 200 m).

According to Sugiura and Yoshimura (1964) waters having the same values of chlorinity and temperature, in a certain sea area, must have equal preformed O_2 and $P.PO_4$ concentrations. According to them when plotting PO_4 against AOU for waters having equal values of chlorinity and temperature a linear relationship may be found, and the y-intercept of the PO_4-AOU line may give the value of preformed phosphate. This cannot be applied to the whole ocean because waters from different areas of the ocean having equal chlorinity and temperature may have different $P.PO_4$, since $P.PO_4$ is not a function of chlorinity and temperature.

Redfield, Ketchum and Richards (1963) proposed a model for the biochemical consumption and liberation of nutrients and O_2 by biological processes, photosynthesis and respiration. As Pytkowicz (1971) states, a plot of AOU versus nutrients is not a proper test of the model of Redfield, Ketchum and Richards (1963) because the preformed nutrients may vary with depth, thus oxidative nutrients should be used instead of total nutrients, but there is not yet a method to determine oxidative nutrients directly.

From Redfield, Ketchum and Richards' (1963) model the AOU: PO_4 ratio should be 138:1 if the units for both are μM, and 3.1:1 if AOU is expressed in ml/l and PO_4 is expressed in μM. Craig (1971) examined the question of a significant rate of "in situ" O_2 consumption in deep water by predicting the deep-water extrema in the O_2-inorganic carbon system as a function of latitude using a vertical-diffusion vertical-advection model with O_2 consumption. His results indicate that "in situ" oxidation and solution of carbon in Pacific deep water occur with time scales roughly comparable to those for circulation and mixing. Culberson (personal communication) suggested that a new method to obtain Redfield, Ketchum and Richards' (1963) ratio is to plot O_2 and nutrients against potential temperature (θ) for the region where the θ-S diagram is straight. The straight line connecting the two boundary points in the θ-nutrients and θ-O_2 diagrams give the "conservative" portion of nutrients and O_2; in other words the data

points would fall on the straight line if the concentrations of nutrients and O_2 between the two boundary points were due only to mixing. If we calculate the area between the straight line and the curved line, for each diagram, and then divide the θ-O_2 area by the respective θ-nutrients areas we may obtain Redfield, Ketchum and Richards' (1963) ratios, i.e., (°C)(ml/l):(°C)(μM) = ml/l:μM.

The method suggested by Culberson is directly applicable only if the θ-preformed nutrients diagrams are straight. We have plotted the θ-S diagram for stations AAH2 and AAH9 (Figure 18), our only two deep stations. A straight line is found between 1300 m and 3600 m depths. Since we already plotted the AOU-PO_4 and AOU-P.PO_4 relationships for the whole water column (Figure 16) it may seem redundant to plot the PO_4-O_2 and P.PO_4-O_2 diagrams for the region where the θ-S diagram is straight. However, we have done so to better see their behavior separately and in an expanded scale (Figure 19). The θ-O_2 diagram is shown in Figure 20 and the θ-PO_4 and θ-P.PO_4 diagrams are shown in Figure 21.

The PO_4-O_2 diagram (Figure 19) has a slope, calculated by a least squares fit, equal to -0.157, equivalent to an O_2 ml/l:PO_4 μM ratio of -6.4:1, more than twice as much as that predicted by Redfield, Ketchum and Richards (1963). It would be a circular argument to explain this by saying that the P.PO_4-O_2 diagram (Figure 19) shows that by adjusting the PO_4 values for differences in P.PO_4 we obtain

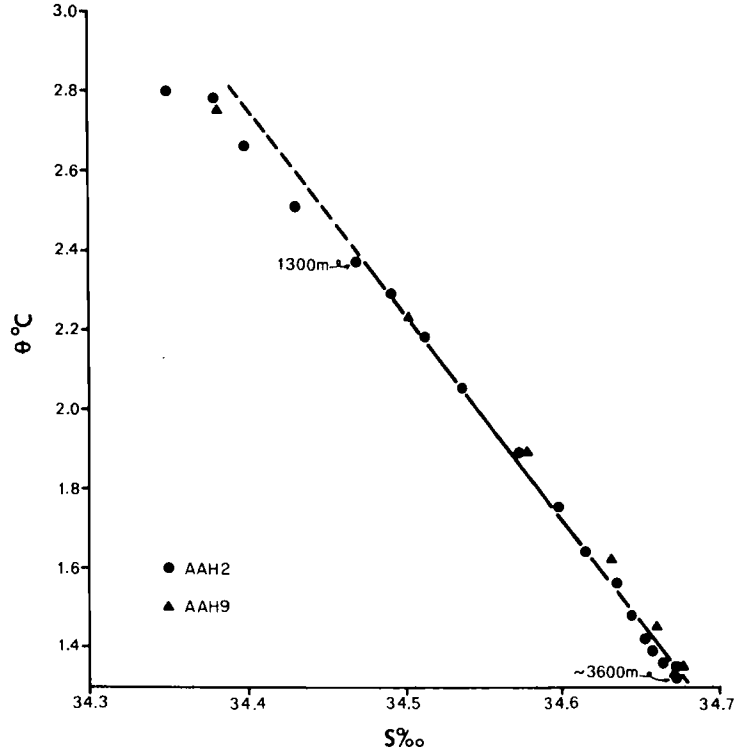

Figure 18. Potential temperature-salinity (θ-S) diagram for the deep waters of stations AAH2 and AAH9. The continuous line marks the straight portion of the diagram.

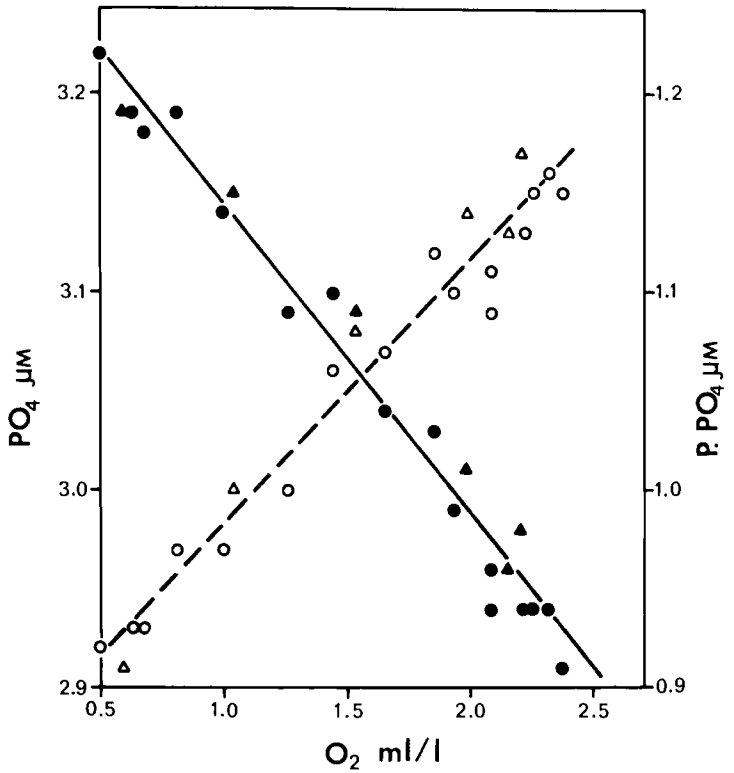

Figure 19. Phosphate-oxygen (PO_4-O_2) and preformed phosphate-oxygen (P. PO_4-O_2) diagrams for the straight portion of the θ-S diagram for stations AAH2 and AAH9. Dark circles and triangles represent PO_4, clear circles and triangles represent P. PO_4.

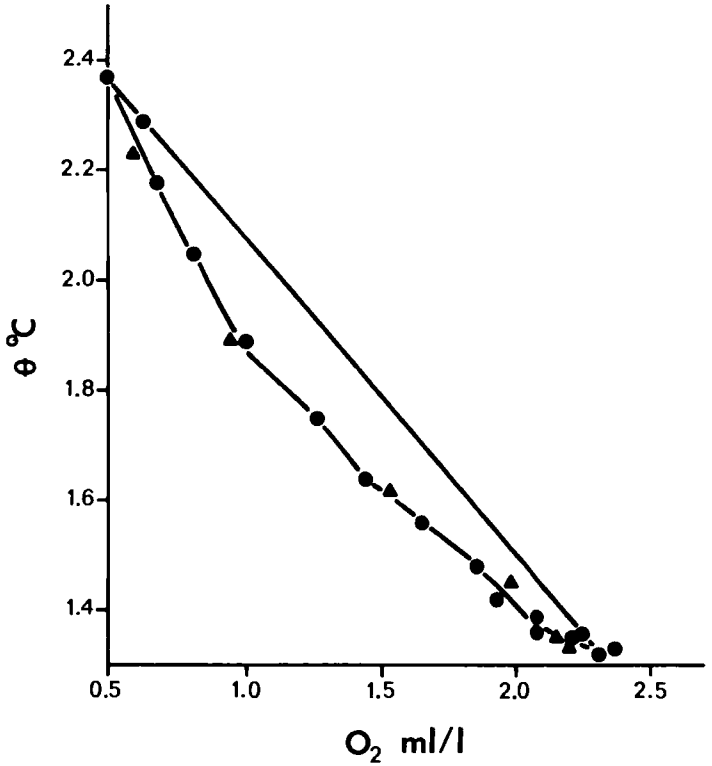

Figure 20. Potential temperature-oxygen (θ-O_2) diagram for the straight portion of the θ-S diagram for stations AAH2 and AAH9. The straight line connects the boundary points.

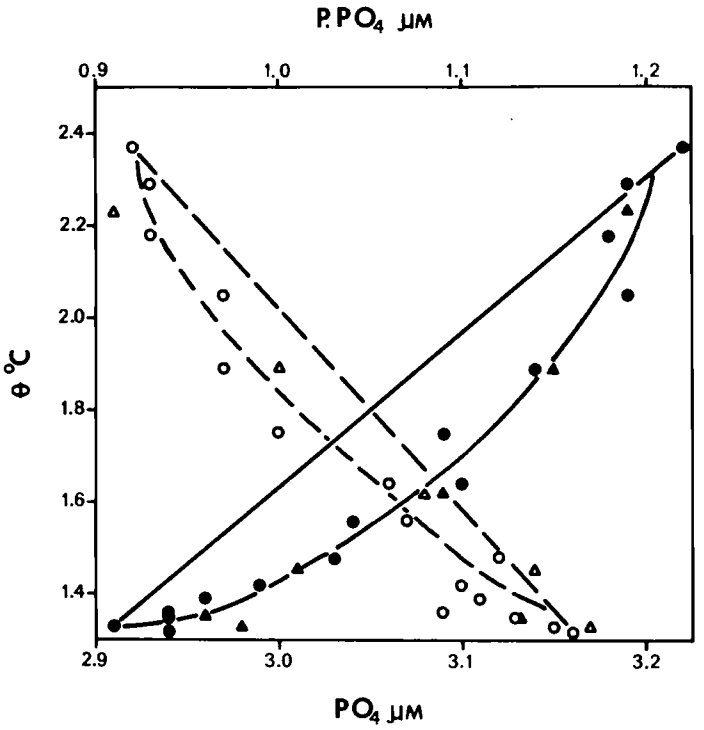

Figure 21. Potential temperature-phosphate (θ-PO_4) and potential temperature-preformed phosphate (θ-P.PO_4) diagrams for the straight portion of the θ-S diagram for stations AAH2 and AAH9. Dark circles and triangles represent PO_4, clear circles and triangles represent P.PO_4. The straight lines connect the boundary points.

Redfield, Ketchum and Richards' (1963) value, since $P.PO_4$ was not determined independently but calculated from equation (11).

The ratio of the θ-O_2 (Figure 20) area to the θ-PO_4 (Figure 21) area is about -4.1 ml/l:1 μM. This is much closer to Redfield, Ketchum and Richards' (1963) value, -3.1 ml/l:1 μM, than the one from the PO_4-O_2 diagram (Figure 19). But the calculated value is still too high. Figure 21 shows that the θ-$P.PO_4$ diagram does not follow a straight line. The precision of $P.PO_4$ is not nearly as high as that of salinity (Pytkowicz and Kester, 1966) but it is statistically significant that most of the data points in the θ-$P.PO_4$ diagram fall to the left of the straight line connecting the boundary points. Since $P.PO_4$ is a conservative quantity (Pytkowicz, 1971) it probably indicates a third water type with temperature and salinity values from the straight line of Figure 18 but with lower $P.PO_4$ value than those of the straight line of the θ-$P.PO_4$ diagram of Figure 21. A straight θ-S diagram is a necessary but not sufficient condition for a two-water type mixing. In other words we probably have three water types A, B and C, as shown in Figure 22, or more than three. $P.PO_4$ is conservative in the same sense salinity is conservative (Pytkowicz and Kester, 1966) in that it is gained or lost only at the sea boundaries, but besides those processes that affect salinity, $P.PO_4$ is gained or lost also because of O_2 air-sea exchange, warming or cooling of surface waters. This can be seen from equations (10) and (11).

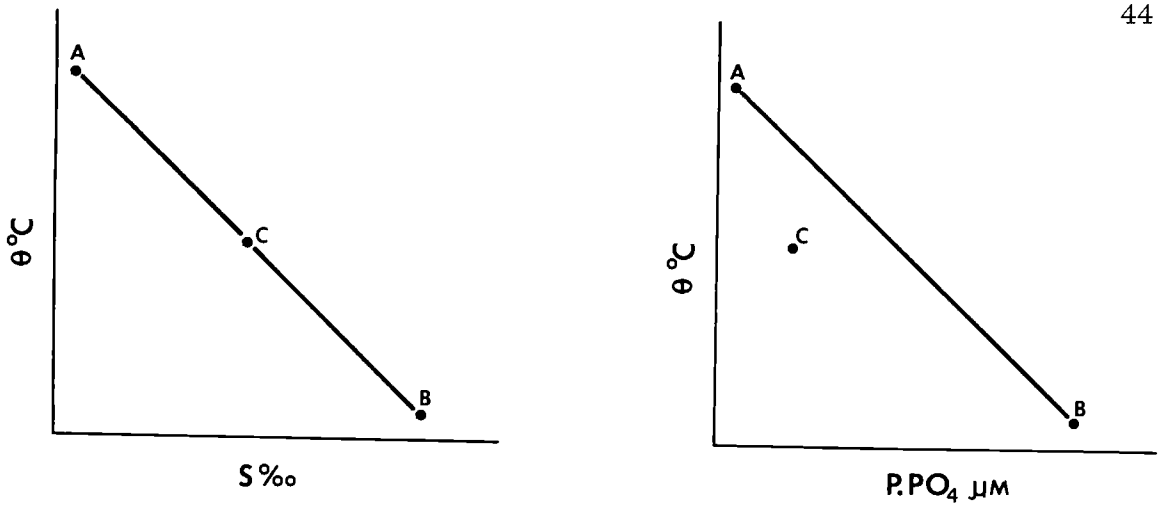

Figure 22. Potential temperature-salinity (θ-S) diagram (a) and potential temperature-preformed phosphate diagram (b). A, B and C represent three water types.

Warming or cooling changes the O_2 solubility, thus changing AOU and $P.PO_4$. Photosynthesis, mixing with deeper waters and upwelling, which cause super or undersaturation with respect to O_2, when coupled with O_2 air-sea exchange cause the $P.PO_4$ to be lost or gained. Without O_2 air-sea exchange these latter phenomena do not affect the $P.PO_4$ differently from the way they affect S‰.

This does not have to be considered when explaining the O_2 distribution by the vertical model as applied by Craig (1971), because the O_2 saturation value when the water mass is at the sea surface does not depend on the $P.PO_4$ values, but on the salinity and temperature of the water, atmospheric pressure, humidity, etc.

The straight line connecting the boundary points of the θ-PO_4 diagram (Figure 21) is supposed to represent the conservative

fraction of PO_4. However the θ-P,PO_4 diagram (Figure 21) is not linear but shows lower P,PO_4 values than those from the linear relationship. Therefore a correction needs to be applied to the θ-PO_4 area before calculating the O_2:PO_4 ratio. This correction consists of adding the θ-P,PO_4 area to the θ-PO_4 area. Since the precision of the calculated values of P,PO_4 is not high consequently the precision of the O_2:PO_4 ratio calculated by this method is not high either. But the main point is demonstrated that by applying this correction the O_2:PO_4 ratio becomes lower. The ratio of the θ-O_2 area (Figure 20) to the sum of the θ-PO_4 and θ-P,PO_4 areas (Figure 21) is about -2.8 ml/l:1 μM, which is closer to Redfield, Ketchum and Richards' (1963) value than the previous two values obtained.

This method to calculate the O_2:PO_4 ratio gives only a point estimation. It does not say anything about the uncertainty of the calculated value. A more valid method, statistically speaking, is to apply a multiple linear regression analysis to our data (Draper and Smith, 1966). We can test the following model to explain the distribution of O_2 as a function of PO_4 and θ°C for the region where the θ-S diagram is a straight line.

$$O_2 = A_I + A_P * PO_4 + A_\theta * \theta \qquad (33)$$

where the A's are constant coefficients, and A_P, in particular, is the O_2:PO_4 ratio. We can statistically test the significance of the values for the different regression coefficients (A's). The conservative

parameter θ explains the changes of O_2 due to mixing, and if A_P is significantly different from zero it means that there is some variation of O_2 due to respiration which has a corresponding variation of PO_4. For the direct application of equation (33) to test Redfield, Ketchum and Richards' (1963) model, we have to have not only a straight θ-S diagram but also a straight θ-P. PO_4 diagram, so that all the "conservative" fraction of PO_4 is represented by the θ term of equation (33), and the PO_4 term only represents the oxidative fraction. Since we do not have a straight θ-P. PO_4 diagram (Figure 21) the application of equation (33) to test Redfield, Ketchum and Richards' (1963) model is only a first approximation, but it is at least statistically more valid than the method applied above.

The multiple linear regression analysis is a least square fit to the given data. The fitting was accomplished by a computer program (SIPS) (Oregon State University, Department of Statistics, 1971). It computes a sequence of multiple linear regression equations in a stepwise manner. At each step one variable is added to the regression equation so that the contribution of each variable to the regression can be evaluated.

The result was found to be as follows:

$$O_2 = 13.2 - 3.4\ (PO_4) - 0.85(\theta) \qquad (34)$$

At the 95% confidence level the interval for A_P is -3.4 ± 1.0. The value -3.4 is closer to Redfield, Ketchum and Richards' (1963) value

of -3.1 than the one obtained by using the area ratio above, without correcting for the θ-P.PO_4 non-linearity. The precision of the A_P value (± 1.0) is too large. Probably this is due to the fact that for the region where the θ-S diagram is straight the range for the O_2 and PO_4 values is not large. For this region PO_4 only changes by about 0.3 μM and O_2 only changes by about 2 ml/l. We need more precise determinations of PO_4 and O_2 when we look at small differences like these.

We did not apply this method to calculate the O_2:NO_3 and O_2:SiO_2 ratios because the NO_3 and SiO_2 systems are more complicated to interpret. Oxidation of NO_2 and NH_3 to NO_3 and non-oxidative dissolution of inorganic SiO_2 with depth make the calculations of preformed-NO_3 and preformed-SiO_2 more complex, if not impossible, without gross assumptions. Figure 16 shows more scattering in the AOU-NO_3 diagram than in the AOU-PO_4 diagram. The curve relationship between AOU and SiO_2, as shown by Figure 16, is due to dissolution of inorganic SiO_2 with depth.

pH, CO_2-system

Alkalinity is lower and "in situ" pH is higher (Figures 10 and 23) at the eastern part of the section than at the western part in the surface waters. This is probably the result of continental runoff, as stated above. The "in situ" pH minimum (Figure 23) is at about the

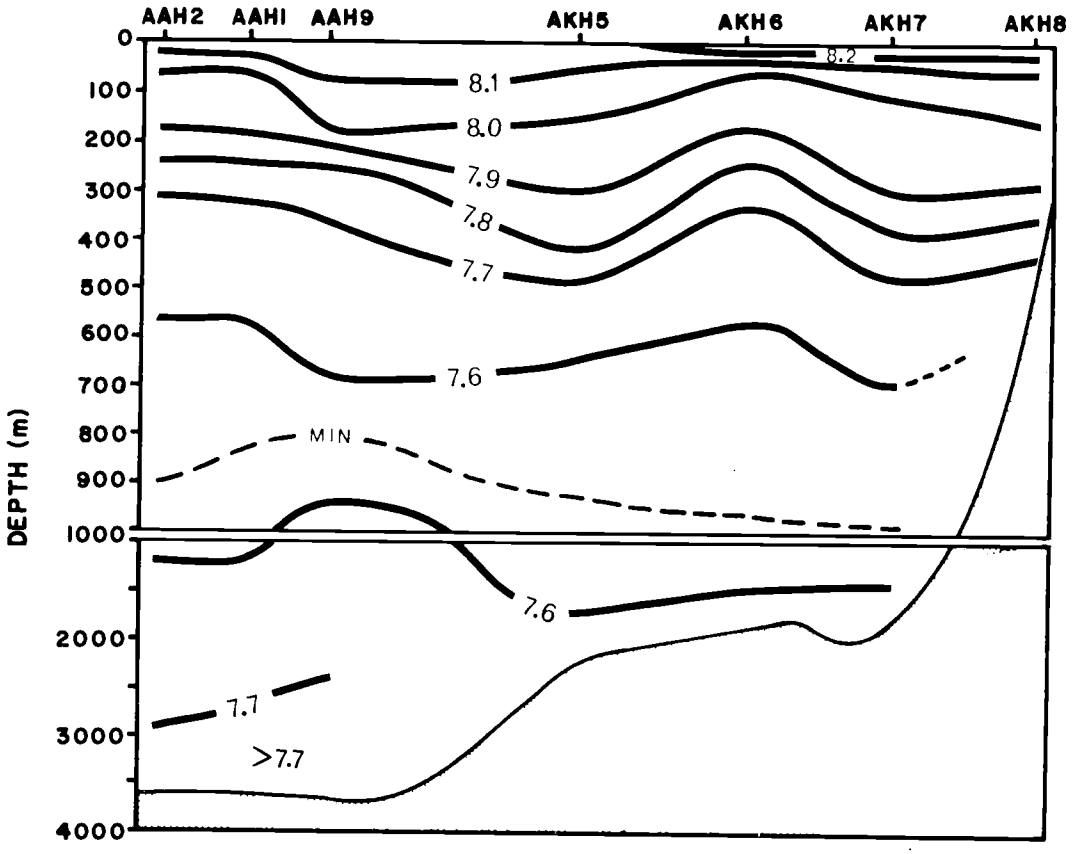

Figure 23. Vertical distribution of "in situ" pH.

same depth as the O_2 minimum, with values of less than 7.6.

The alkalinity:chlorinity ratio (Figure 24) increases monotonically with depth from about 0.128 in the surface waters to more than 0.132 in the deep waters. Since we measure salinity instead of chlorinity, during oceanographic cruises, it is more proper to calculate alkalinity:salinity ratio than to calculate alkalinity:chlorinity ratio. But we calculated alkalinity:chlorinity ratio to compare our results with Ivanenkov's (1964). Ivanenkov (1964) reports somewhat lower values for the Western Bering Sea, 0.126 for surface waters

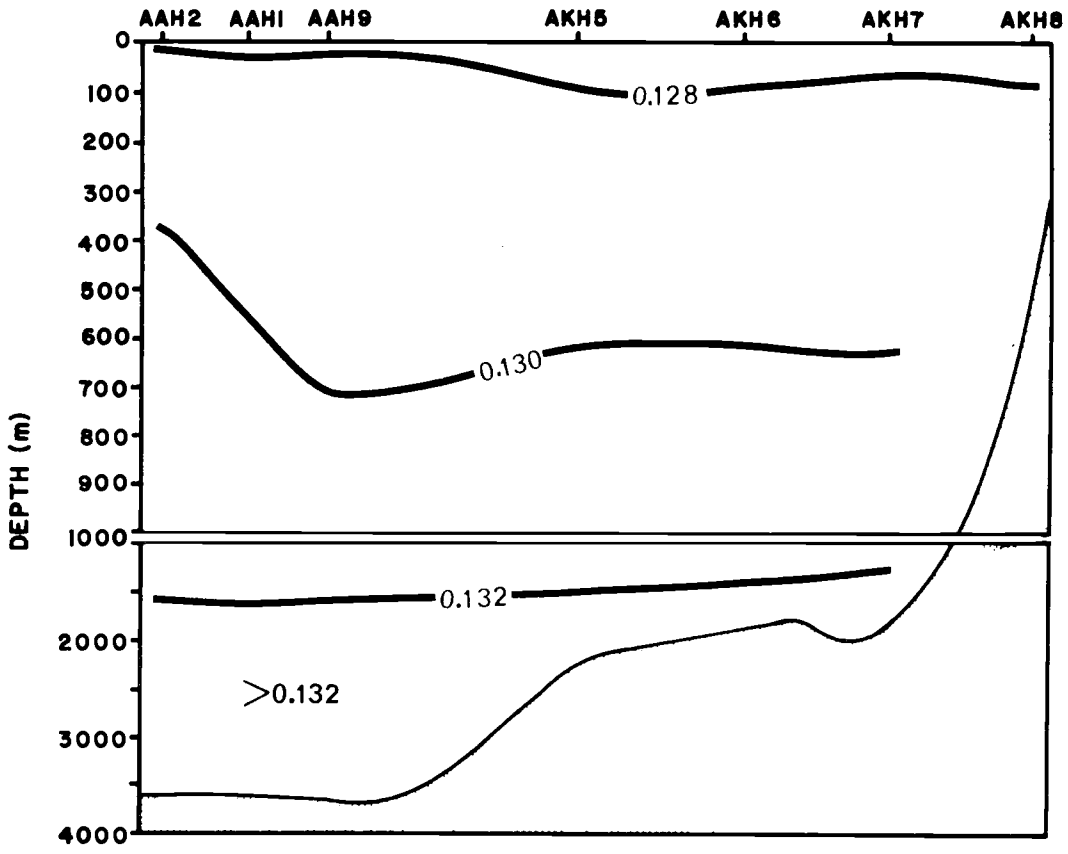

Figure 24. Vertical distribution of alkalinity-chlorinity ratio (meq/l:‰).

and 0.131 for deep waters. But, since the precision of the calculated values of the alkalinity:chlorinity ratio is ± 1-2%, the ranges for his values and our values overlap. In both cases there is an increase of about 0.005 in the ratio from shallow to deep waters. This increase corresponds to a hypothetical $CaCO_3$ dissolution of 0.05 mM of $CaCO_3$ to the surface water to obtain the deep-water alkalinity: chlorinity ratio.

The atmospheric P_{CO_2} was not measured during YALOC-66

but very likely it was near 320 ppm. Kelley, Longerich and Hood (1971) report that for the southeastern region of the Bering Sea the values of the atmospheric P_{CO_2} were 327 ppm during June and 314 ppm during September of 1970. According to Kelley (1968) this type of decrease in the atmospheric P_{CO_2} is due to uptake of CO_2 from the atmosphere during the summer plant bloom. In Figure 25 the 320 ppm isogram for sea water is shown by a dashed line. Surface waters were shown to be undersaturated with respect to CO_2 (Figure 25) at station AAH9 and from station AKH6 to the east, and

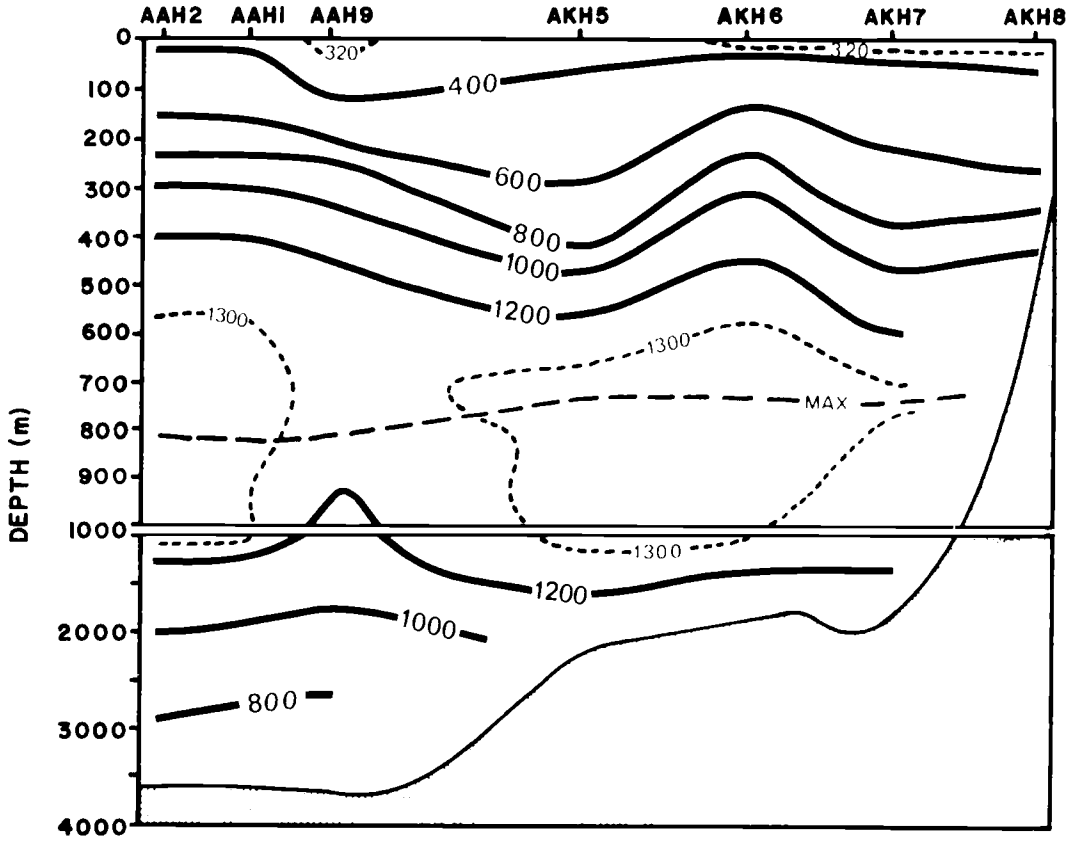

Figure 25. Vertical distribution of the "in situ" partial pressure of carbon dioxide (ppm).

supersaturated everywhere else in the section. Gordon, Park, Hager and Parsons (1971) (and previous authors cited therein) have shown that rarely is surface sea water in equilibrium with the atmosphere with respect to CO_2. The surface pH and P_{CO_2} values (Figures 23 and 25) correlate very well, with high values of pH where the P_{CO_2} is low and vice versa. At station AAH9, where P_{CO_2} is low, there is a high surface pH value of 8.19, although it is not shown in Figure 23. The low P_{CO_2} surface values at the eastern part of the section are also due to the low alkalinity values (Figure 10). At this part of the section low P_{CO_2} values also correlate with O_2 values higher than 7.5 ml/l (Figures 5 and 25).

Although not shown in Figure 25 the highest P_{CO_2} surface value, 380 ppm, was found at station AAH1. Gordon, Park, Hager and Parsons (1971) report a maximum value of about 400 ppm south of the Aleutian chain near 47°N, 170°E, during March-April, 1969. Miyake and Sugimura (1969) found a high correlation between the P_{CO_2} of surface waters and the depth of the pycnocline between Japan and Antarctica; this indicates that vertical mixing of the water column affects considerably the surface P_{CO_2} values.

The P_{CO_2} maximum of about 1300 ppm was found at 800 m at AAH2 and gradually decreasing in depth eastward to about 700 m at AKH7.

Figures 26 and 27 show the vertical distribution of the percent

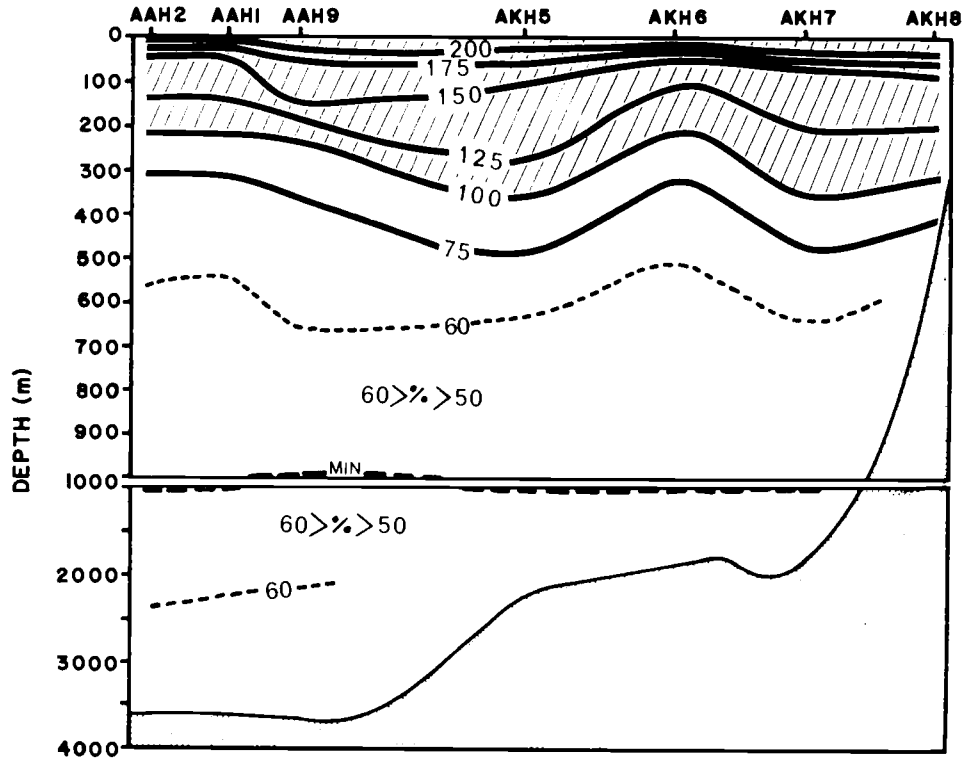

Figure 26. Vertical distribution of the percent saturation of calcite.

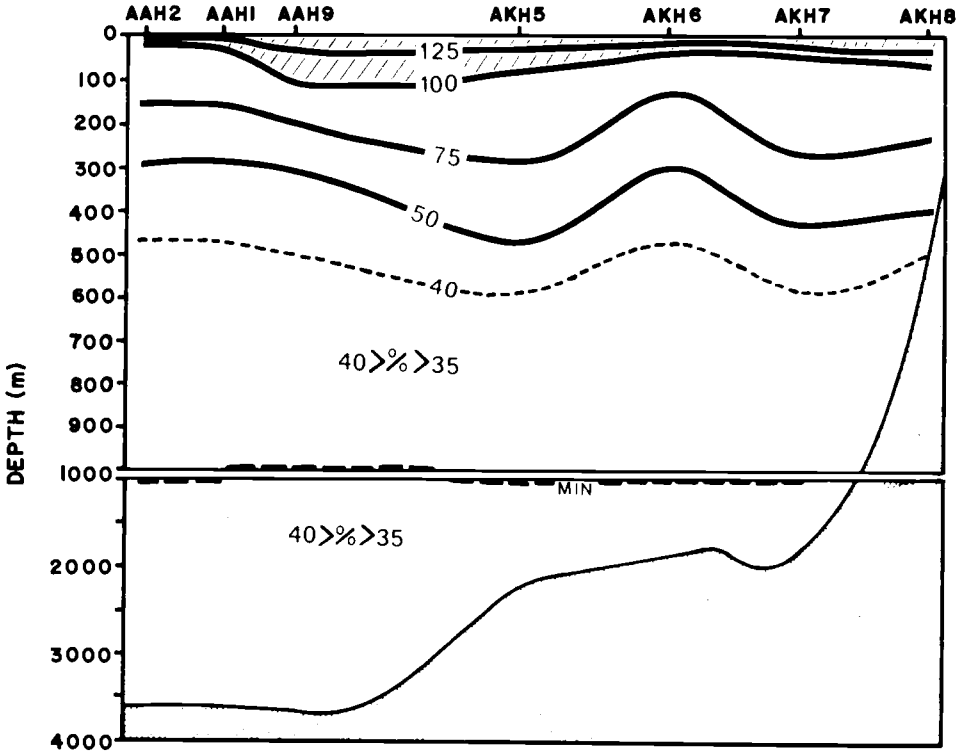

Figure 27. Vertical distribution of the percent saturation of aragonite.

saturation of sea water with respect to calcite and aragonite, respectively. The upper layer is supersaturated from the sea surface to about 250 m with calcite, and to about 100 m with aragonite. Below these depths sea water is undersaturated with respect to these two minerals, with minima at 1000 m. The saturations at the minima are 55% for calcite and 35% for aragonite. In the deep waters the saturation of calcite is about 60% and that of aragonite is about 40%.

There has been controversy concerning estimates of calcium carbonate saturation by different methods. Recently Ben-Yaakov and Kaplan (1971) have developed a technique to measure the degree of saturation of sea water with respect to calcium carbonate "in situ." They present a comparison of calcite saturation profiles around latitude 30°N in the Pacific Ocean obtained by different authors. Their results are in disagreement with those of Lyahkin (1968), Hawley and Pytkowicz (1969) and Li, Takahashi and Broecker (1969). Our method of estimating the percent saturation of calcium carbonate is essentially the same as that of Hawley and Pytkowicz (1969). The results of Lyahkin (1968) and Hawley and Pytkowicz (1969) are essentially in good agreement for deep waters (i.e. below 1000 m). They used very much the same method for their estimations. The results of Li, Takahashi and Broecker (1969) show that sea water is undersaturated with respect to calcite only below about 2500 m; they calculated the percent saturation of calcite from field measurements

of P_{CO_2} and ΣCO_2. Ben-Yaakov and Kaplan's (1971) direct measurements show that sea water becomes undersaturated with respect to calcite at approximately 400 m and remains so to a depth of about 1600 m where it is saturated, then below 2500 m it appears to be undersaturated again.

Further studies are needed to solve this controversy. Either something is wrong with the data obtained at sea, or something is wrong with the literature values of the dissociation constants of carbonic acid, or the solubility of calcium carbonate, used in indirect estimations.

In Figure 4 of Ben-Yaakov and Kaplan's (1971) paper the profile for the results of Hawley and Pytkowicz (1969) is not shown completely, and some important features are missing, tending to give the impression that their results are different from those of Ben-Yaakov not only in the absolute values but also in their behavior with depth. We have drawn the profile here, using the calculated data from table 3 of Hawley and Pytkowicz (1969) (Figure 28), together with one from YALOC-70 cruise to show that, as Hawley and Pytkowicz (1969) say in their text, there is a minimum and a maximum in the profile, as in the case of Ben-Yaakov and Kaplan's (1971) results. These extrema are explained by Hawley and Pytkowicz (1969) in terms of the concurrent effect of pH and pressure. Alvarez-Borrego (1970) showed that by shifting the pH values up by as much as 0.2 of a pH unit the

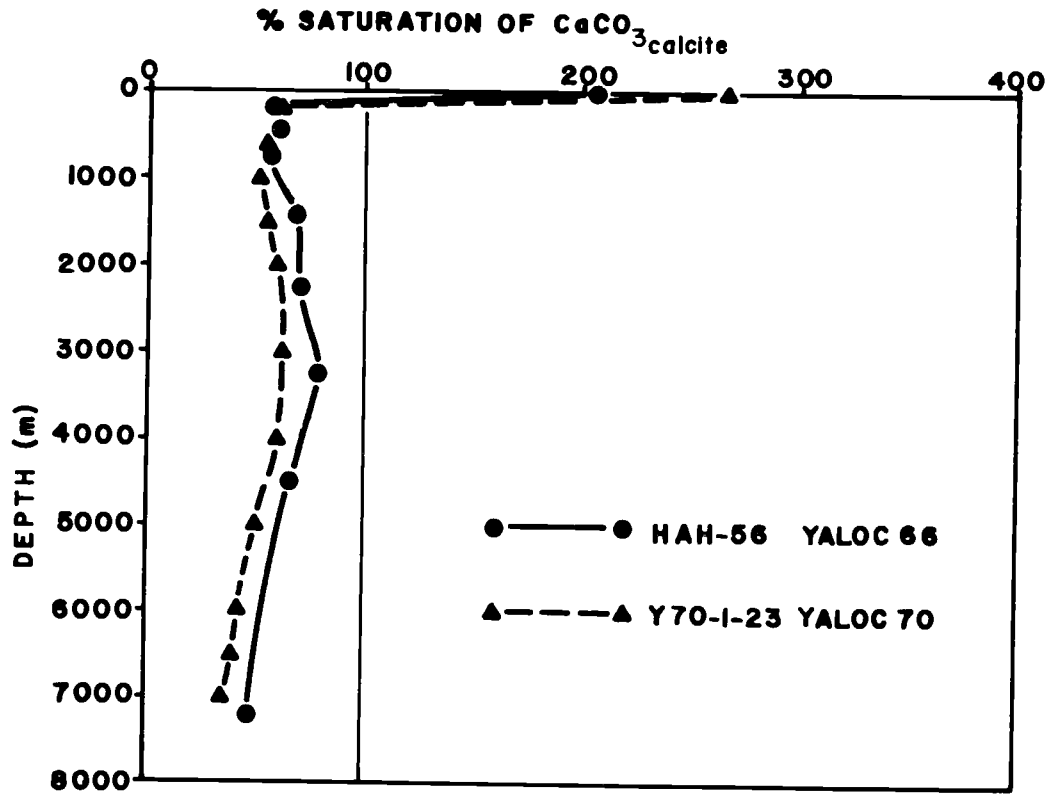

Figure 28. Vertical profiles of the percent saturation of calcite at stations HAH56 of YALOC-66 cruise (data from table 3 of Hawley and Pytkowicz, 1969) (50°27.5'N, 176°13.8'W) and Y70-1-23 of YALOC-70 cruise (45°00.0'N, 174°02.6'E).

whole profile for calcite is shifted towards saturation with similar results to those obtained by Ben-Yaakov and Kaplan (1971), in this area of the ocean. That is a very high increment for the pH, which indicates that if our method is incorrect and Ben-Yaakov and Kaplan's (1971) is correct, it is not because of faulty pH data, but because of failures in the literature data and a revision of the values of the different constants involved in the calculations would be necessary.

Pytkowicz (1972) indicates that definitive work on the solubility of calcium carbonate in sea water will have to take cognizance of the

history and nature of the samples used, because of the effect of adsorption of other ions such as magnesium (Berner, 1966; Weyl, 1967; Pytkowicz and Fowler, 1967). In general, hysteresis effects which strongly affect the solution behavior of pure calcite (Weyl, 1967) such as was used by Ben-Yaakov and Kaplan (1971), should be carefully examined in the laboratory before what may seem to be obviously direct field data are interpreted. Frank Millero of the University of Miami and Robert Berner of Yale University (personal communications) concluded from partial molal volume estimates that sea water is even more undersaturated than our results indicate, instead of being more saturated as was observed by Ben-Yaakov and Kaplan (1971). The differences between the various sets of results may be the consequence of the pretreatment of samples, their history, and the adsorption of impurities.

Figure 29 shows the relationship between pH (at 25° C and one atmosphere) and AOU, pH and alkalinity, and AOU and TCO_2, for the whole water column, at the seven stations under consideration. Using data from YALOC-66 cruise Park (1968) stated that the two major processes that affect the vertical distribution of apparent pH (the pH measured by using glass and calomel electrodes, at 25° C and one atmosphere pressure) in the Subarctic region of the Northeastern Pacific Ocean are apparent oxygen utilization by marine organisms and carbonate dissolution, the effect of the first being

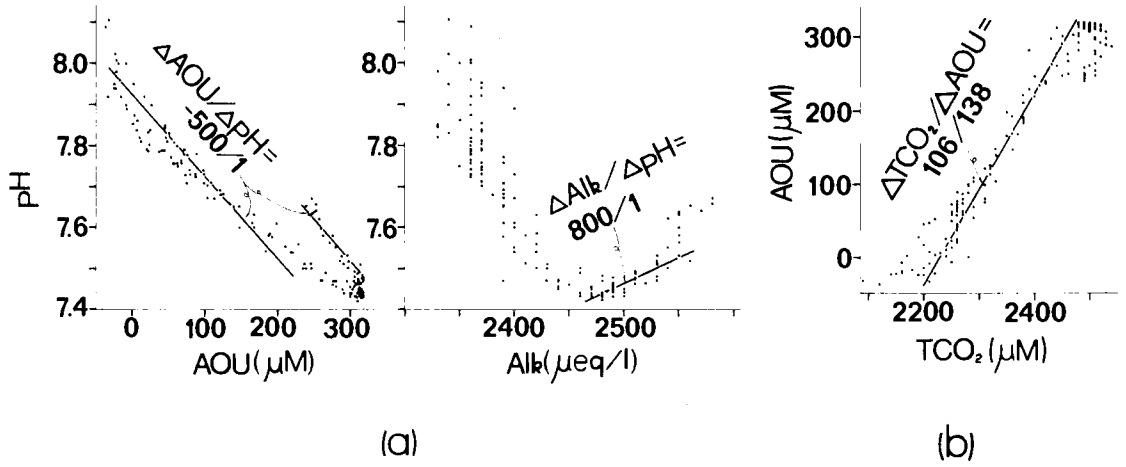

Figure 29. pH (at 25° C and one atmosphere)-apparent oxygen utilization, and pH-alkalinity relationships (a); and apparent oxygen utilization-total carbon dioxide relationship (b). The straight lines do not represent the data points, they are lines with slopes as proposed by Park (1968) (a), and as proposed by Redfield, Ketchum and Richards (1963) (b).

much greater than that of the second. In Figure 29a we have drawn lines with slopes as proposed by Park (1968). The lines do not represent the data points, they are to be taken as a frame of reference to compare Park's (1968) model to our data. In Figure 29a the data points showing the pH-AOU relationship follow a curve trajectory. At the pH minimum this trajectory has a zero slope. This is not inconsistent with the model of Redfield, Ketchum and Richards (1963) used by Park (1968) to express the relationship between pH and AOU. The effect is a result of calcium carbonate dissolution.

Since alkalinity changes as a function of salinity, the ratio ΔAlk:ΔpH does not correspond exactly to the ratio $\Delta CO_3^{=}$:ΔpH, but, as

a first approximation, we have drawn the line for the alkalinity-pH relationship as if the changes of alkalinity were only due to carbonate dissolution. This serves the purpose of showing that the greater effect of alkalinity on apparent pH is at the region where the calcium carbonate degree of saturation with respect to calcite and aragonite is minimum (Figures 26, 27 and 29a). In Figure 29b we have drawn a line with a slope according to the model of Redfield, Ketchum and Richards (1963). Culberson and Pytkowicz (1970) have shown that when changes in TCO_2 due to all the processes other than oxidation are compensated for, linear correlations between AOU and TCO_2 with essentially the slope predicted by Redfield, Ketchum and Richards (1963) are found.

Conclusions

The horizontal distribution of O_2 at 2000 m and 2500 m depth throughout the Bering Sea, as presented by Ivanenkov (1964), indicates that deep water is flowing from the Pacific Ocean, through the Kamchatka Strait, and then northward and eastward in the Bering Sea. This is in disagreement with the results obtained by Arsen'ev (1967) who calculated geostrophic flow at the 2000 db surface relative to the 3000 db surface. But, as Favorite (1972) states, there are still questions concerning not only how well the averaged data that Arsen'ev (1967) used denote actual conditions, but also whether or not geostrophic

flow is a good indicator of actual circulation in the Bering Sea. Further studies are needed to solve this problem.

Based on the O_2 distribution it is estimated that it takes roughly 20 years for the water to move from the Kamchatka Strait to the farthest parts of the basins, at 2000 m depth; and, at 2500 m depth, it takes about 20 years for the water to move from the Kamchatka Strait to the southeastern part of the eastern basin, and about 30 years to move from the Kamchatka Strait to the northern part of the eastern and western basins.

In the upper 1000 m, sigma-t shows a wavy distribution. In general the isograms of the different chemical parameters follow the same pattern as the sigma-t isograms.

The surface concentration of nutrients is higher in the Bering Sea than in the North Pacific Ocean, probably because of upwelling and intense vertical mixing in the Bering Sea. The vertical distribution of nutrients in the deep waters of the Southeastern Bering Sea is very nearly the same as in the deep waters of the North Pacific Ocean, with similar levels of concentration, probably because it is the same deep Pacific water mass.

It is shown "a priori" that whenever mixing occurs between two water types a straight PO_4-O_2 diagram is only to be expected when the two component lines, the one generated by mixing and the one generated by oxidation, have the same slope. In the case of the

PO_4-AOU diagram this condition is satisfied by having the same P.PO_4 concentration in the two water types. The PO_4-AOU diagram for a portion of the water column would be straight only when P.PO_4 is constant or, by chance, the P.PO_4-AOU diagram is straight for that portion of the water column. The latter seems to be the case for the Southeastern Bering Sea. Straight P.PO_4-AOU, and consequently PO_4-AOU, diagrams were found for the region where the AOU values are higher than $\sim$100 μM (deeper than $\sim$ 200 m).

A multivariable regression analysis of O_2 as a function of PO_4 and θ°C was applied for the region where the θ°C-S‰ diagram is straight in stations AAH2 and AAH9; and the confidence interval of the PO_4 coefficient, at the 95% probability level, -3.4 ± 1.0, was found consistent with the model of Redfield, Ketchum and Richards (1963).

The "in situ" P_{CO_2} maximum with values of about 1300 ppm is located near 800 m depth. The calcium carbonate saturation calculations show that the Bering Sea is supersaturated with aragonite in the upper 100 m, and with calcite in the upper 250 m. Below these depths sea water is undersaturated with respect to these two minerals, with minima at 1000 m. The percent saturation at the minima are 55% for calcite and 35% for aragonite. There is at present controversy concerning the results of calcium carbonate saturation determinations by different methods. A further definitive study is needed to solve this controversy.

III. OXYGEN-NUTRIENT RELATIONSHIPS IN THE PACIFIC OCEAN

When biological oxidation of organic matter occurs in the oceans, coupled with physical and geochemical processes, the concentrations of dissolved oxygen (O_2) nutrients (PO_4, NO_3, SiO_2, etc.), and total inorganic carbon dioxide (ΣCO_2), vary in a complicated way. Redfield (1934) proposed a model to explain the proportions of organic derivatives in sea water based on O_2, PO_4, NO_3 and ΣCO_2 data from the western Atlantic Ocean and on the composition of plankton. Although there have been some modifications to the model since Redfield proposed it in 1934, we will call it, in this work, Redfield's model. The model is based on the assumption that, when biological oxidation occurs, the ratios of the consumption of dissolved oxygen to the production of nutrients and carbon dioxide are constant. So that, if we want to know the contribution of biological oxidation to the concentration of nutrients and total inorganic carbon dioxide, we need only calculate the amount of dissolved oxygen that has been utilized and multiply it by the respective constants associated with each of the nutrients and the inorganic carbon dioxide. Simple as it may seem at first, there have been misinterpretations of the model due to failures in properly considering all non-biological factors when testing it with field data.

Riley (1951) estimated the oxidative ratios (O_2 consumption to

PO_4 regeneration, etc.) for ocean water and found them to vary with depth. According to Redfield, Ketchum and Richards (1963) this was due to Riley (1951) not taking into consideration the variation of preformed nutrients (Redfield, 1942) with depth.

Postma (1964) plotted measured dissolved oxygen concentrations (O_2) versus measured phosphate concentrations (PO_4) using data from stations at different latitudes (55°N to 62°S) in the Pacific Ocean, and did not find a constant ΔO_2:ΔPO_4 ratio with depth. Pytkowicz (1964) and Park (1967a) using data from off the Oregon coast, plotted O_2 versus PO_4 and found a linear relationship above the O_2 minimum zone with a ΔO_2:ΔPO_4 ratio near the value predicted by Redfield's model. Pytkowicz (1964) concluded from theoretical considerations that when mixing occurs between two water types the O_2-PO_4 relationship is linear only when the proportions (f_z) of the two water types in the mixture is the same at all depths. Alvarez-Borrego, Gordon, Jones, Park and Pytkowicz (1972) have shown "a priori" that, if the ΔPO_4:ΔO_2 ratio is constant for the biological oxidation, whenever mixing occurs between two water types a straight PO_4-O_2 diagram is only to be expected when two component lines, one generated by mixing and the other generated by oxidation, have the same slope. This condition is satisfied by either having f_z constant with depth or by having ($P.PO_4 + a_R O'_2$) constant with depth; where $P.PO_4$ is the preformed phosphate, a_R is the ΔPO_4:ΔO_2 ratio for the biological oxidation, and O'_2 is the

concentration of dissolved oxygen at saturation. The second case is more likely. Alvarez-Borrego, Gordon, Jones, Park and Pytkowicz (1972) also showed that when mixing occurs between n water types the phosphate versus apparent oxygen utilization (PO_4-AOU) diagram is linear if the P.PO_4 concentrations in all n water types is the same, or if by chance the P.PO_4-AOU diagram is linear.

Postma (1964) and Craig (1969) questioned the validity of Redfield's model because they did not find a linear relationship between O_2 and ΣCO_2. But Culberson and Pytkowicz (1970) have shown that when changes in ΣCO_2 due to all the processes other than oxidation are compensated for, linear relationships between AOU and ΣCO_2 with essentially the slope predicted by Redfield's model are found. Using multiple regression analysis Ben-Yaakov (1971) has shown that there is a linear relation between ΣCO_2, total alkalinity and temperature along vertical profiles in the Eastern Pacific, and that the confidence interval of the regression coefficient for oxygen, at the 95% confidence level, is consistent with Redfield's model. Culberson (1972) showed that the vertical and horizontal distribution of ΣCO_2 in the Pacific, Indian, and South Atlantic Oceans conform to Redfield's model.

Alvarez-Borrego, Gordon, Jones, Park and Pytkowicz (1972) applied multiple regression analysis to express O_2 as a function of PO_4 and potential temperature (θ° C), for the region in the Southeastern

Bering Sea where the θ°C-S‰ diagram is straight; the confidence interval of the PO_4 regression coefficient, at the 95% confidence level, was found consistent with Redfield's model. They indicate that, since the θ°C-P. PO_4 diagram is not a straight line for that portion of the water column, the application of their regression equation to test Redfield's model is only a first approximation.

Theoretically, the best way to test Redfield's model would be to plot the utilization of dissolved oxygen versus the increase in the concentration of nutrients and ΣCO_2 arising from biological oxidation. Since there are not yet methods to measure these changes directly, only approximations can be made, and in the case of the nutrients these changes cannot yet be calculated independently of Redfield's model. As Pytkowicz (1971) states, a plot of AOU versus nutrients is not a proper test of Redfield's model because the preformed nutrients may vary with depth.

The purpose of this work is to study the O_2-PO_4 and O_2-NO_3 relationships for different parts of the ocean, with special attention to the Northeastern Pacific Ocean and Southeastern Bering Sea, and to test Redfield's model for these relationships. To test the model multiple regression analysis is applied to the field data. After the field data are found to be consistent with the model, the model is used to calculate preformed nutrients. Preformed nutrients versus θ°C diagrams are then used to detect water masses that are not very well

identified by θ°C-S‰ diagrams.

Sources of data

For this study we used salinity, temperature, oxygen, phosphate and nitrate data from stations 3801 and 3804 of the 26th cruise of VITYAZ (November, 1957) in the Central Pacific Ocean (National Oceanographic Data Center); from several stations of R/V ANTON BRUUN cruise 2 (May-July, 1964) in the Indian Ocean (WHOI, 1964); from station 116 of the BOREAS expedition (winter, 1966) (SIO, reference 66-24) in the Subarctic Pacific region; from several stations of YALOC-66 (summer, 1966) (Barstow, Gilbert, Park, Still and Wyatt, 1968) from Hawaii to Adak, Alaska, and the Southeastern Bering Sea; from several station of the SCORPIO expedition (May, 1967) (SIO, reference 69-15; WHOI, reference 59-45) in the South Pacific Ocean; from stations 34 and 35 of the SOUTHERN CROSS cruise (December, 1968) (Horibe, 1970) off New Zealand; from a GEOSECS intercalibration and test station (summer, 1970) (Spencer, 1970; unpublished manuscript) in the Atlantic Ocean; and from station GOGO-1 of a GEOSECS intercalibration and test cruise (November, 1971) (unpublished data taken by Oregon State University's chemical oceanography group) off California. The positions of these stations are shown in Figures 30 and 31.

Nutrient determinations for GOGO-1 were made by a Technicon

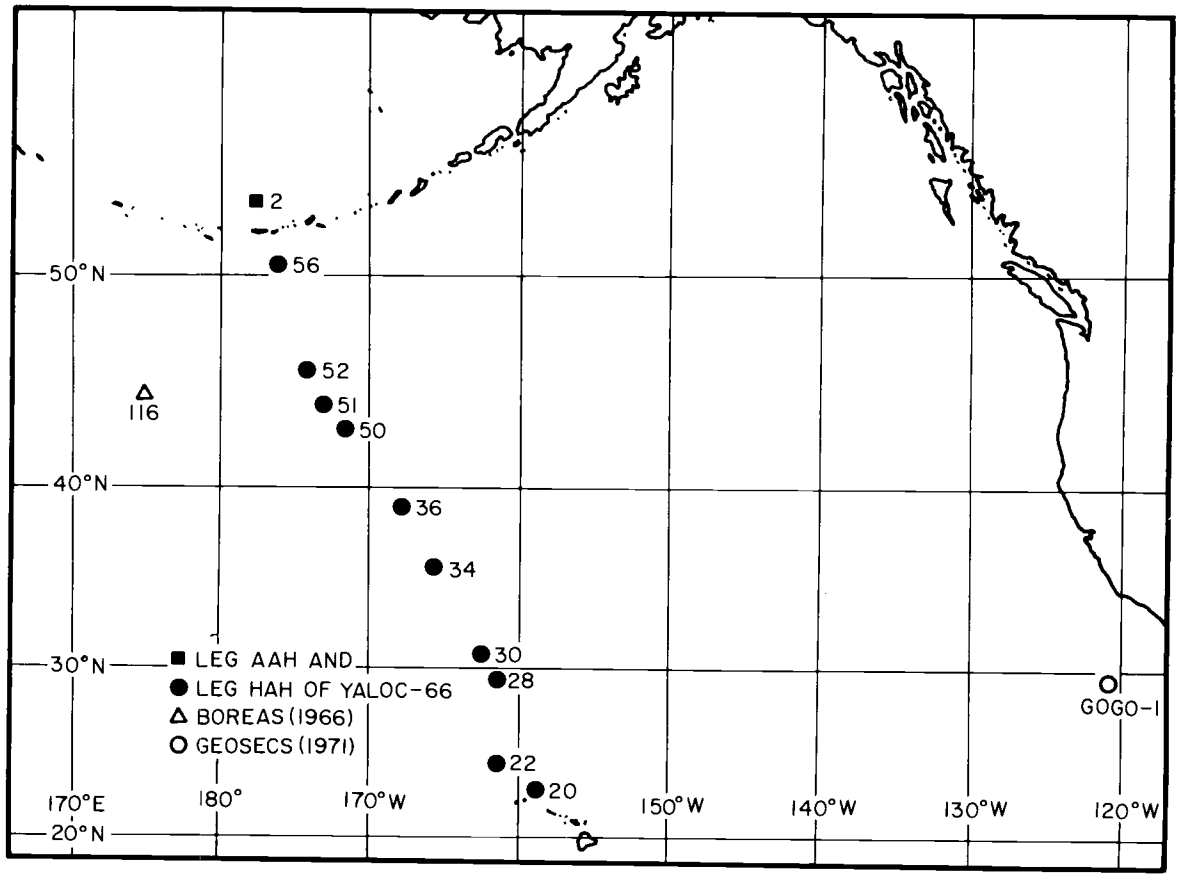

Figure 30. Location of station GOGO-1, station 116 of BOREAS expedition and the stations from YALOC-66 that were used in this study.

AutoAnalyzer® (AA-II, basic industrial model), and the determinations of all three nutrients (PO_4, NO_3 and SiO_2) have a precision of ±1% or better.

Results

In the Northeastern Pacific Ocean the O_2-PO_4 and O_2-NO_3 relationships for the region of the water column above the O_2 minimum zone vary systematically with latitude (Figures 32 and 33). A similar but less pronounced variation is found below the O_2 minimum

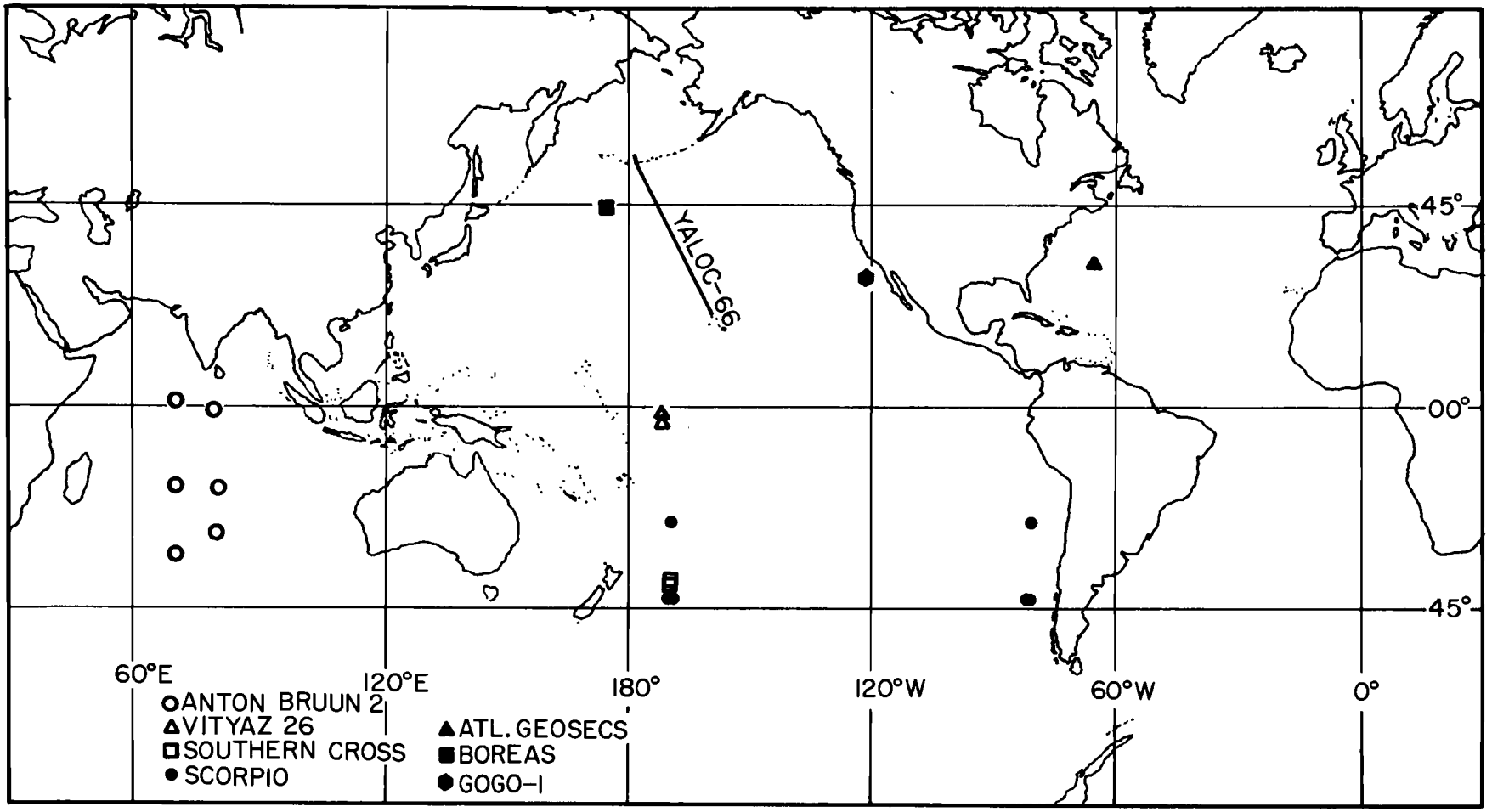

Figure 31. Location of station GOGO-1, the Atlantic GEOSECS intercalibration station, and the stations from the 26th expedition of the VITYAZ, the ANTON BRUUN cruise 2, the BOREAS expedition, the SOUTHERN CROSS cruise, and the SCORPIO expedition that were used in this study.

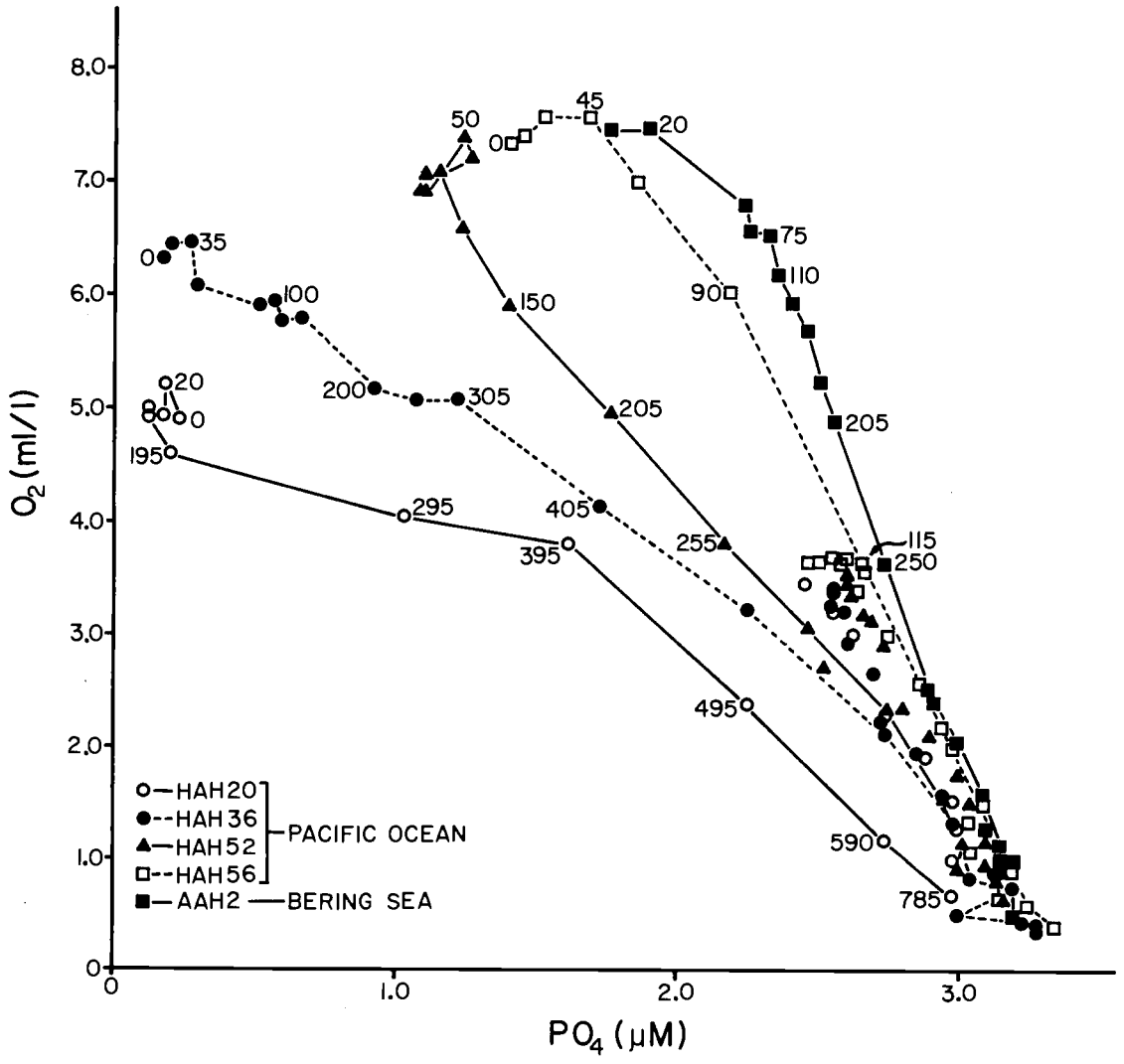

Figure 32. Oxygen-phosphate diagram. The numbers by the data points represent depth in meters. The lines are joining the data points above the oxygen minimum zone. The positions of the stations are: HAH20 (22°53.8'N, 158°54.7'W), HAH36 (38°53.3'N, 168°13.6'W), HAH52 (45°52.8'N, 174°02.3'W), HAH56 (50°27.5'N, 176°13.8'W), AAH2 (52°56.1'N, 177°55.0'W).

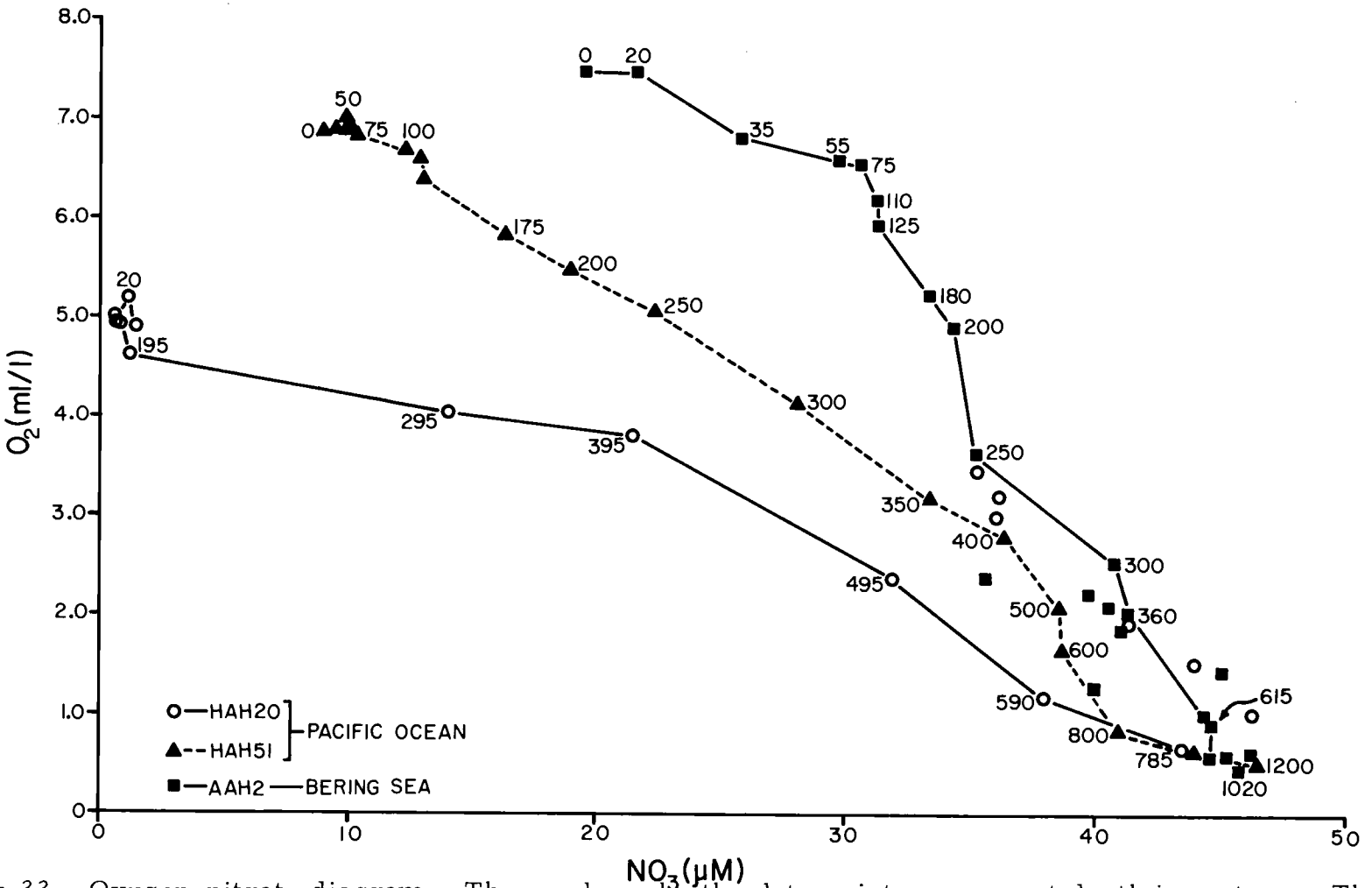

Figure 33. Oxygen-nitrate diagram. The numbers by the data points represent depth in meters. The lines are joining the data points above the oxygen minimum zone. The positions of the stations are: HAH20 (22°53.8'N, 158°54.7'W), HAH51 (44°17.0'N, 173°06.3'W), AAH2 (52°56.1'N, 177°55.0'W).

zone (Figures 34 and 35). The slopes of these relationships in general increase with increasing latitude. In the entire water column, these slopes vary with depth (Figures 32 and 33). An effect on the slopes of the O_2-PO_4 and O_2-NO_3 relationships, similar to that observed when decreasing latitude, is observed when comparing winter versus summer data. The winter slopes are higher than the summer slopes (Figures 36 and 37).

The slope of the NO_3-PO_4 relationship for the region of the water column above the O_2 minimum zone also changes with latitude but in a much less pronounced way than the slopes for the O_2-PO_4 and O_2-NO_3 relationships (Figure 38). Below the O_2 minimum zone there is a pronounced variation of the NO_3-PO_4 relationship with latitude (Figure 39). The summer value for the NO_3-PO_4 slope is higher than the winter value (Figure 40).

These variations of the O_2-PO_4, O_2-NO_3 and NO_3-PO_4 slopes were estimated by applying the least-squares method to the O_2, PO_4 and NO_3 field data. The confidence intervals were estimated at the 95% confidence level. O_2 is expressed in ml/l and PO_4 and NO_3 in μM. Above the O_2 minimum zone the slope of the O_2-PO_4 diagram varies from -1.40 ± 0.20 near Hawaii, to -5.26 ± 0.70 in the Southeastern Bering Sea (Figure 32); the slope of the O_2-NO_3 diagram varies from -0.095 ± 0.014 near Hawaii, to -0.278 ± 0.060 in the Southeastern Bering Sea (Figure 33); and the slope of the NO_3-PO_4

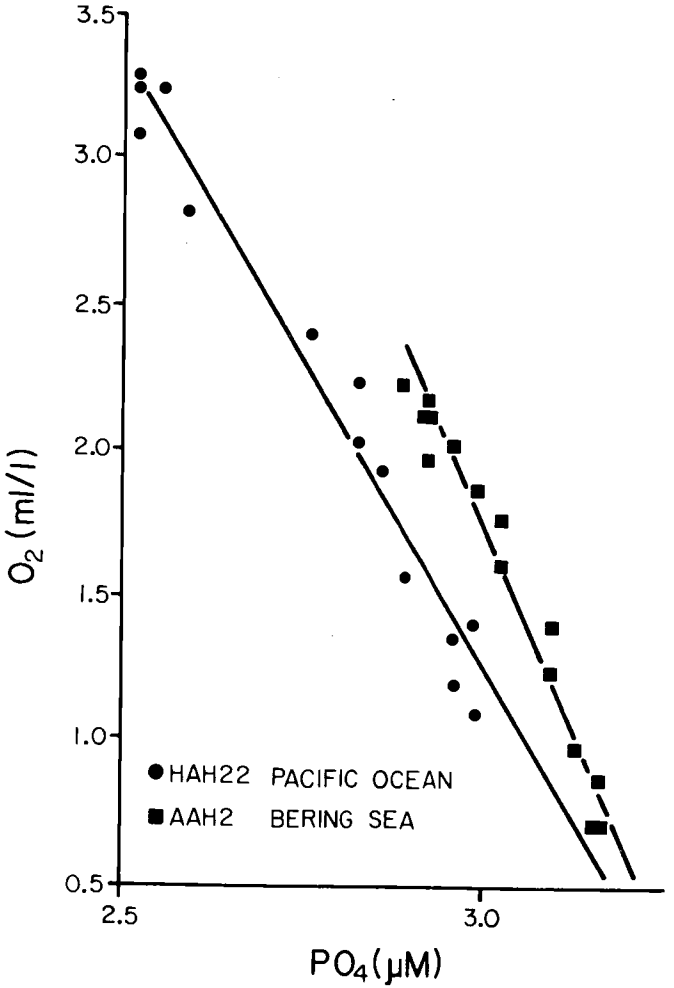

Figure 34. Oxygen-phosphate diagram for the region of the water column below the oxygen minimum zone. The lines are the least squares fits. The positions of the stations are: HAH22 (24°30.6'N, 161°30.0'W), AAH2 (52°56.1'N, 177°55.0'W).

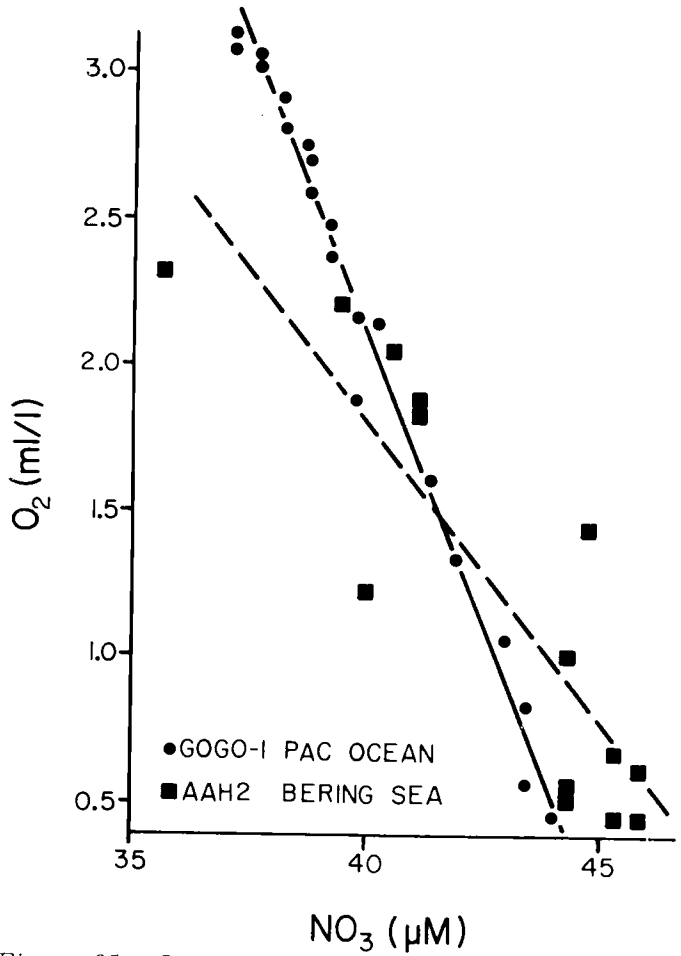

Figure 35. Oxygen-nitrate diagram for the region of the water column below the oxygen minimum zone. The lines are the least squares fits. The positions of the stations are: GOGO-1 (28°29.0'N, 121°38.0'W), AAH2 (52°56.1'N, 177°55.0'W).

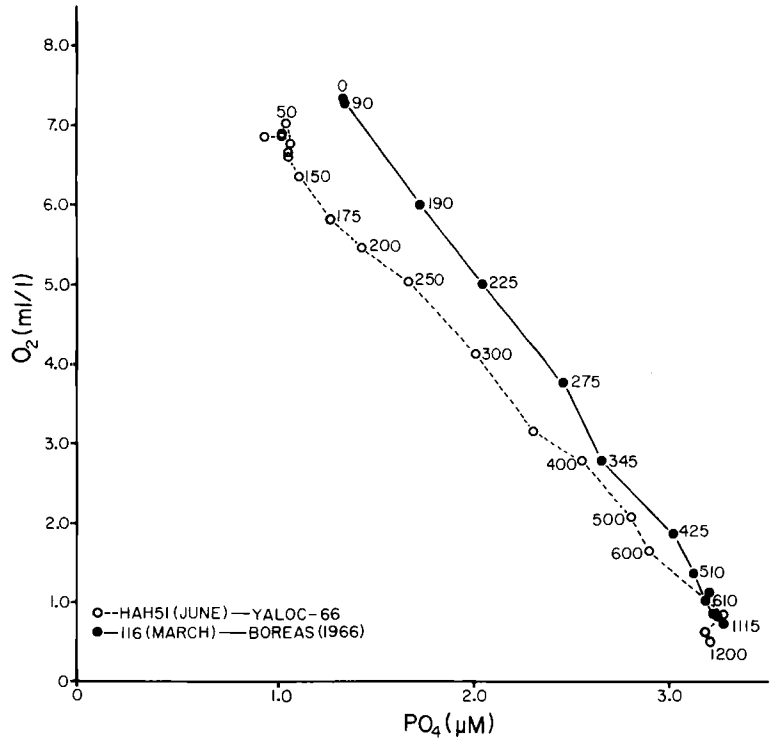

Figure 36. Oxygen-phosphate diagram. Comparison between winter and summer data. The numbers by the data points represent depth in meters. The positions of the stations are: HAH51 (44°17.0'N, 173°06.3'W), 116 (44°51.0'N, 174°57.0'E).

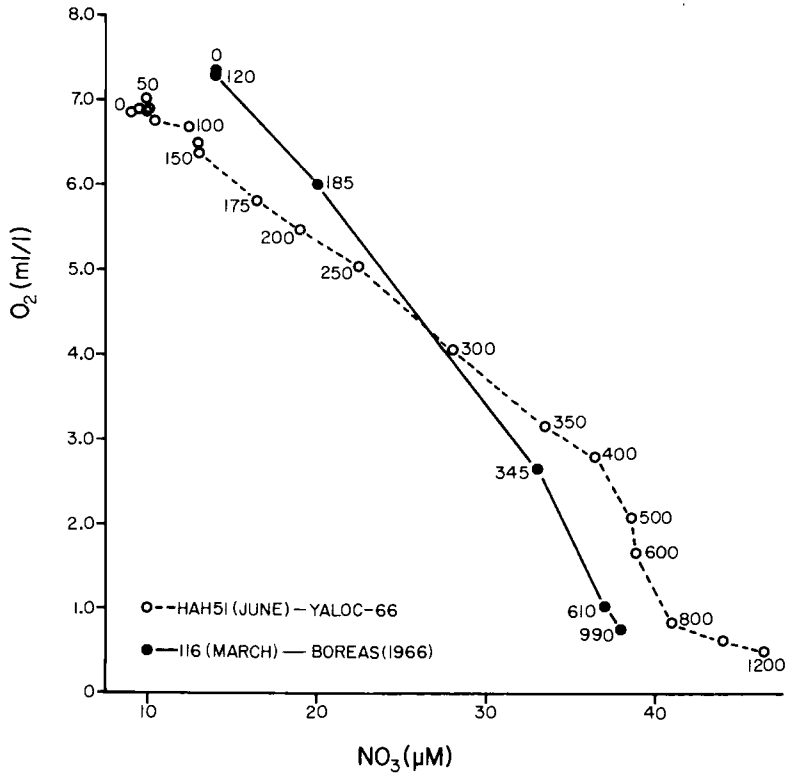

Figure 37. Oxygen-nitrate diagram. Comparison between winter and summer data. The numbers by the data points represent depth in meters. The positions of the stations are: HAH51 (44°17.0'N, 173°06.3'W), 116 (44°51.0'N, 174°57.0'E).

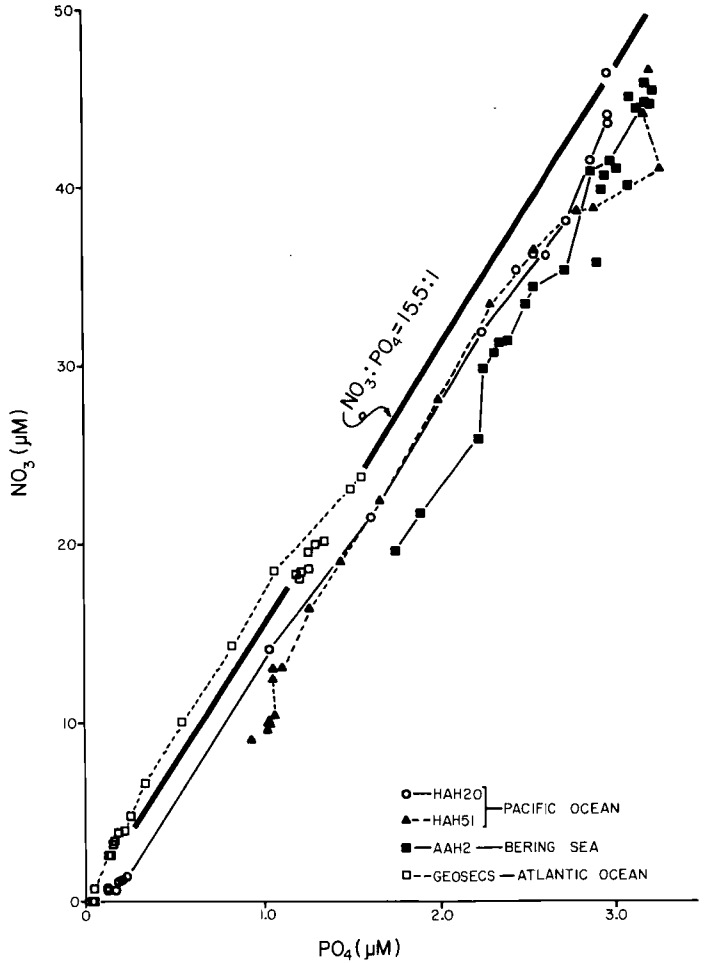

Figure 38. Nitrate-phosphate diagram. The thick straight line has a slope equal to the mean nitrogen: phosphorus ratio in phytoplankton reported by Fleming (1941). The positions of the stations are: HAH20 (22°53.8'N, 158°54.7'W), HAH51 (44°17.0'N, 173°06.3'W), AAH2 (52°56.1'N, 177°55.0'W), GEOSECS (35°46.0'N, 67°58.0'W).

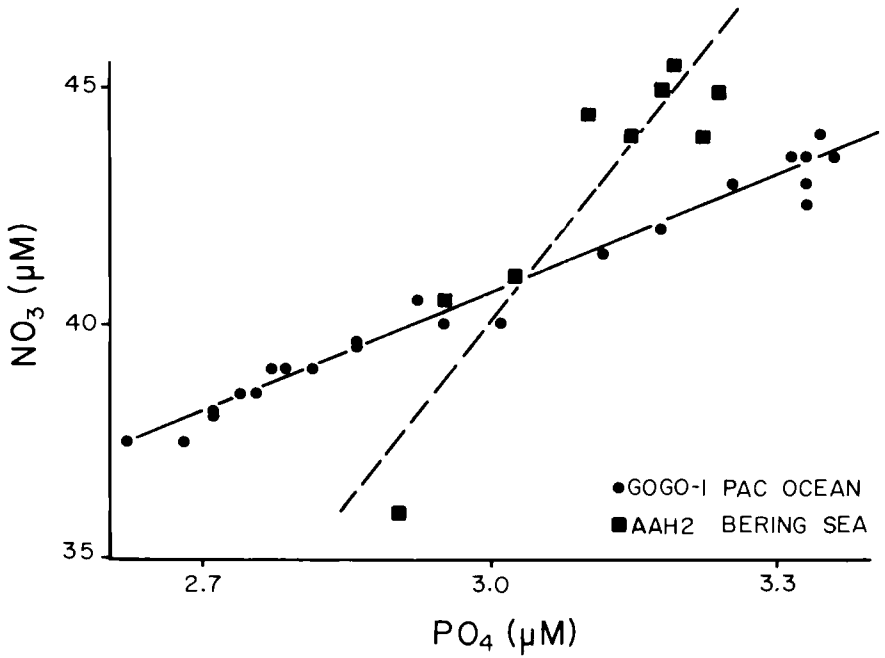

Figure 39. Nitrate-phosphate diagram for the region of the water column below the oxygen minimum zone. The lines are the least squares fits. The positions of the stations are: GOGO-1 (28°29.0'N, 121°38.0'W), AAH2 (52°56.1'N, 177°55.0'W).

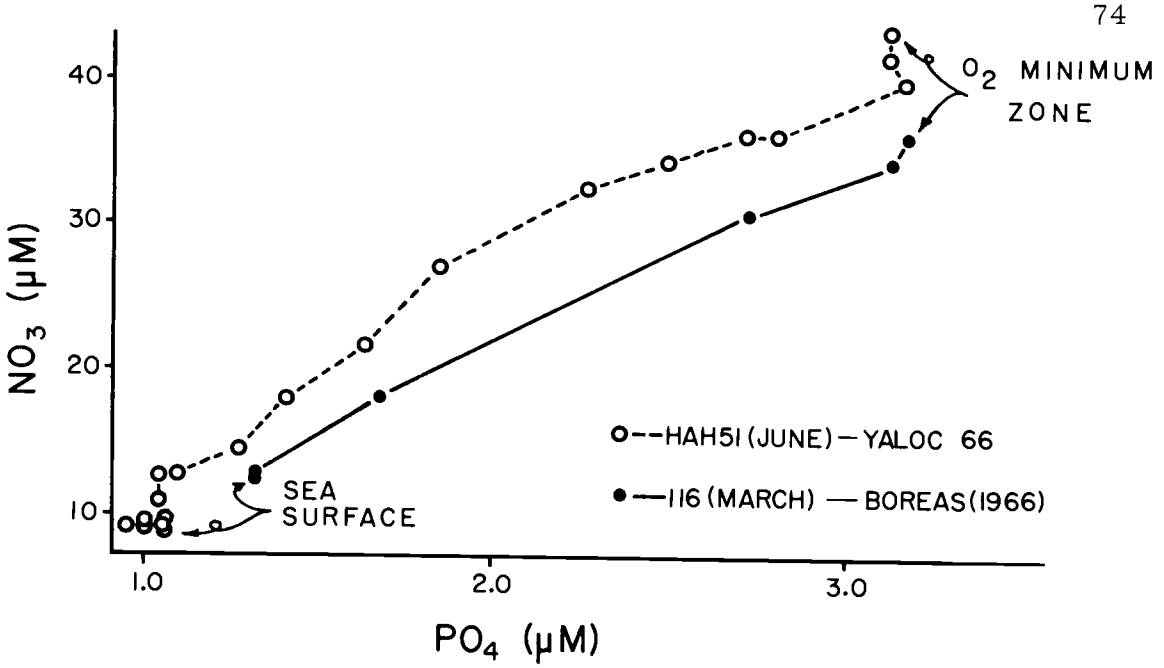

Figure 40. Nitrate-phosphate diagram. Comparison between winter and summer data. The positions of the stations are: HAH51 (44°17.0'N, 173°06.3'W), 116 (44°51.0'N, 174°57.0'E).

diagram varies from 14.8 ± 0.4 near Hawaii, to 17.7 ± 1.6 in the Southeastern Bering Sea (Figure 38). Near 45°N the slopes of the O_2-PO_4, O_2-NO_3 and NO_3-PO_4 relationships, for the region of the water column above the O_2 minimum zone, have values very near those predicted by Redfield's model (Figures 32, 33 and 38).

Below the O_2 minimum zone the O_2-PO_4 slope varies from -4.24 ± 0.70 near Hawaii, to -6.01 ± 0.50 in the Southeastern Bering Sea (Figure 34); the O_2-NO_3 slope varies from -0.169 ± 0.012 near 28°N (off California), to -0.404 ± 0.022 in the Southeastern Bering Sea (Figure 35); and the NO_3-PO_4 slope varies from 8.5 ± 0.8 near 28°N (off California), to 25.1 ± 6.8 in the Southeastern Bering Sea (Figure 39).

Above the O_2 minimum zone, near 45°N, 180°, the O_2-PO_4 slope varies from -3.38 ± 0.08 in March, to -2.74 ± 0.10 in June (Figure 36); the O_2-NO_3 slope varies from -0.270 ± 0.020 in March, to -0.169 ± 0.012 in June (Figure 37); and the NO_3-PO_4 slope varies from 12.4 ± 0.6 in March, to 15.3 ± 0.9 in June (Figure 40).

Discussion

The regeneration of nitrate in sea water is more complicated than that of phosphate. Nitrogen is released from organic combination as ammonia and is subsequently oxidized to nitrite, and then to nitrate (Redfield, Ketchum and Richards, 1963). Von Brand and Rakestraw's (1941) experiments showed the successive appearance and disappearance of the fractions as decomposition proceeded. Phosphate on the other hand stays at the same oxidation state during the biochemical oxidation in the ocean.

In the deep sea, ammonia does not ordinarily occur in significant quantities below the photosynthetic zone, except in anoxic basins (Redfield, Ketchum and Richards, 1963). Rakestraw (1936) showed that in the Northwestern Atlantic Ocean, below ~ 150 m depth, nitrite does not exceed 0.1 μM. Data from the SOUTHERN CROSS cruise (Horibe, 1970) and the SCORPIO expedition (SIO, reference 69-15; WHOI, reference 69-56) show that nitrite concentrations rarely exceed 0.1 μM below ~ 150 m depth in the Pacific Ocean. Thus, in our

discussion we will assume that all the nitrogen derived from biological oxidation is in the form of nitrate.

Originally Redfield (1934) proposed the values 20:1 for the ΔNO_3: ΔPO_4 ratio and 6: 1 for the ΔO_2:ΔNO_3 ratio, when O_2, PO_4, and NO_3 are expressed in μM. But Cooper (1937) (cited by Fleming, 1941) indicated that Redfield's (1934) PO_4 data had to be corrected for the salt error. Fleming (1941) assembled more extensive data for the composition of plankton and proposed the ratios 106:16:1 for the C:N:P, by atoms. Based on Fleming's (1941) values Redfield, Ketchum and Richards (1963) proposed that for each atom of phosphorus that is released by biological oxidation 276 atoms of oxygen are consumed from sea water. When O_2 is expressed in ml/l, and PO_4 and NO_3 are expressed in μM, the ratios proposed by Redfield, Ketchum and Richards (1963) are: ΔO_2:$\Delta PO_4 \doteq -3.1$, ΔO_2:$\Delta NO_3 \doteq -0.19$ and ΔNO_3: $\Delta PO_4 \doteq 16$.

Fleming (1941) only reported the means of his estimates of the C:N:P ratios in phytoplankton and zooplankton. They are only point estimates that do not provide any information about the uncertainty of the values. Fleming (1941) wrote: "... The available data show a considerable range, ... Consequently, although the method of treatment is valid, the numerical values must be considered as tentative and subject to some revision when additional data are available."

The maximum and minimum values of the proportions of carbon,

nitrogen and phosphorus in plankton, in parts by weight, that Redfield (1934) used (Table 2 of Redfield, 1934) were: C to N maximum = 100: 8.1, minimum = 100:25.6; and C to P maximum = 100:1.06, minimum = 100:2.26. This gives an idea of the variability of the data on plankton composition used to support the model.

According to Vinogradov (1953) (cited by Redfield, Ketchum and Richards, 1963) the species composition of the biomass is observably variable both in time and space, and each species may be expected to have a composition which differs somewhat from others. For these reasons, as Redfield, Ketchum and Richards (1963) indicated, statistical uniformity in composition is probably approached only in large masses of water, where deviations of this sort are averaged out.

From Redfield (1942):

$$AOU = O'_2 - O_2 \tag{35}$$

$$PO_4 = PO_{4_{ox}} + P.PO_4 \tag{36}$$

$$PO_{4_{ox}} \doteq (AOU)/3.1 \tag{37}$$

similarly for NO_3:

$$NO_3 = NO_{3_{ox}} + P.NO_3 \tag{38}$$

$$NO_{3_{ox}} \doteq (AOU)/0.19 \tag{39}$$

where O'_2 is the calculated concentration of dissolved oxygen at saturation; $PO_{4_{ox}}$ and $NO_{3_{ox}}$ are the phosphate and nitrate released

by biological oxidation; and $P.NO_3$ is the preformed nitrate. From equations (35), (36) and (37) we have

$$O_2 \doteq -3.1\ PO_4 + (O'_2 + 3.1\ P.PO_4) \tag{40}$$

and from equations (35), (38) and (39) we have

$$O_2 \doteq -0.19\ NO_3 + (O'_2 + 0.19\ P.NO_3) \tag{41}$$

From equations (40) and (41) we can see that if Redfield's model is correct, the variation of the O_2-PO_4 and O_2-NO_3 slopes with geographic location, depth and time of the year (Figures 32, 33, 34, 35, 36 and 37) is due to mixing between different water types with different conservative portions of O_2, PO_4 and NO_3, namely (O'_2 + 3.1 $P.PO_4$) and (O'_2 + 0.19 $P.NO_3$).

From equations (40) and (41) we have

$$NO_3 \doteq 16\ PO_4 + (P.NO_3 - 16\ P.PO_4) \tag{42}$$

From equation (42) we can see that if Redfield's model is correct, the variation of the NO_3-PO_4 relationship with geographic location, depth and time of the year (Figures 38, 39 and 40) is due to mixing between different water types with not only different $P.PO_4$'s and $P.NO_3$'s, but furthermore with $P.NO_3$:$P.PO_4$ ratios different from 16.

As a possible explanation of the variation of the ΔO_2:ΔPO_4 ratio with depth Wattenberg (1938) (cited by Postma, 1964) suggested that the decomposition of organic matter takes place stepwise in such a

manner that, during the sinking of the organic particles, parts with different phosphorus content are oxidized at different depths. Pytkowicz (1964) found that off the Oregon coast the value of the $\Delta O_2:\Delta PO_4$ ratio varies seasonally, being lowest in summer and highest in winter. He explained this in terms of possible variations in the composition of the organic matter being oxidized at different times of the year. If these explanations were true, the O_2-PO_4, O_2-NO_3 and NO_3-PO_4 relationships would give an indication of the composition of organic matter at different depths in the ocean and on different seasons of the year.

Pytkowicz (1971) states that differences in the $\Delta O_2:\Delta PO_4$ ratio may be due to variation of $P_\circ PO_4$ with depth. Calculating $P_\circ PO_4$ by using Redfield's (1942) definition

$$P_\circ PO_4 = PO_4 - (AOU)/3.1 \qquad (43)$$

and plotting it versus O_2 for three stations at different latitudes (Figure 41), we can see that the relationship between O_2 and $P_\circ PO_4$ varies with depth and latitude. $P_\circ PO_4$ is about constant for station HAH51 (near 45°N), with values around 1.0 μM. South of 45°N, $P_\circ PO_4$ changes from lower values at the surface to about 1.0 μM at the O_2 minimum zone. North of 45°N, $P_\circ PO_4$ changes from higher values at the surface to about 1.0 μM at the O_2 minimum zone (Figure 41). This is merely illustrative and cannot be used to explain the disagreement between the variable slope of the O_2-PO_4

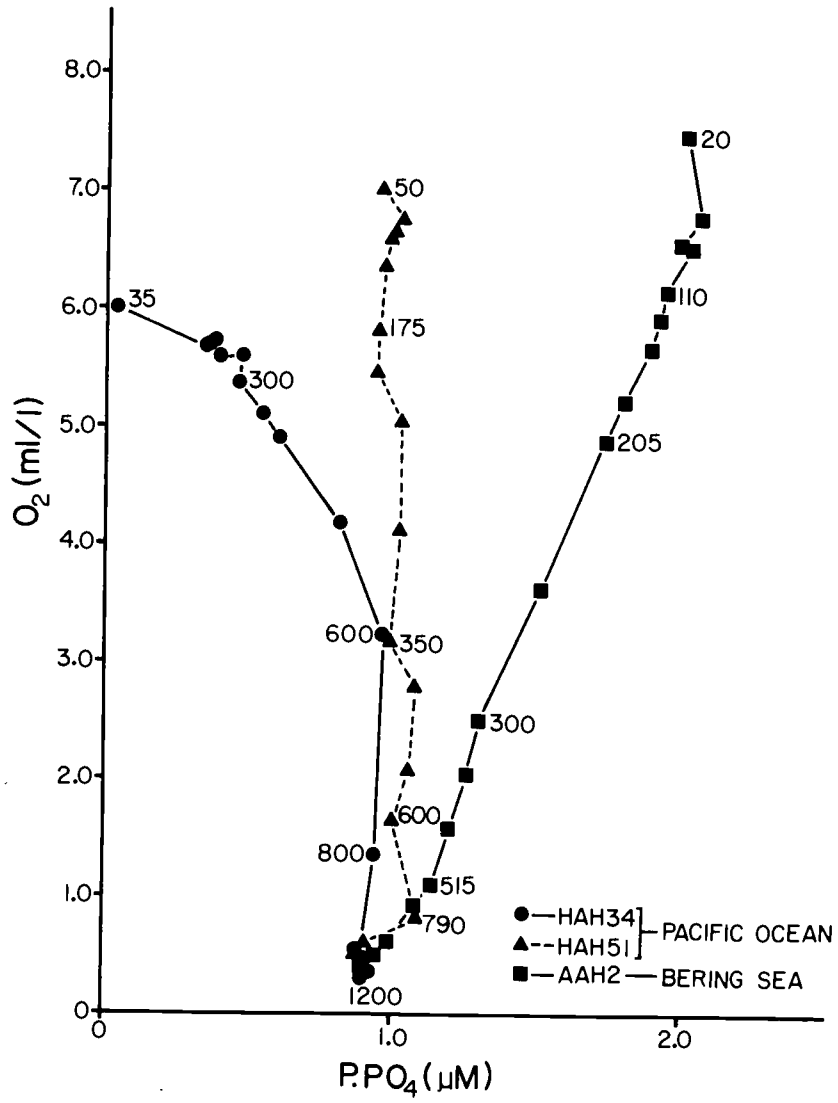

Figure 41. Oxygen-preformed phosphate diagram. The numbers by the data points represent depth in meters. The positions of the stations are: HAH34 (35°26.5'N, 165°97.8'W), HAH51 (44°17.0'N, 173°06.3'W), AAH2 (52°56.1'N, 177°55.0'W).

relationship, found by plotting field data, and the constant value predicted by Redfield's model. It would be a circular argument because P.PO_4 values were not calculated independently of Redfield's model.

Test of Redfield's model by using regression analysis

One way to test Redfield's model is by using regression analysis on the field data. $P.PO_4$ is conservative in the same sense salinity and temperature are conservative (Pytkowicz and Kester, 1966). Physical processes such as mixing and advection affect $P.PO_4$ in the same way they affect salinity and temperature. O'_2 is conservative in the sense that it is not affected by biological processes. If we make a regression of O_2 on PO_4, temperature and/or salinity, the temperature and/or salinity terms may represent the conservative fraction of phosphate and oxygen, namely $(O'_2 + 3.1\ P.PO_4)$, so that the PO_4 term represents only the non-conservative fractions. The same type of approach may be used for the O_2-NO_3 relationship.

Ben-Yaakov (1971) applied regression analysis to ΣCO_2, O_2, total alkalinity, S‰ and temperature data. He indicated that, when dealing with a water mass which results from the mixing of n water types, at least n-1 conservative parameters are needed in the regression equation.

According to what is explained above, multiple linear regression analysis (Draper and Smith, 1966) was applied to O_2, PO_4, NO_3 and θ°C data. θ°C is preferred to "in situ" temperature to avoid the adiabatic heating effect of hydrostatic pressure. Temperature is preferred to S‰ because O'_2 depends more on temperature than on

S‰ in the ocean.

A discussion follows on the application of regression analysis to test Redfield's model for the $\Delta O_2:\Delta PO_4$ ratio. The same procedure is then applied to test Redfield's model for the $\Delta O_2:\Delta NO_3$ ratio.

To test the hypothesis that the $\Delta O_2:\Delta PO_4$ ratio is equal to -3.1, the regression equation

$$O_2 = a_o + a_1 PO_4 + a_2 \theta^\circ C + O_{2_{res}} \tag{44}$$

was applied to the data, where $O_{2_{res}}$ are the O_2 residuals after regression of O_2 on PO_4 and $\theta^\circ C$; a_o, a_1 and a_2 are constant regression coefficients. $a_1 = \Delta O_2:\Delta PO_4$.

At first it may seem that to properly apply equation (44) to the field data we need to choose a portion of the water column where mixing between no more than two water types is occurring, since we only have one conservative variable in the equation. But, by comparing equations (40) and (44) we can see that the only necessary and sufficient condition for the proper application of equation (44) is that the conservative quantity $(O'_2 + a_1 P.PO_4)$ be a linear function of $\theta^\circ C$, that is

$$O'_2 + a_1 P.PO_4 = a_o + a_2 \theta^\circ C \tag{45}$$

This is equivalent to saying that equation (44) must be applied to data from a portion of the water column where the diagram of $(O'_2 + a_1 P.PO_4)$ versus $\theta^\circ C$ is able to detect only two-water-types mixing.

A classical way to detect two-water-types mixing has been to

look for straight portions of the temperature-salinity (T-S) diagram. But, a straight T-S diagram is a necessary but not sufficient condition for two-water types mixing. The $(O'_2 + a_1\ P.PO_4)$ versus $\theta°C$ or other diagrams may show water types that the T-S diagram does not show, and vice versa. To choose the portion of the water column where $(O'_2 + a_1 P.PO_4)$ is a linear function of $\theta°C$ it is not proper to calculate $P.PO_4$ by using Redfield's definition, and then plot $(O'_2 + 3.1\ P.PO_4)$ versus $\theta°C$, because we would fall into a circular argument. We must decide where to apply the regression independently of Redfield's model.

There is a statistical method to decide where to apply equation (44) properly. If equation (44) is applied to the proper portion of the water column, a plot of $O_{2_{res}}$ versus $\theta°C$ should be completely random, because $O_{2_{res}}$ should result from only the random errors in the measurements of O_2, PO_4, and $\theta°C$. Thus, if we apply equation (44) to the whole water column and plot $O_{2_{res}}$ versus $\theta°C$, the pattern shown by the diagram, if any, would give us an indication of how to separate the water column into suitable portions.

Suppose we have data from the whole water column of a certain station, and suppose the $(O'_2 + a_1 P.PO_4)$ versus $\theta°C$ diagram is like the one shown in Figure 42a where at least three water types A, B and C are being detected. Since $(O'_2 + a_1\ P.PO_4)$ is not a linear function of $\theta°C$, the plot of $O_{2_{res}}$ versus $\theta°C$ would generate a diagram as shown in Figure 42b which would detect the three water types A, B

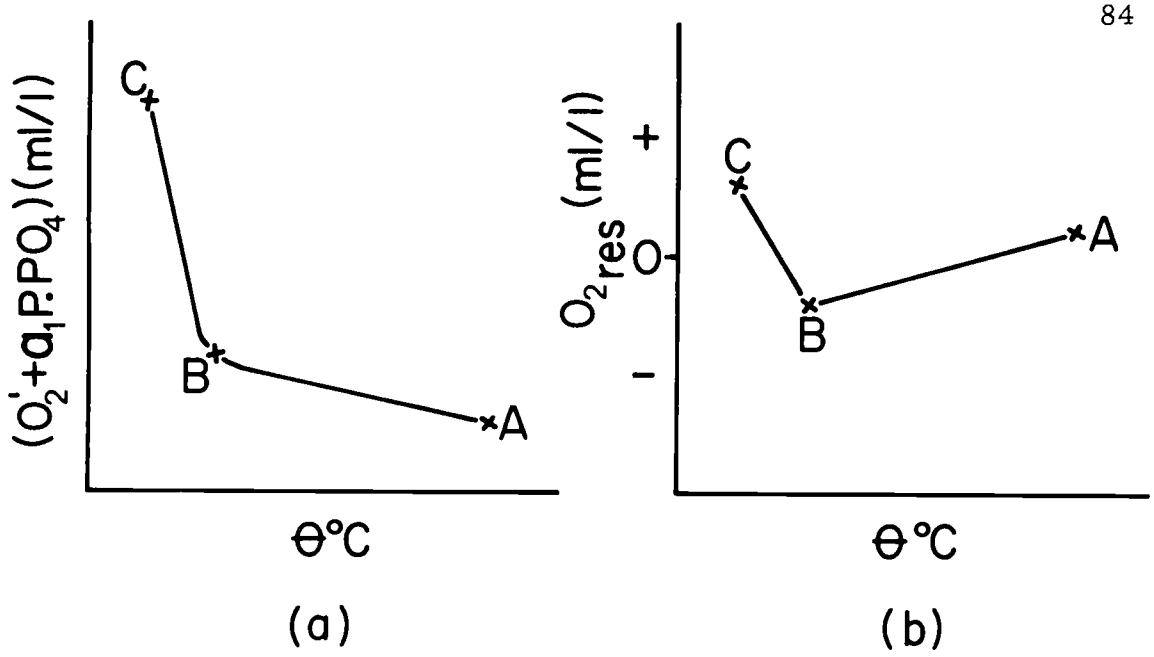

Figure 42. $(O'_2 + a_1 P.PO_4)$ versus θ°C diagram (a), and $O_{2_{res}}$ versus θ°C diagram (b), of a hypothetical station.

and C. Thus, each minimum and maximum in the $O_{2_{res}}$ versus θ°C diagram represents a different water type.

This procedure was applied to data from station HAH30 of YALOC-66 (30°55.4'N, 162°37.4'W) (Figure 30)(Barstow, Gilbert, Park, Still and Wyatt, 1968). This station was chosen because samples were obtained from 49 different depths. Most of the published data contain no more than 30 observations per station. The number of observations is very important because the more degrees of freedom we have, when applying regression analysis to a set of data, the smaller the standard errors of the regression coefficients. The multiple linear regression analysis is a least square fit to the given

data. The fitting was accomplished by a computer program (SIPS) (Oregon State University, Department of Statistics, 1971). For each of the coefficients of all the following regression equations, 95% confidence intervals are given.

The results are as follows. Regressing O_2 on PO_4 and $\theta°C$ in a stepwise manner (Draper and Smith, 1966) for the whole water column (0 to 5275 m), we find the regression equations

$$\text{with } PO_4 \text{ only: } O_2 = (5.79 \pm 0.36) - (1.27 \pm 0.17)PO_4 \tag{46}$$

$$\text{with } PO_4 \text{ and } \theta°C: \quad O_2 = (10.65 \pm 0.78) - (0.27 \pm 0.04)\theta°C + - (2.85 \pm 0.26)PO_4 \tag{47}$$

equation (47) has a coefficient of determination $R^2 = 0.969$.

Figure 43 shows a definite dependency of $O_{2_{res}}$ on $\theta°C$. Since the O'_2 versus $\theta°C$ diagram is a smooth curve (Figure 44) the pattern shown in Figure 43 is almost entirely due to differences in $P.PO_4$ between the different water types. In Figure 43, A is the surface water, C is the Subarctic Intermediate water (S‰ minimum), D almost coincides with the O_2 minimum, E is the Pacific Bottom water. The θ-S diagram (Figure 45) does not show B and D distinctly as water types, but the fact that in the vicinity of both of them the θ-S diagram is not a straight line suggests their presence.

Reid (1965) studied the intermediate waters of the Pacific Ocean by plotting different physico-chemical properties on surfaces of

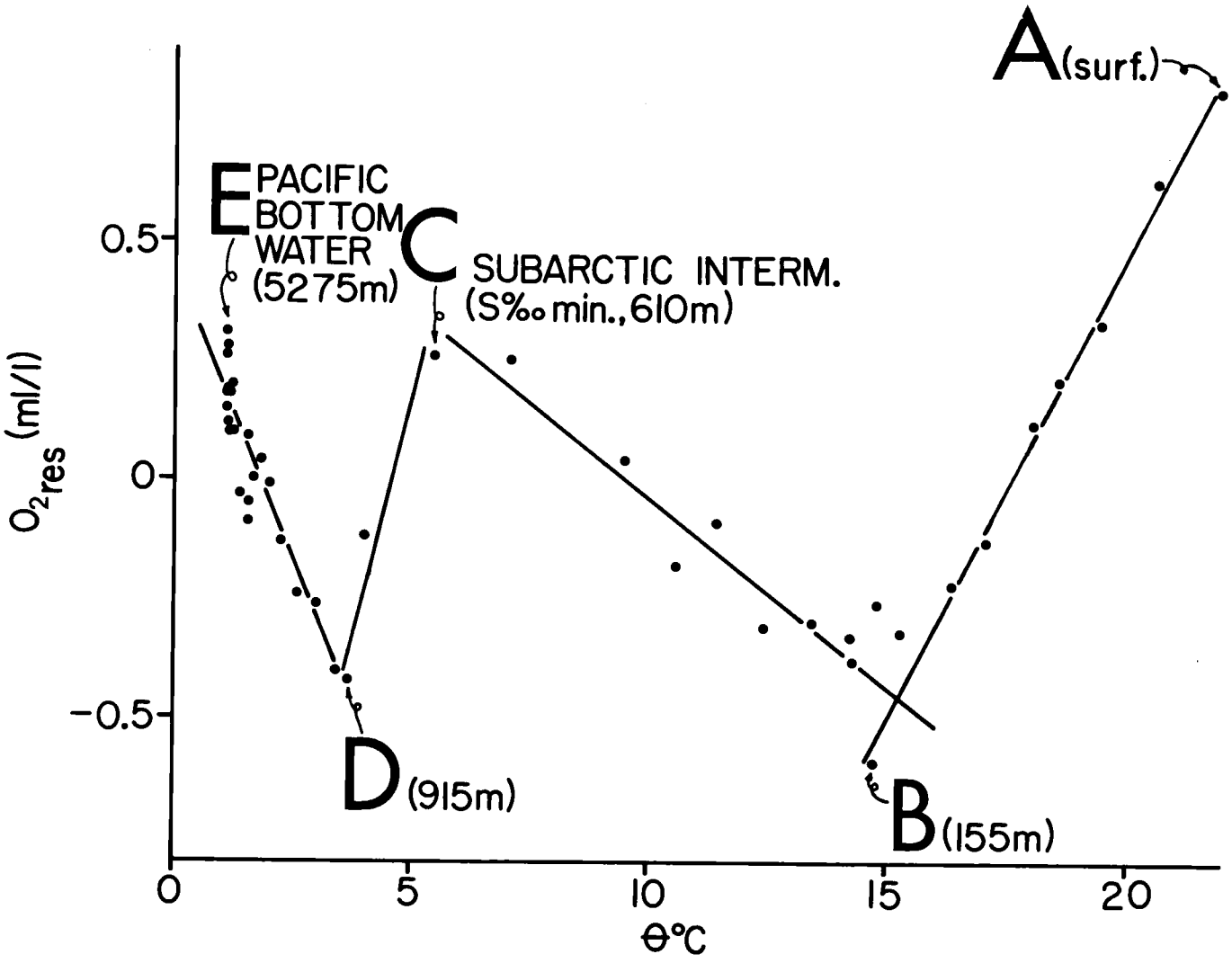

Figure 43. $O_{2_{res}}$ versus θ°C diagram for the whole water column of station HAH30 (30°55.4'N, 162°37.4'W). A, B, C, D and E denote water types.

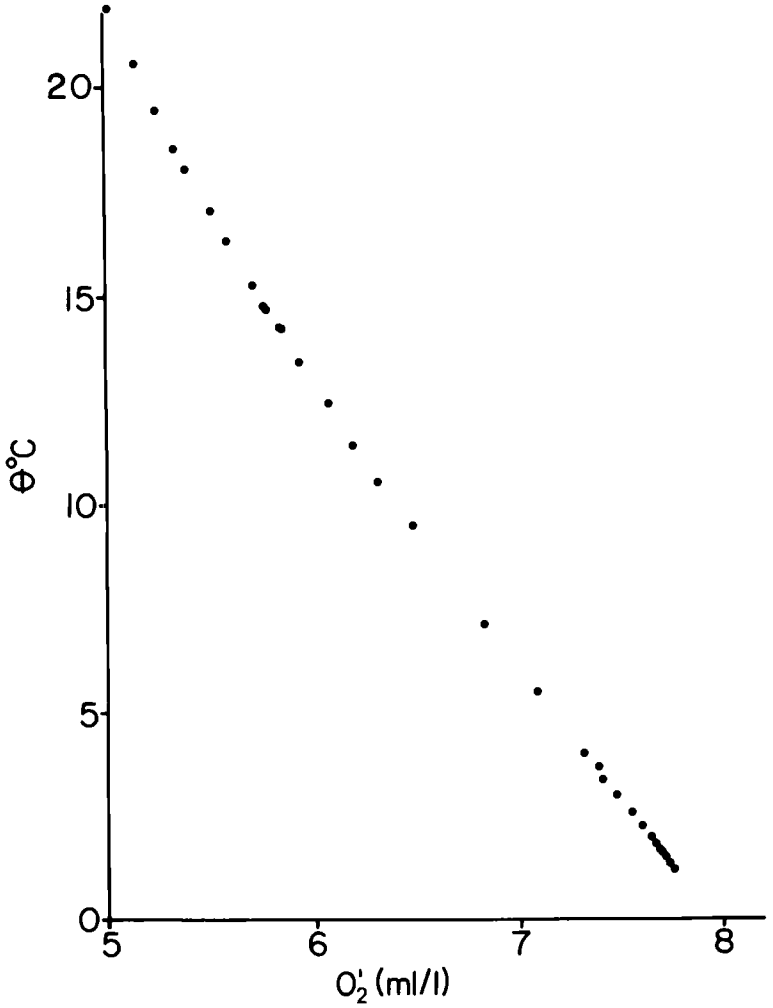

Figure 44. O'_2 versus θ° C diagram for the whole water column of station HAH30 (30° 55.4'N, 162° 37.4'W).

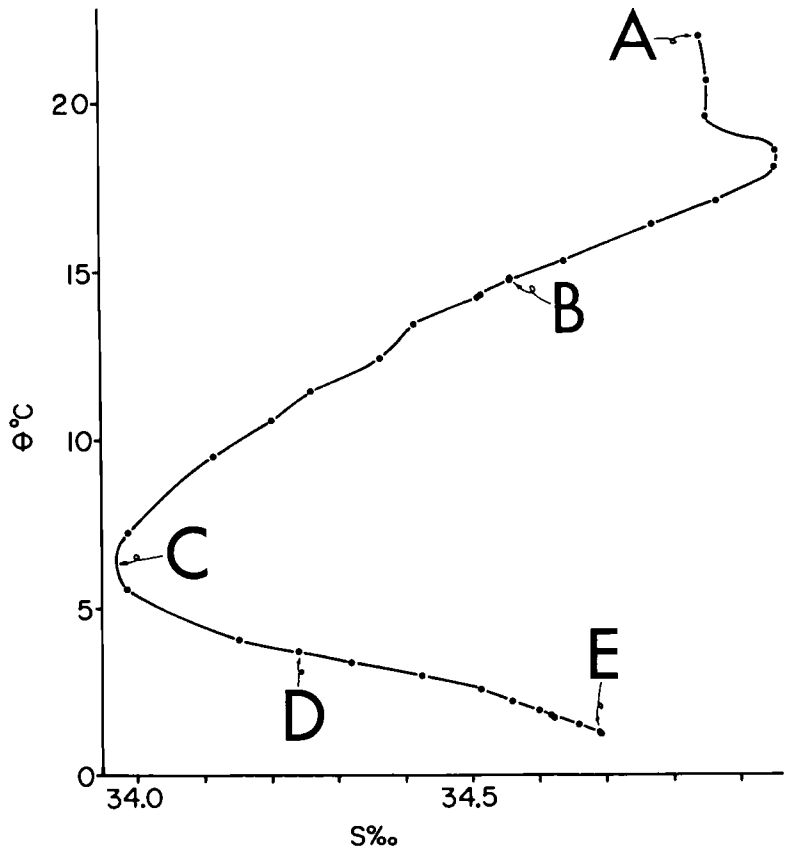

Figure 45. θ° C-S‰ diagram for station HAH30 (30° 55.4'N, 162° 37.4'W). A, B, C, D and E denote water types.

constant potential density. For the Antarctic Intermediate water he chose the surface of thermosteric anomaly (δ_t) equal to 80 cl/ton, ($\sigma_t = 27.28$). Water D (Figure 43) has a sigma-t value of 27.32.

The confidence interval for the PO_4 regression coefficient of equation (47), -2.59 to -3.11, is consistent with the value predicted by Redfield's model. The agreement should be considered fortuitous since, according to Figure 43, there is no oceanological nor statistical basis to justify the coefficient for $\theta°C$ as a valid one.

A separation of the data from HAH30 into three sets was done; one from A to B, another from B to C, and another from D to E. Between C and D (Figure 43) there is only one data point, therefore no regression was applied to that portion of the water column.

The results of the regressions are as follows.

for A-B

with PO_4: $O_2 = (5.54 \pm 0.15) - (1.12 \pm 0.80)PO_4$ (48)

with PO_4 and $\theta°C$: $O_2 = (7.08 \pm 0.60) - (0.07 \pm 0.03)\theta°C + - (2.50 \pm 0.64)PO_4$ (49)

equation (44) has a coefficient of determination $R^2 = 0.915$

for B-C

with PO_4: $O_2 = (5.71 \pm 0.24) - (1.20 \pm 0.20)PO_4$ (50)

with PO_4 and $\theta°C$: $O_2 = (10.91 \pm 1.84) - (0.32 \pm 0.12)\theta°C + - (2.71 \pm 0.54)PO_4$ (51)

equation (51) has a coefficient of determination $R^2 = 0.988$

with PO_4: $O_2 = (14.18 \pm 0.70) - (4.32 \pm 0.26)PO_4$ (52)

for D-E with PO_4 and $\theta°C$: $O_2 = (11.27 \pm 0.78) - (0.49 \pm 0.12)\theta°C + - (2.93 \pm 0.36)PO_4$ (53)

equation (53) has a coefficient of determination $R^2 = 0.996$

$O_{2_{res}}$ versus $\theta°C$ diagrams for these three sets of data do not show any particular trend (Figure 46a, b, c). This indicates that $O_{2_{res}}$ result from only the random errors in the measurements of O_2, PO_4 and $\theta°C$ data, and that equations (49), (51) and (53) are properly describing the data.

The PO_4 regression coefficients of equations (48), (50) and (52) are the least-squares slopes we would get by plotting O_2 versus PO_4 directly. It is interesting to notice that before adding $\theta°C$ to the regression equations [equations (48), (50) and (52)] the PO_4 regression coefficients for A-B and B-C are smaller than the value predicted by Redfield's model (-3.1) while the one for D-E is greater; and after

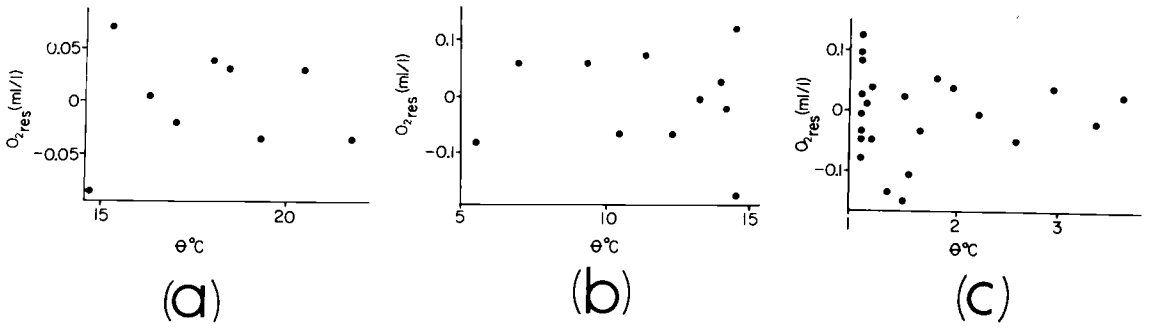

Figure 46. $O_{2_{res}}$ versus $\theta°C$ diagrams for the portions of the water column between (a) 0 and 155 m, (b) 155 and 610 m, and (c) 915 and 5275 m of station HAH30 (30°55.4'N, 162°37.4'W).

adding θ°C to the equations [equations (49), (51) and (53)] the adjustment changes the PO_4 coefficients towards -3.1 in all three cases.

To test the hypothesis that the $\Delta O_2 : \Delta NO_3$ ratio is equal to -0.19, the regression equation

$$O_2 = b_o + b_1 NO_3 + b_2 \theta°C + O_{2_{res'}} \quad (54)$$

was applied to the data, where $O_{2_{res'}}$ are the O_2 residuals after regression of O_2 on NO_3 and θ°C; b_o, b_1 and b_2 are constant regression coefficients. $b_1 = \Delta O_2 : \Delta NO_3$.

Applying equation (54) to data from HAH30 station (35 to 5275 m) (there are no NO_3 data for the upper 35 m) we obtained the following results

$$\text{with } NO_3 \text{ only: } O_2 = (5.71 \pm 0.42) - (0.089 \pm 0.014) NO_3 \quad (55)$$

$$\text{with } NO_3 \text{ and } \theta°C: \; O_2 = (10.98 \pm 1.08) - (0.33 \pm 0.12)\theta°C + - (0.21 \pm 0.02) NO_3 \quad (56)$$

equation (56) has a coefficient of determination $R^2 = 0.953$.

Figure 47 shows a definite dependency of $O_{2_{res'}}$ on θ°C. It also shows very clearly the Subarctic Intermediate water and water type D shown in Figure 43. Below 3725 m depth the values for $O_{2_{res'}}$ increase and decrease without any particular trend. This is not very noticeable from Figure 47 because the difference in θ°C from point to point is very small. The fact that the data points are more spread in

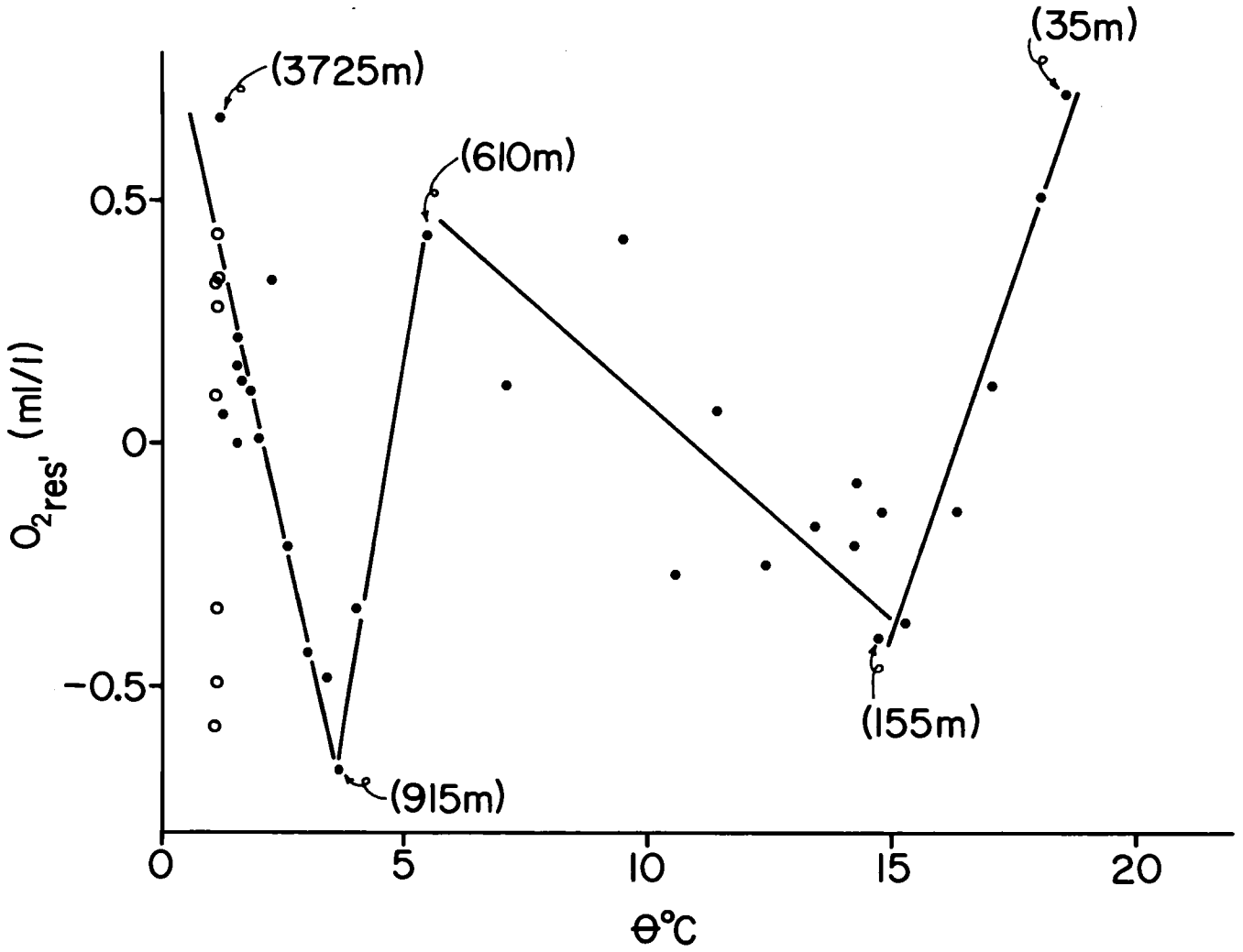

Figure 47. $O_{2_{res'}}$ versus θ° C diagram for the whole water column of station HAH30 (30° 55.4'N, 162° 37.4'W). Open circles represent data from below 3725 m depth.

Figure 47 than in Figure 43 indicates that NO_3 data are not as precise as PO_4 data from this station. During YALOC-66 cruise, PO_4 samples were analyzed aboard the ship as soon as they were collected, but NO_3 samples were frozen and analyzed later ashore (Barstow, Gilbert, Park, Still and Wyatt, 1968).

The confidence interval for the NO_3 regression coefficient of equation (56), -0.19 to -0.23, is consistent with the value predicted by Redfield's model. We again consider the agreement fortuitous since, according to Figure 47, there is no oceanological nor statistical basis to justify the coefficient for θ° C as a valid one. According to Figure 47 equation (56) is not properly describing the field data.

The data were divided into three sets, from 35 to 155 m, from 155 to 610 m, and from 915 to 3725 m. The regression for the 35-155 m depth range was not significant, there are only 6 data points for that region of the water column (Figure 47).

for 155-610 m

with NO_3 only: $O_2 = (5.57 \pm 0.22) - (0.081 \pm 0.014)NO_3$ (57)

with NO_3 and θ° C: $O_2 = (9.56 \pm 2.82) - (0.26 \pm 0.18)\theta°C + - (0.16 \pm 0.06)NO_3$ (58)

equation (58) has a coefficient of determination $R^2 = 0.966$

for 915-3725 m:

with NO_3 only: $O_2 = (16.76 \pm 4.56) - (0.364 \pm 0.110)NO_3$ (59)

with NO_3 and θ°C: $O_2 = (9.36 \pm 2.26) - (0.87 \pm 0.20)\theta°C + - (0.14 \pm 0.06)NO_3$ (60)

equation (60) has a coefficient of determination $R^2 = 0.978$

The $O_{2_{res'}}$ versus θ°C diagrams for these two sets of data do not show any particular trend (Figure 48a, b). This indicates that $O_{2_{res'}}$ result from only the random errors of O_2, NO_3 and θ°C data, and that equations (58) and (60) are properly describing the data.

The NO_3 regression coefficients of equations (57) and (59) are the least-squares slopes we would get by plotting O_2 versus NO_3 directly.

The confidence intervals for the PO_4 regression coefficients of equations (49), (51) and (53), and for the NO_3 regression coefficients of equations (58) and (60) are the sets of acceptable hypotheses at the 95% confidence level. Based on these results we cannot reject the

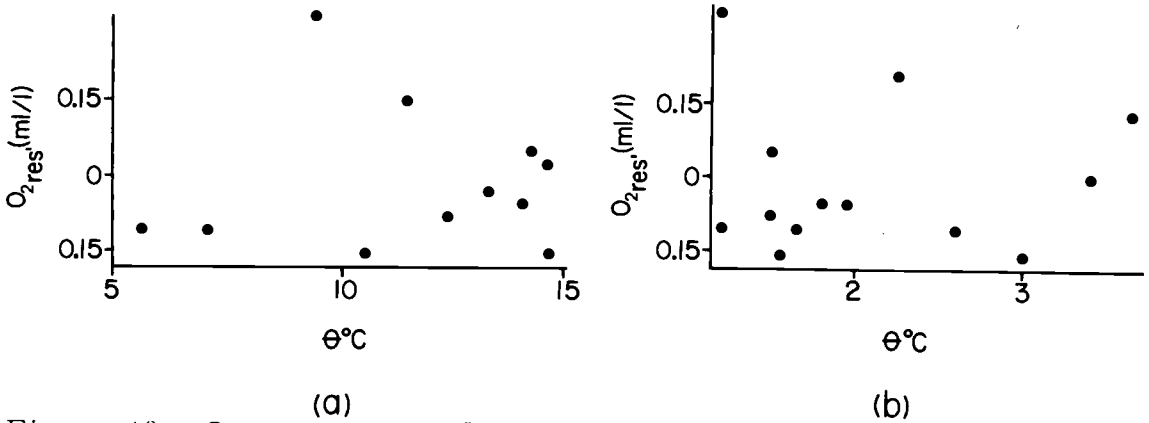

Figure 48. $O_{2_{res'}}$ versus θ°C diagrams for the portions of the water column between (a) 155 and 610 m, and (b) 915 and 3725 m of station HAH30 (30°55.4'N, 162°37.4'W).

values predicted by Redfield's model for the $\Delta O_2:\Delta PO_4$ and $\Delta O_2:\Delta NO_3$ ratios.

Something important to consider is that when we properly apply equations (44) and/or (54) to a certain region of the water column, the fact that the PO_4 and NO_3 regression coefficients are significantly different from zero does not provide any information as to where, geographically, the main bulk of the biological oxidation occurred. It only proves that at least part of the changes in O_2, PO_4 and NO_3 are due to biological oxidation, but not that those changes occurred at the geographic location of the hydrographic station where the data are from.

Equations (44) and (54) were applied to data from other stations to see what kind of results we could get from different geographic locations. The results are shown in Tables 1 and 2. For station HAH52 (Figure 30), in the Subarctic Pacific region, there is no NO_3 data available (Barstow, Gilbert, Park, Still and Wyatt, 1968). For the Atlantic GEOSECS station the Scripps Institution of Oceanography's O_2 data set was used (Spencer, 1970; unpublished manuscript).

The graphs that were constructed to decide on the separation of the water column into regions, for each station, and to test for the proper application of the regression analysis, are not reproduced here. Their use is well illustrated in the treatment of data from station HAH30. The regression equations for the whole water column

Table 1. Regression equations of O_2 on PO_4 and θ°C, on PO_4 and S‰, on NO_3 and θ°C, and on NO_3 and S‰. The confidence intervals are at the 95% confidence level. Stations HAH52, AAH2, and SCORPIO 71 and 72.

Station	Depth range (meters)	Regression equations (showing 95% confidence intervals)	R^2	n-p-1*
HAH52 (45°52.8'N, 174°2.3'W)	125-405	with PO_4 only: $O_2 = (9.90 \pm 0.39) - (2.78 \pm 0.20)PO_4$		4
		with PO_4 & θ°C: $O_2 = (14.02 \pm 3.91) - (3.49 \pm 0.58)PO_4 - (0.50 \pm 0.48)\theta°C$	0.999	3
	405-1765	with PO_4 only: $O_2 = (12.59 \pm 2.02) - (3.75 \pm 0.66)PO_4$	0.978	5
		with PO_4 & θ°C: $O_2 = (13.24 \pm 7.67) - (3.92 \pm 1.95)PO_4 - (0.05 \pm 0.55)\theta°C$	0.979	4
AAH2 (52°56.1'N, 179°55'W)	75-300	with PO_4 only: $O_2 = (22.87 \pm 0.90) - (7.05 \pm 0.35)PO_4$		6
		with PO_4 & S‰: $O_2 = (186 \pm 96) - (2.9 \pm 2.6)PO_4 - (5.2 \pm 3.1)S‰$	0.999	5
	360-1020	with PO_4 only: $O_2 = (24.4 \pm 6.4) - (7.4 \pm 2.0)PO_4$		7
		with PO_4 & S‰: $O_2 = (74.4 \pm 23.5) - (3.3 \pm 2.2)PO_4 - (1.85 \pm 0.86)S‰$	0.985	6
	1215-3200	with PO_4 only: $O_2 = (20.33 \pm 2.04) - (6.15 \pm 0.66)PO_4$		11
		with PO_4 & S‰: $O_2 = -(74.9 \pm 50.8) - (4.21 \pm 1.14)PO_4 + (2.58 \pm 1.28)S‰$	0.987	10
	515-3500	with NO_3 only: $O_2 = (14.03 \pm 2.06) - (0.297 \pm 0.046)NO_3$		12
		with NO_3 & S‰: $O_2 = -(40.2 \pm 36.7) - (0.224 \pm 0.060)NO_3 + (1.5 \pm 1.0)S‰$	0.961	11
SCORPIO 71 & 72 (off Chile)	90-865	with PO_4 only: $O_2 = (6.88 \pm 1.06) - (0.82 \pm 0.62)PO_4$		24
		with PO_4 & θ°C: $O_2 = (13.80 \pm 0.70) - (3.12 \pm 0.26)PO_4 - (0.45 \pm 0.04)\theta°C$	0.962	23
	80-840	with NO_3 only: $O_2 = (6.49 \pm 0.92) - (0.04 \pm 0.04)NO_3$		24
		with NO_3 & θ°C: $O_2 = (15.91 \pm 1.48) - (0.26 \pm 0.04)NO_3 - (0.62 \pm 0.10)\theta°C$	0.902	23

*n-p-1 are the residual degrees of freedom, n is the number of observations and p is the number of independent variables already in the regression equation.

Table 2. Regression equations of O_2 on PO_4 and θ°C and on NO_3 and θ°C. The confidence intervals are at the 95% confidence level. North Pacific and North Atlantic GEOSECS intercalibration stations.

Station	Depth range (meters)	Regression equations (showing 95% confidence intervals)	R^2	n-p-1*
GOGO I (GEOSECS) (28°29'N, 121°38'W) (off Baja California)	260-800	with PO_4 only: $O_2 = 7.60 \pm 0.57) - (2.22 \pm 0.21)PO_4$		6
		with PO_4 & θ°C: $O_2 = (10.78 \pm 1.20) - (2.82 \pm 0.23)PO_4 - (0.23 \pm 0.07)\theta$°C	0.999	5
	1200-4200	with PO_4 only: $O_2 = (12.81 \pm 0.44) - (3.61 \pm 0.16)PO_4$		16
		with PO_4 & θ°C: $O_2 = (11.50 \pm 1.54) - (3.05 \pm 0.66)PO_4 - (0.19 \pm 0.21)\theta$°C	0.994	15
	905-2005	with NO_3 only: $O_2 = (17.17 \pm 4.16) - (0.38 \pm 0.10)NO_3$		5
		with NO_3 & θ°C: $O_2 = (9.77 \pm 3.36) - (0.18 \pm 0.08)NO_3 - (0.36 \pm 0.14)\theta$°C	0.997	4
	2005-4200	with NO_3 only: $O_2 = (17.91 \pm 2.64) - (0.39 \pm 0.07)NO_3$		12
		with NO_3 & θ°C: $O_2 = (8.90 \pm 2.4) - (0.12 \pm 0.07)NO_3 - (1.19 \pm 0.28)\theta$°C	0.992	11
ATLANTIC STATION (GEOSECS) (35°46.0'N, 67°58.0'W)	430-860	with PO_4 only: $O_2 = (5.17 \pm 0.11) - (1.58 \pm 0.20)PO_4$		4
		with PO_4 & θ°C: $O_2 = (8.52 \pm 3.84) - (2.72 \pm 1.31)PO_4 - (0.18 \pm 0.17)\theta$°C	0.998	3
	860-1840	with PO_4 only: $O_2 = (9.11 \pm 6.67) - (3.18 \pm 5.29)PO_4$		8
		with PO_4 & θ°C: $O_2 = (10.49 \pm 0.74) - (2.62 \pm 0.53)PO_4 - (0.35 \pm 0.02)\theta$°C	0.993	7
	150-580	with NO_3 only: $O_2 = (4.97 \pm 0.29) - (0.041 \pm 0.059)NO_3$		5
		with NO_3 & θ°C: $O_2 = (11.09 \pm 3.44) - (0.18 \pm 0.08)NO_3 - (0.31 \pm 0.17)\theta$°C	0.905	4
	860-1840	with NO_3 only: $O_2 = (12.18 \pm 5.75) - (0.36 \pm 0.28)NO_3$		8
		with NO_3 & θ°C: $O_2 = (10.82 \pm 0.67) - (0.20 \pm 0.04)NO_3 - (0.30 \pm 0.03)\theta$°C	0.995	7
	1840-4915	with NO_3 only: $O_2 = (7.43 \pm 1.12) - (0.07 \pm 0.06)NO_3$		14
		with NO_3 & θ°C: $O_2 = (9.26 \pm 1.54) - (0.16 \pm 0.08)NO_3 - (0.11 \pm 0.08)\theta$°C	0.571	13

*n-p-1 are the residual degrees of freedom, n is the number of observations and p is the number of independent variables already in the regression equation.

are not reproduced either, again because their use is illustrated with the case of station HAH30 and they are not considered as final results.

In Tables 1 and 2 the regression equations without the θ°C term are given for comparison of the O_2-PO_4 and O_2-NO_3 slopes before and after the mixing effect is extracted.

The precision of the regression coefficients depend not only on the random errors of the O_2, PO_4, NO_3 and θ°C measurements, but also on the ranges of variability of these properties, for the region of the water column under consideration, and on the degrees of freedom of the residuals. Poor precision does not necessarily mean bad field data. Tables 1 and 2 show that in some cases the residuals only had 3 degrees of freedom. With 3 degrees of freedom the value for $t_{(\alpha/2)}$ is 3.18, where α is, in our case, 0.05.

For the regions of the water column, at each station, that are not tabulated in Tables 1 and 2, either the O_2, PO_4 and NO_3 ranges were too small or there were not enough data points to apply the regression analysis.

The Central North Pacific Ocean, around 30°N, has a relatively uniform water column, with respect to the $O_{2_{res}}$-θ°C and $O_{2_{res'}}$-θ°C diagrams (Figures 43 and 47). That, together with the fact that the sampling for HAH30 was appropriate for performing the regression analysis, produced very satisfactory results, as we have shown. But, other parts of the ocean may have many different water types being

mixed and, of course, the hydrocasts have not been designed to meet the necessities of the regression analysis. A hydrocast designed to meet the necessities of this type of regression analysis should have the sampling bottles spaced according to the changes of θ°C, not according to depth. As many samples as possible should be collected from the regions where the $O2_{res}$-θ°C and $O2_{res'}$-θ°C diagrams are relatively straight. To decide on this in advance historical data may be used.

For station AAH2, in the Southeastern Bering Sea, the presence of the temperature minimum and maximum in the upper 400 m (Alvarez-Borrego, Gordon, Jones, Park and Pytkowicz, 1972) made the S‰ a better parameter to be used for the regressions. At HAH52 the temperature minimum and maximum are also present but θ°C was used in the regression with satisfactory results (Table 1).

For GOGO-1 the 7 deepest observations were not used (from 4207 to 4289 m depth). θ°C, O_2, PO_4 and NO_3 do not change significantly in that depth range.

In the Atlantic and in the South Pacific Oceans, changes of O_2, PO_4 and NO_3 are not as great as in the North Pacific Ocean. When changes in these properties are small, the random errors of the determinations are bigger percentagewise.

SCORPIO stations 71 and 72 were chosen because they are geographically very close (43°14.7'S, 80°02.0'W; and 43°19.0'S,

79°01.5'W, respectively) (Figure 31). The difference in location is mainly in longitude. By looking at SCORPIO data we can see that the distribution of physical and chemical properties is almost the same when longitude changes by few degrees, in that part of the ocean. The two stations were treated together to have more degrees of freedom when doing the regression. Another reason for choosing this part of the South Pacific to test Redfield's model is that the ranges for O_2, NO_3 and PO_4 are larger off Chile than at other locations along the same latitude. The two SCORPIO legs were on lines of constant latitude (SIO, reference 69-15; WHOI, reference 69-56).

With few exceptions, most of the results are consistent with Redfield's model (Tables 1 and 2). For the 1200-4200 m depth range of GOGO-1 (Table 2), the θ°C regression coefficient is not significantly different from zero. Nevertheless, the adjustment for the PO_4 regression coefficient was made to a proper interval. This means that if we had chosen a confidence level lower than 95%, i.e. 90%, the result for that depth range would have been consistent with Redfield's model.

For the 405-1765 depth range of HAH52 (Table 1), the θ°C regression coefficient is not significantly different from zero even at very low probability levels. The confidence interval of the PO_4 coefficient, for this depth range, is consistent with Redfield's value with or without adding the θ°C term to the equation.

For stations 71 and 72 of SCORPIO cruise the PO_4 regression coefficient is consistent with Redfield's model. But the NO_3 regression coefficient is slightly higher than the value predicted by Redfield's model. The adjustment of the NO_3 regression coefficient, by adding $\theta°C$ to the equation, was done in the "right" direction, but it went a little too far (Table 1).

In some cases the PO_4 and NO_3 regression coefficients were not significantly different from zero before the $\theta°C$ was added to the equations, but they were adjusted to intervals consistent with Redfield's model when the $\theta°C$ was added to the equations (Tables 1 and 2).

For the depth range of 1215 to 3200 m of station AAH2 the confidence interval for the PO_4 regression coefficient, after $\theta°C$ is added to the equation, is -4.21 ± 1.14 (Table 1). Alvarez-Borrego, Gordon, Jones, Park and Pytkowicz (1972) applied regression analysis to the region of the water column where the $\theta°C$-S‰ diagram is straight (1300 to 3600 m). They treated data from stations AAH2 and AAH9 (also in the Southeastern Bering Sea) together, and obtained a PO_4 regression coefficient of -3.4 ± 1.0. The confidence interval in our case is larger because we have less degrees of freedom. Alvarez-Borrego, Gordon, Jones, Park and Pytkowicz (1972) calculated $P.PO_4$ by using Redfield's model and plotted it versus $\theta°C$ for the region of the water column where they applied the regression. They found a significant, although not very pronounced departure of the $P.PO_4$-$\theta°C$

diagram from linearity. Based on this they indicated that their application of regression analysis to test Redfield's model was a first approximation. Although not shown here, the $O2_{res}$-θ°C diagram for the whole water column of station AAH2 does not detect the presence of a third water type for the depth range 1215 to 3200 m. Unless we have very precise data, the $O_{2_{res}}$-θ°C diagram is able to clearly detect the different water types only when there are abrupt inflections in the $(O'_2 + a_1 P.PO_4)$ versus θ°C diagram. The two confidence intervals, the one obtained by Alvarez-Borrego, Gordon, Jones, Park and Pytkowicz (1972) and the one obtained in this work, are consistent with Redfield's model.

Use of the $O_{2_{res}}$-θ°C diagram for the qualitative study of the proportions of water types

When we began testing Redfield's model for the South Pacific Ocean, we used data from the SOUTHERN CROSS cruise (Horibe, 1970). Due to the ranges for O_2, PO_4 and θ°C being smaller than in the North Pacific Ocean, we did not obtain significant regressions by applying our method to data from one station. Because of this, we tried applying equation (44) to data from two stations simultaneously (off New Zealand) (Figure 31). But, the $O_{2_{res}}$-θ°C diagram (Figure 49) shows that the proportions of the different water types is different at each station. We cannot represent the data from both stations with

the same set of regression equations. Nevertheless, Figure 49 serves the purpose to illustrate that when equation (44) has been applied to data from two stations that are geographically close, the $O_{2_{res}}$-θ°C diagram may be useful to indicate which station has a higher proportion of a certain water type. The $O_{2_{res}}$-θ°C diagram (Figure 49) and the θ-S‰ diagram (Figure 50) show that station 35 has a higher proportion of Antarctic Intermediate water (35 is farther south than 34). Although not shown here, for stations 71 and 72 of SCORPIO cruise, the $O_{2_{res}}$-θ°C diagram does not show any differentiation.

Use of the θ°C-P.PO_4 diagram to trace water masses

Once the field O_2, PO_4 and NO_3 data have been found consistent with Redfield's model, we can calculate quantities by using the model and rely with more certainty on them to describe the ocean. Since PO_4 data from YALOC-66 cruise is more precise than NO_3 data we will use, in this work, only the calculated P.PO_4's to construct θ°C-P.PO_4 diagrams. In most of the cases both diagrams, θ°C-P.PO_4 and θ°C-P.NO_3, provide the same information. Pytkowicz (1968) used T°C-P.PO_4 diagrams to characterize water masses in the Southern Ocean.

Figures 51a-d, 52a-d, and 53a, b, show the θ°C-P.PO_4 diagrams for different parts of the Pacific Ocean and the Southeastern Bering Sea. Figures 51c, d, and 52a, b show a P.PO_4 maximum and a deeper

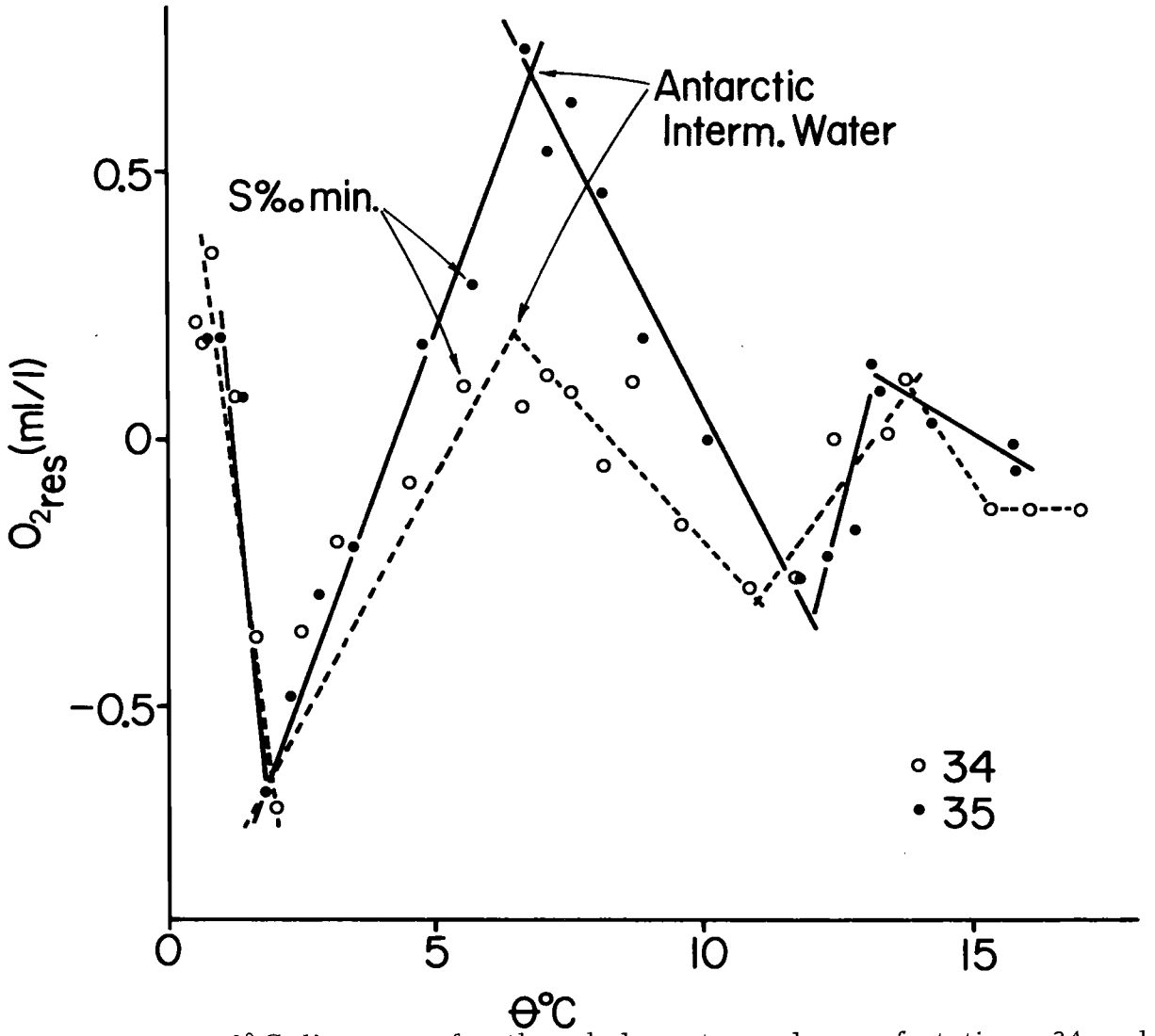

Figure 49. $O_{2_{res}}$ versus θ° C diagrams for the whole water column of stations 34 and 35 of the SOUTHERN CROSS cruise (39°59.5'S, 170°03.2'W and 42°01.2'S, 170°01.8'W, respectively).

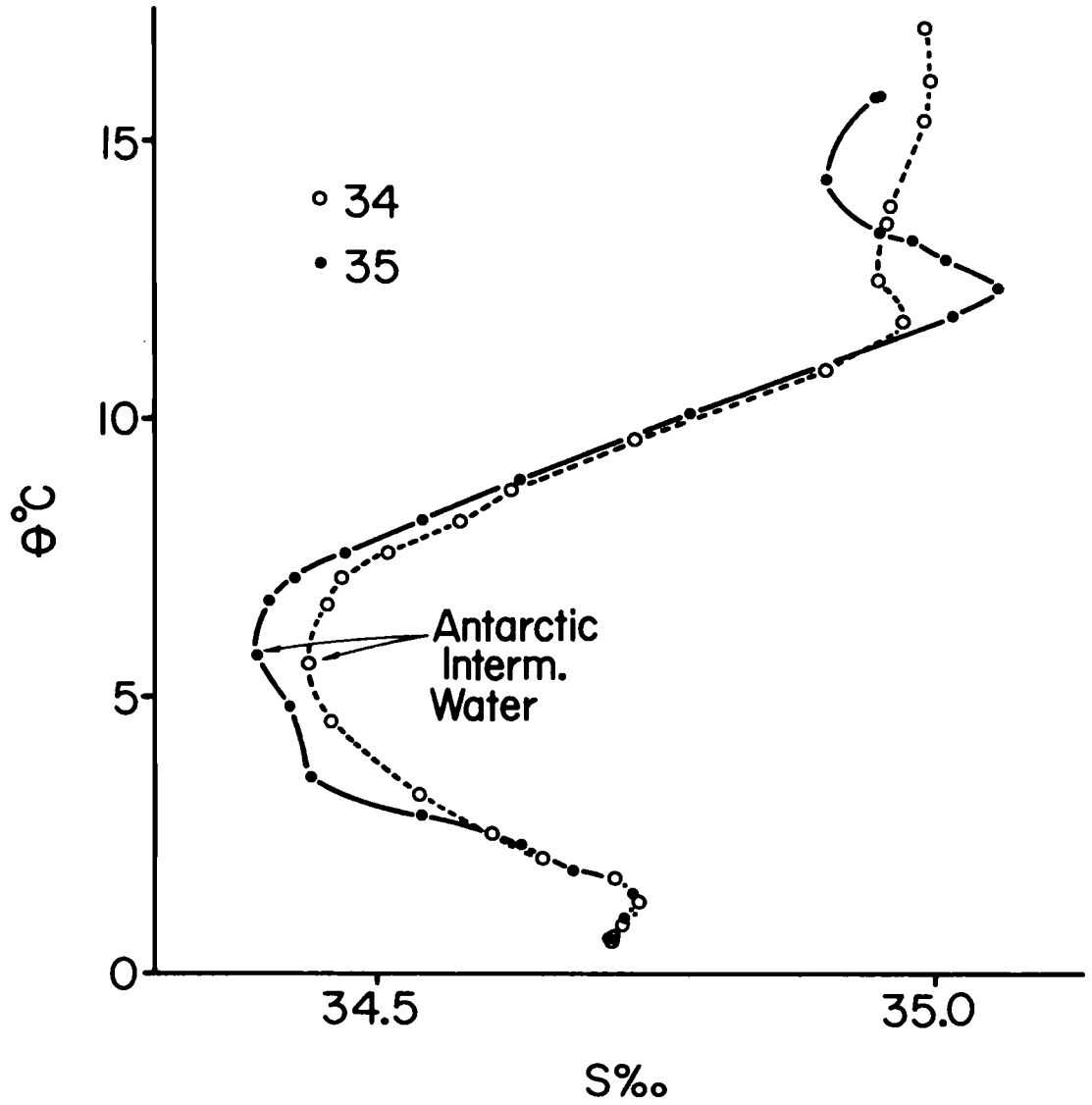

Figure 50. θ° C-S‰ diagrams for stations 34 and 35 of the SOUTHERN CROSS cruise (39°59.5'S, 170°03.2'W and 42°01.2'S, 170°01.8'W, respectively).

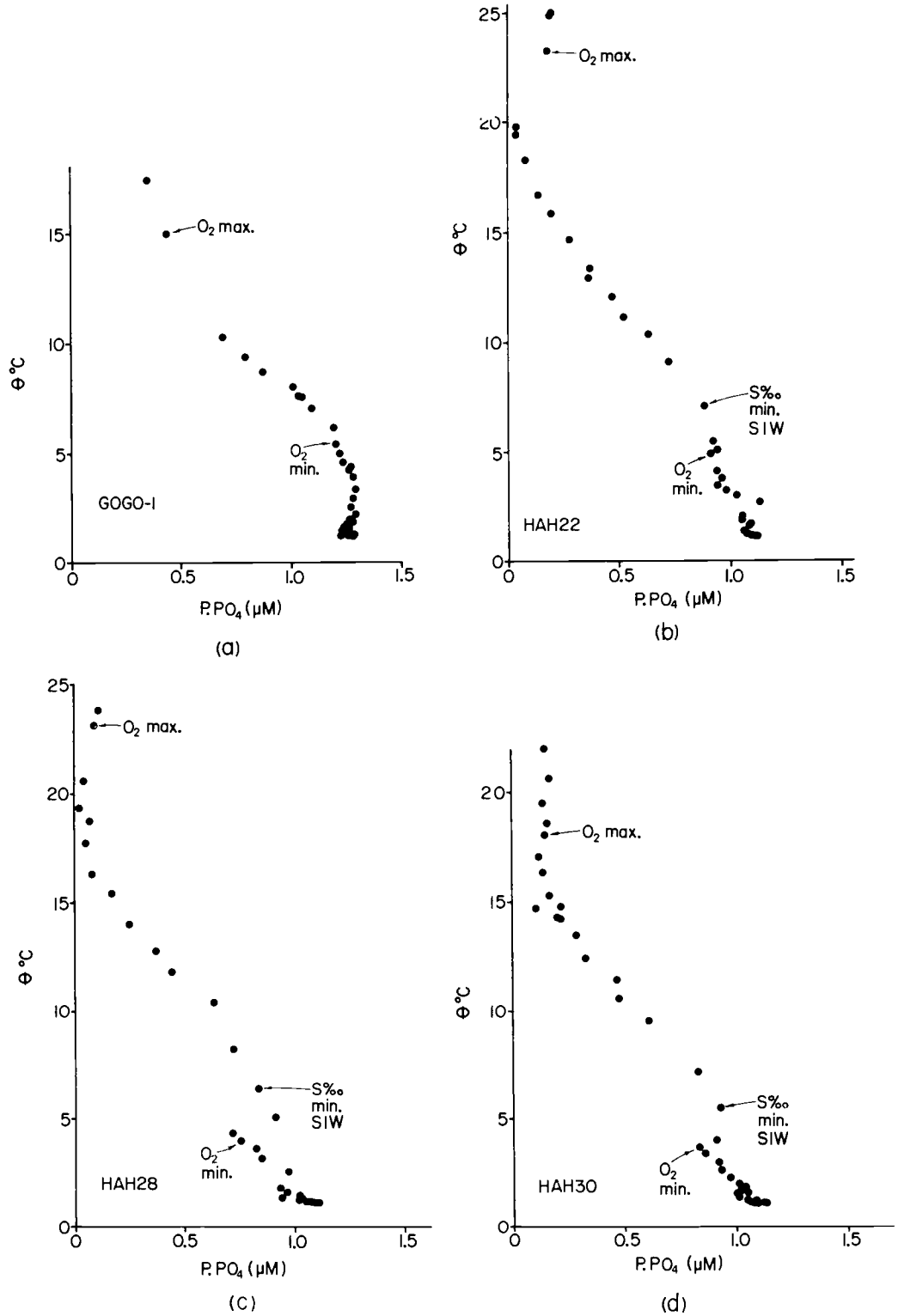

Figure 51. θ°C versus P. PO_4 diagrams for stations GOGO-1 (a) (28°29.0'N, 121°38.0'W), (b) HAH22 (24°30.6'N, 161°30.0'W), (c) HAH28 (29°10.0'N, 161°28.0'W), and (d) HAH30 (30°55.4'N, 162°37.4'W). SIW means Subarctic Intermediate water.

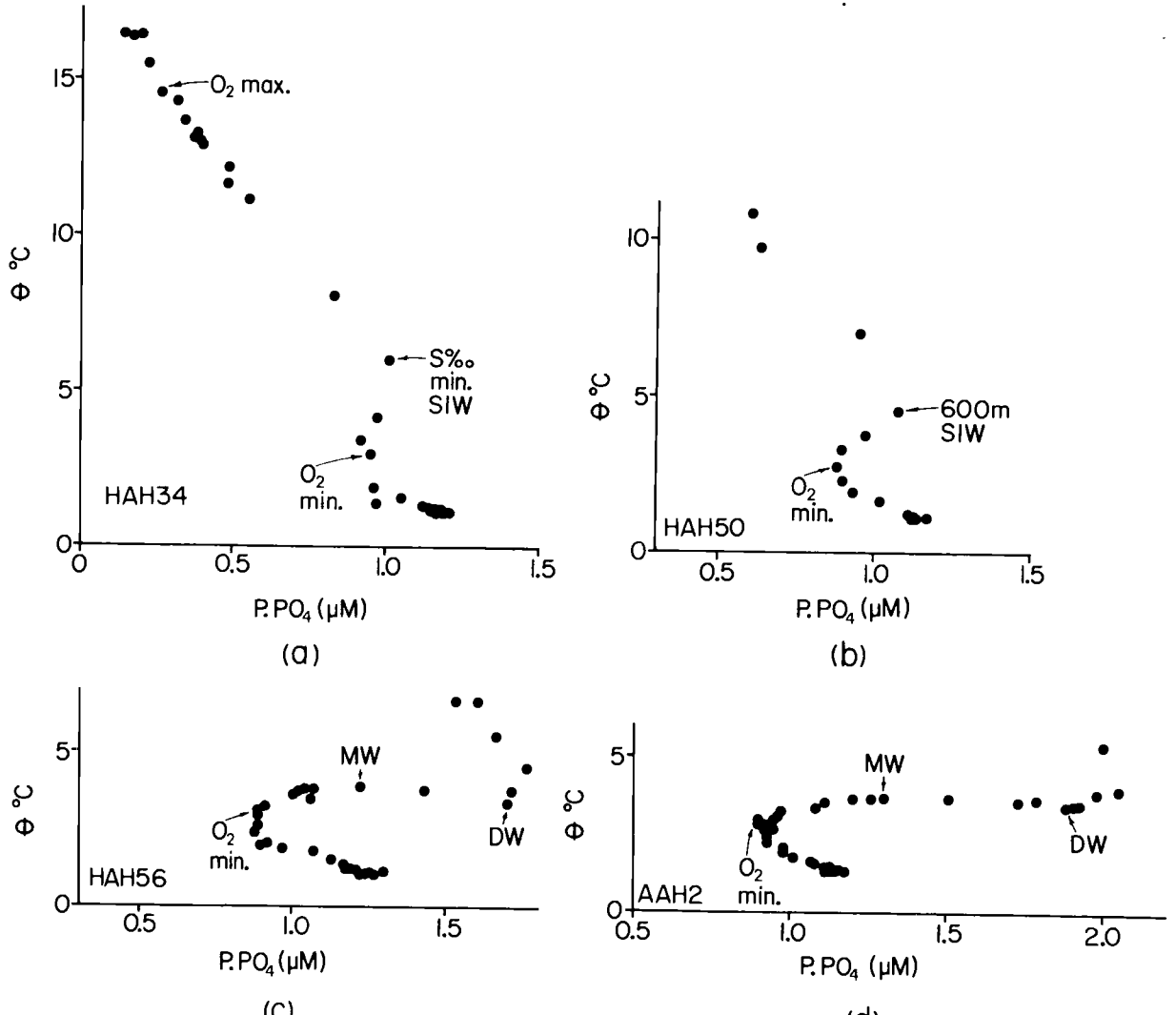

Figure 52. θ°C versus P. PO_4 diagrams for stations HAH34 (a) (35°26.5'N, 165°47.8'W), (b) HAH50 (43°04.6'N, 171°25.0'W) (c) HAH56 (50°27.5'N, 176°13.8'W), and (d) AAH2 (52°56.1'N, 177°55.0'W). SIW means Subarctic Intermediate water.

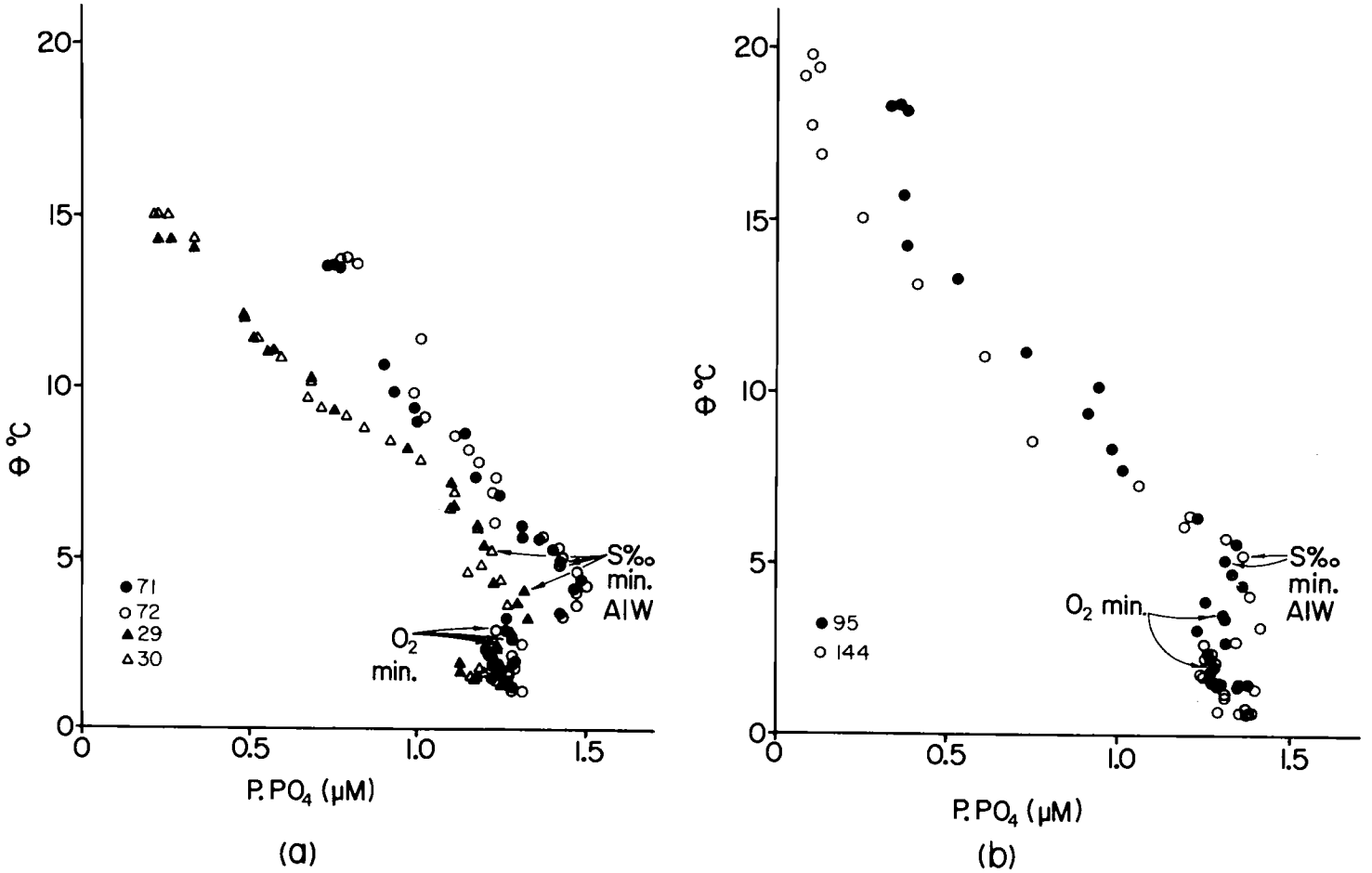

Figure 53. θ° C versus P. PO_4 diagrams for stations 29, 30, 71 and 72 (a), and for stations 95 and 144 (b), of SCORPIO expedition. The position of the stations are: 29 (43°15.0'S, 169° 50.0'W), 30 (43°15.0'S, 169°04.5'W), 71 (43°14.7'S, 80°02.0'W), 72 (43°19.0'S, 79° 01.5'W), 95 (28°15.7'S, 79°07.3'W) and 144 (28°15.7'S, 170°14.8'W). AIW means Antarctic Intermediate water.

$P.PO_4$ minimum. The $P.PO_4$ maximum indicates the presence of the Subarctic Intermediate water. Park (1967b) used $P.PO_4$ to characterize the Subarctic Intermediate water in a section constructed with data from leg HAH of YALOC-66. The Subarctic Intermediate water has been classically characterized by a S‰ minimum. According to Reid (1965) this S‰ minimum is recognizable as far south as ~10°N, along 160°W. Park's (1967b) section also shows the deeper $P.PO_4$ minimum. The $P.PO_4$ minimum (Figures 51c,d and 52a-d) coincides with the O_2 minimum. Alvarez-Borrego, Gordon, Jones, Park and Pytkowicz (1972) found the $P.PO_4$ minimum in the Southeastern Bering Sea. They indicated that possibly this $P.PO_4$ minimum is the core of a water mass which when at the sea surface had undergone intense photosynthesis with depletion of PO_4 to very low values.

Off Baja California and near Hawaii (stations GOGO-1 and HAH22) (Figures 30, 51a, b) neither the $P.PO_4$ maximum nor the minimum are apparent. At station HAH30 the $P.PO_4$ minimum of Figure 51d corresponds to water D in Figure 43. It almost coincides with the sigma-t surface of 27.28 that Reid (1965) used to study the Antarctic Intermediate water. According to Reid (1965) this sigma-t surface lies more than 350 m below the sea surface everywhere in the North Pacific. If the explanation given by Alvarez-Borrego, Gordon, Jones, Park and Pytkowicz (1972) for the $P.PO_4$ minimum is correct, the source of this water should not be in the North Pacific

Ocean.

Figures 53a, b show that the Antarctic Intermediate water is not characterized by a $P.PO_4$ minimum in the South Pacific. Thus, the $P.PO_4$ minimum present in the North Pacific Ocean and Southeastern Bering Sea is not formed at the Pacific sector of the Antarctic convergence. Figure 53a shows that for stations 71 and 72 (off Chile), of SCORPIO expedition, the Antarctic Intermediate water is characterized by a well-defined $P.PO_4$ maximum. Redfield (1942) found this $P.PO_4$ maximum from the Antarctic convergence to about 10°N in the Atlantic Ocean. Figure 53a shows that for stations 29 and 30 (off New Zealand) of SCORPIO expedition, the $P.PO_4$ maximum is not very apparent. Stations 29, 30, 71 and 72 are at the same latitude (Figure 31). Although Figure 53a does not show the $\theta°C$-$P.PO_4$ diagrams for stations located between 30 and 71 and between New Zealand and the Southern Australian coast, the $P.PO_4$ maximum diminishes gradually from east to west at this latitude in the South Pacific. Station 71 has almost the same geographic location as station 72, and station 29 has almost the same geographic location as station 30. We have plotted the $\theta°C$-$P.PO_4$ diagrams for both 71 and 72, and both 29 and 30, to check for consistency of the data.

If the $P.PO_4$ minimum observed in the North Pacific Ocean is formed at the Antarctic convergence, the only possibility left would be that it is formed in the Eastern Atlantic Ocean and Western Indian

Ocean sectors. It would have to be transported through the Indian Ocean and through the Celebes Sea, north of Australia, into the Pacific Ocean. This is a very remote possibility indeed, but in order not to leave it out we have plotted the θ°C-P.PO_4 diagrams for several stations of the ANTON BRUUN cruise 2. Figures 54a, b show that there is no P.PO_4 minimum nor maximum in the Indian Ocean between 35°S and 00°. The P.PO_4 values of deep waters decrease as we go north in the Indian Ocean (Figure 54a, b) possibly because of

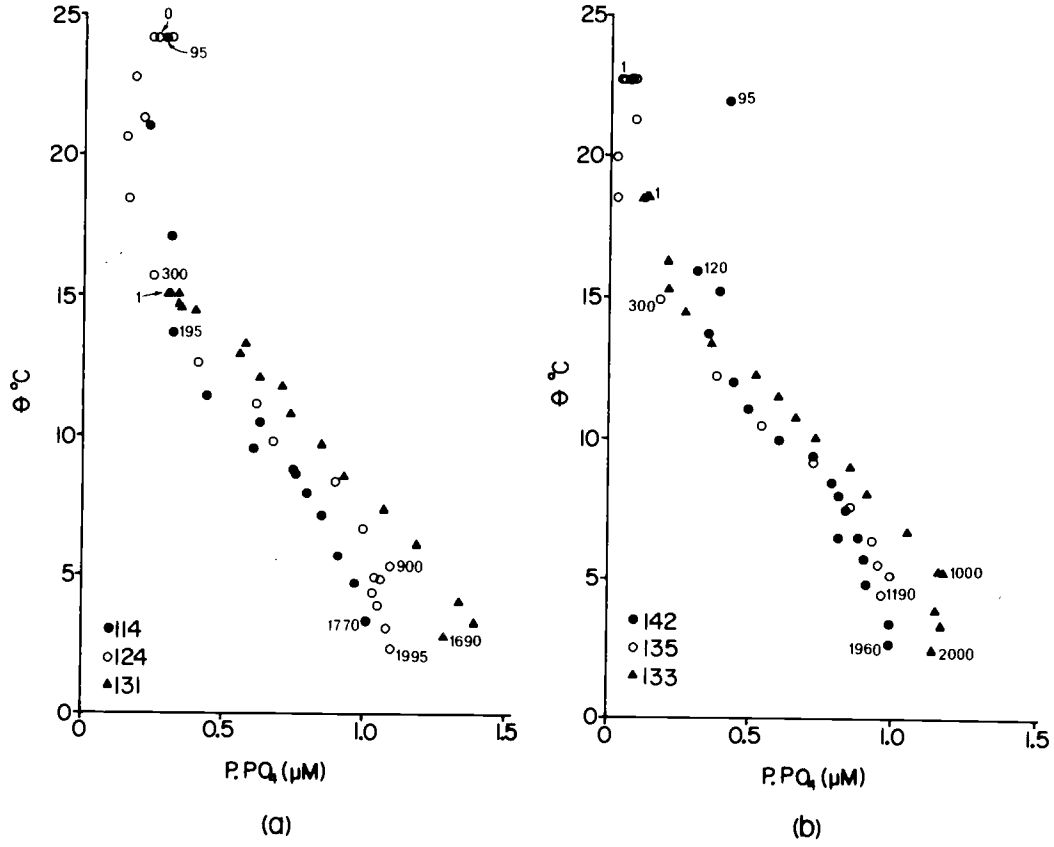

Figure 54. θ°C versus P.PO_4 diagrams for stations 114, 124 and 131 (a) and for stations 133, 135 and 142 (b) of the ANTON BRUUN cruise 2. The positions of the stations are: 114 (01°N, 70°01'E), 124 (19°30'S, 69°51'E), 131 (35°09'S, 69°59'E), 133 (30°11'S, 79°42'S), 135 20°02'S, 79°50'E) and 142 (00°33'S 80°08'E).

mixing with surface water with low $P.PO_4$. Thus, the $P.PO_4$ minimum present at intermediate depths in the North Pacific Ocean and Southeastern Bering Sea is not formed as such in any sea surface source.

Figures 55a, b show the $\theta°C$-$P.PO_4$ diagrams for two stations of the 25th cruise of VITYAZ in the Central Pacific Ocean (near the equator). Unfortunately there are only few data points for those two stations (the near surface data points with $\theta°C > 20°$ were not plotted). Nevertheless, we can see, from Figures 55a, b that in the Central Pacific Ocean the $\theta°C$-$P.PO_4$ diagram for waters below few hundred meters depth does not show any minimum nor maximum. At

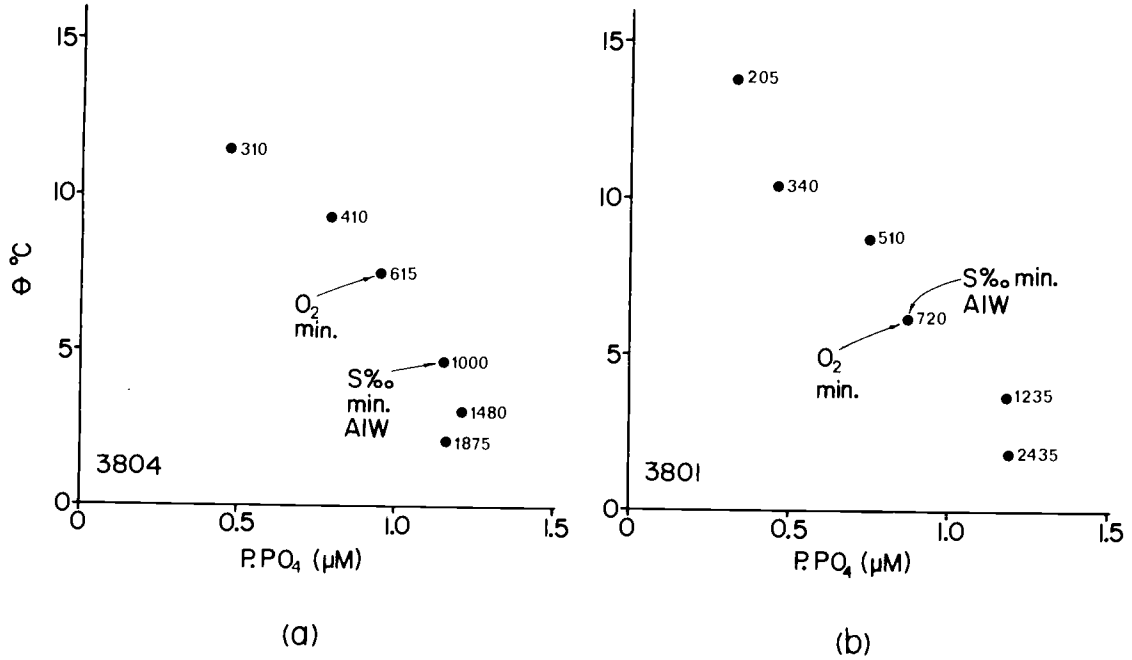

Figure 55. $\theta°C$ versus $P.PO_4$ diagrams for stations (a) 3804 and (b) 3801 of the 26th expedition of the VITYAZ. The numbers by the data points represent depth in meters. The positions of the stations are: 3801 (02°25'S, 173°27'W) and 3804 (04°57'S, 172°36'W). AIW means Antarctic Intermediate water.

this geographic location (Figures 55a, b) the Antarctic Intermediate water has lower values of $P.PO_4$ than the deeper waters, and higher values than the shallower waters. Figure 56a illustrates diagrammatically how the $P.PO_4$ maximum characterizing the Antarctic Intermediate water in the South Pacific is eroded, as it moves northward, by mixing with shallower waters with lower $P.PO_4$ values; and Figure 56b shows how the $P.PO_4$ minimum is formed at intermediate depths as the shallower waters are characterized by higher $P.PO_4$ values. The higher $P.PO_4$ values of the Subarctic Intermediate water

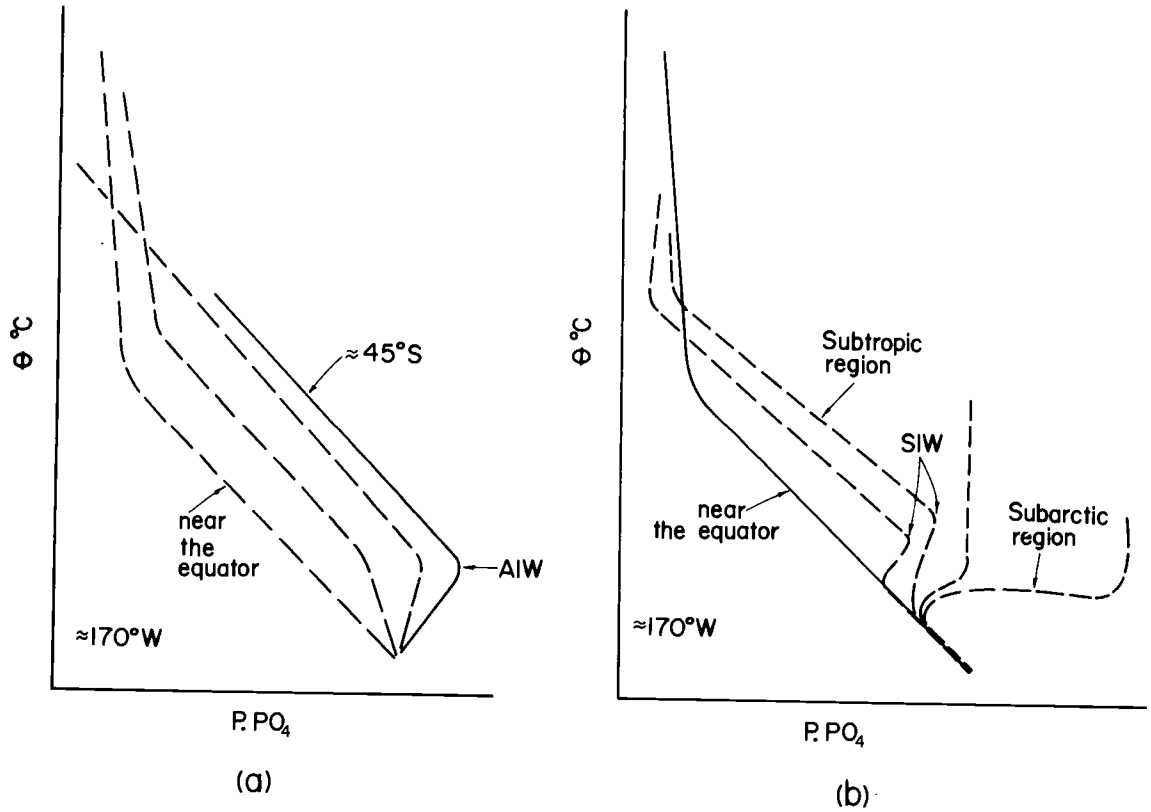

Figure 56. θ°C versus $P.PO_4$ diagrams for the (a) South Pacific Ocean and (b) North Pacific Ocean. AIW and SIW mean Antarctic Intermediate water and Subarctic Intermediate water respectively.

and of the surface waters of the Subarctic region make the $P.PO_4$ values at intermediate depths to be minimum. Thus, the $P.PO_4$ minimum observed at high latitudes in the North Pacific is just the product of having high $P.PO_4$ values in the surface waters of this region of the ocean.

There is a trend, for the sigma-t values that correspond to the $P.PO_4$ minimum, to increase as latitude increases. At HAH28 the $P.PO_4$ minimum is at the sigma-t surface of 27.11 while at HAH50 it is at the sigma-t surface of 27.44. North of HAH50 (Figure 30) the sigma-t values that correspond to the $P.PO_4$ minimum do not change significantly.

The $P.PO_4$ values for the near bottom waters of the different stations studied (Figures 51, 52 and 53) differ in some cases, from station to station, and specially from cruise to cruise, by as much as 0.2 μM. This is probably due to the fact that there is not yet an international standard for PO_4 determinations. Standards for PO_4 still have to be prepared manually for each station. However, the main problem with PO_4 analysis is still not the accuracy but the precision. Steps should be taken to improve the precision of the methods before an international standard can be accepted. Data from GOGO-1 station were the most precise we used in this study.

Diagrammatic illustration of the extraction of the mixing effect

Station HAH22 has an almost straight $P.PO_4$-$\theta°C$ diagram (Figure 51b) for the region of the water column from 75 to 4550 m depth (below the near surface O_2 maximum). Although not shown here, its O_2'-$\theta°C$ diagram is very similar to the one for HAH30 (Figure 44). This gives us an opportunity to illustrate diagrammatically, in a very clear way, the extraction of the mixing effect by adding a term with a conservative property, such as $\theta°C$, to the regression equation.

The O_2-PO_4 diagram for station HAH22 (Figure 57) is not linear, it has a hook-like shape at the lower O_2's. If this is due to variation in the preformed quantities, $\theta°C$ should extract the mixing effect and leave a linear relationship between O_2 and PO_4. In the case of HAH22 it is only to a first approximation because the O_2'-$\theta°C$ and $P.PO_4$-$\theta°C$ diagrams are not completely linear.

When regressing O_2 on PO_4 and $\theta°C$, since PO_4 and $\theta°C$ are correlated to a certain extent, the PO_4 term represents the regression of the residuals of O_2, after regression on $\theta°C$, on the residuals of PO_4, after regression on $\theta°C$. In other words, if we do the regression in a stepwise manner, adding $\theta°C$ first we have

$$O_2 = c_o + c_1 \theta°C + O_{2_r} \qquad (61)$$

and implicitly and simultaneously

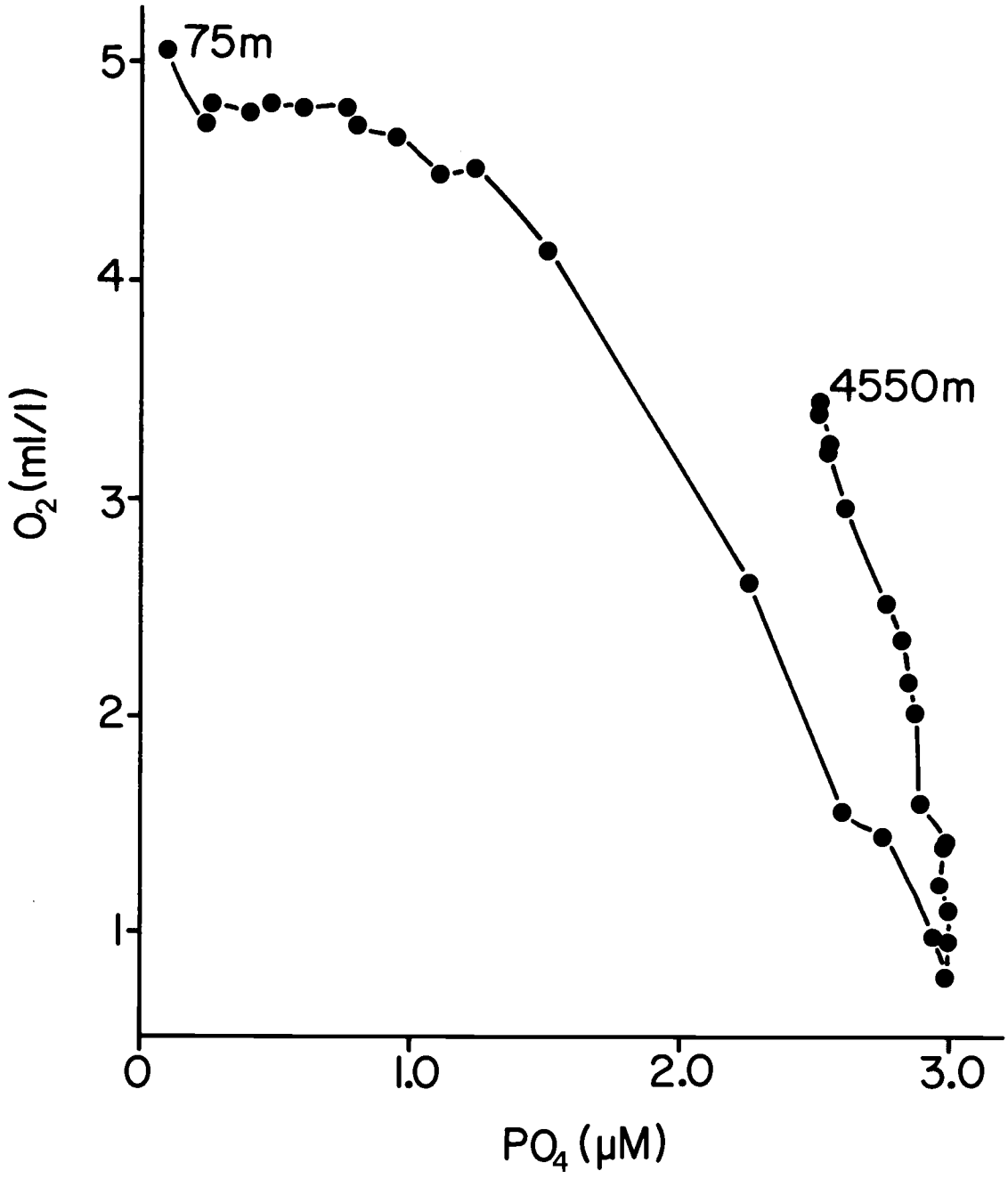

Figure 57. Oxygen-phosphate diagram for station HAH22 (24°30.6'N, 161°30.0'W).

$$PO_4 = d_o + d_1\theta°C + PO_{4_r} \tag{62}$$

where c_o, c_1, d_o, and d_1 are constant regression coefficients and O_{2_r} and PO_{4_r} are the O_2 and PO_4 residuals after regression on $\theta°C$.

When we add PO_4 to regression equation (61), what we are doing is regressing O_{2_r} on PO_{4_r}

$$O_{2_r} = f_o + a_1 PO_{4_r} + O_{2_{res}} \tag{63}$$

where f_o and a_1 are constant regression coefficients and $O_{2_{res}}$ is as defined for equation (44); substituting the value of PO_{4_r} from equation (62) into equation (63) we have

$$O_{2_r} = (f_o - a_1 d_o) + a_1 PO_4 - a_1 d_1 \theta°C + O_{2_{res}} \tag{64}$$

substituting equation (64) into equation (61)

$$O_2 = (c_o + f_o - a_1 d_o) + a_1 PO_4 + (c_1 - a_1 d_1)\theta°C + O_{2_{res}} \tag{65}$$

$(c_o + f_o - a_1 d_o)$ and $(c_1 - a_1 d_1)$ are constants, we can represent them by the symbols a_o and a_2 respectively; equation (65) is the same as equation (44). The PO_4 regression coefficient of equation (44), a_1, is the slope of the O_{2_r} versus PO_{4_r} diagram.

For station HAH22 the O_2-PO_4, O_2-$\theta°C$ and PO_4-$\theta°C$ correlation coefficients are, respectively, -0.91, 0.75 and -0.95. Applying equations (61) and (62) we have

$$O_2 = (1.68 \pm 0.56) + (0.18 \pm 0.06)\theta°C \tag{66}$$

$$PO_4 = (3.19 \pm 0.18) - (0.16 \pm 0.02)\theta°C \tag{67}$$

Figure 58 shows the O_{2_r} versus PO_{4_r} diagram. The hook-like shape shown by Figure 57 has disappeared after the θ°C has extracted the mixing effect. The O_{2_r}-PO_{4_r} correlation coefficient is -0.99 and the confidence interval for the O_{2_r}-PO_{4_r} slope is -3.03±0.14, which is consistent with Redfield's model. In Figure 58 the data points do not follow a sequence, with reference to depth, along the line. In other words, the points at one end are not necessarily the near surface points, and the points at the other end are not necessarily the deep points. The data points at the lower end of the O_{2_r}-PO_{4_r} diagram correspond to the O_2 minimum zone.

O_{2_r} and PO_{4_r} should not be regarded as the non-conservative fractions of O_2 and PO_4. By definition the O_{2_r}'s and PO_{4_r}'s add to zero, respectively. For this station the calculated ranges for AOU and $PO_{4_{ox}}$ are 0.16 to 6.40 ml/l and 0.05 to 2.05 μM, respectively. The ranges for O_{2_r} and PO_{4_r} are only about half the size of the ranges for AOU and $PO_{4_{ox}}$ (Figure 58). This is due to the AOU and $PO_{4_{ox}}$ not being completely geometrically uncorrelated with θ°C. In nature AOU and $PO_{4_{ox}}$ do not depend on θ°C but, nevertheless, their correlation coefficients are not zero. Thus, when we make the step-wise regression adding θ°C first (equation 61), the θ°C term already contains not only the information about (O_2' + 3.1 PO_4), but also some fraction of the AOU and $PO_{4_{ox}}$.

This means that although the fact that the PO_4 regression

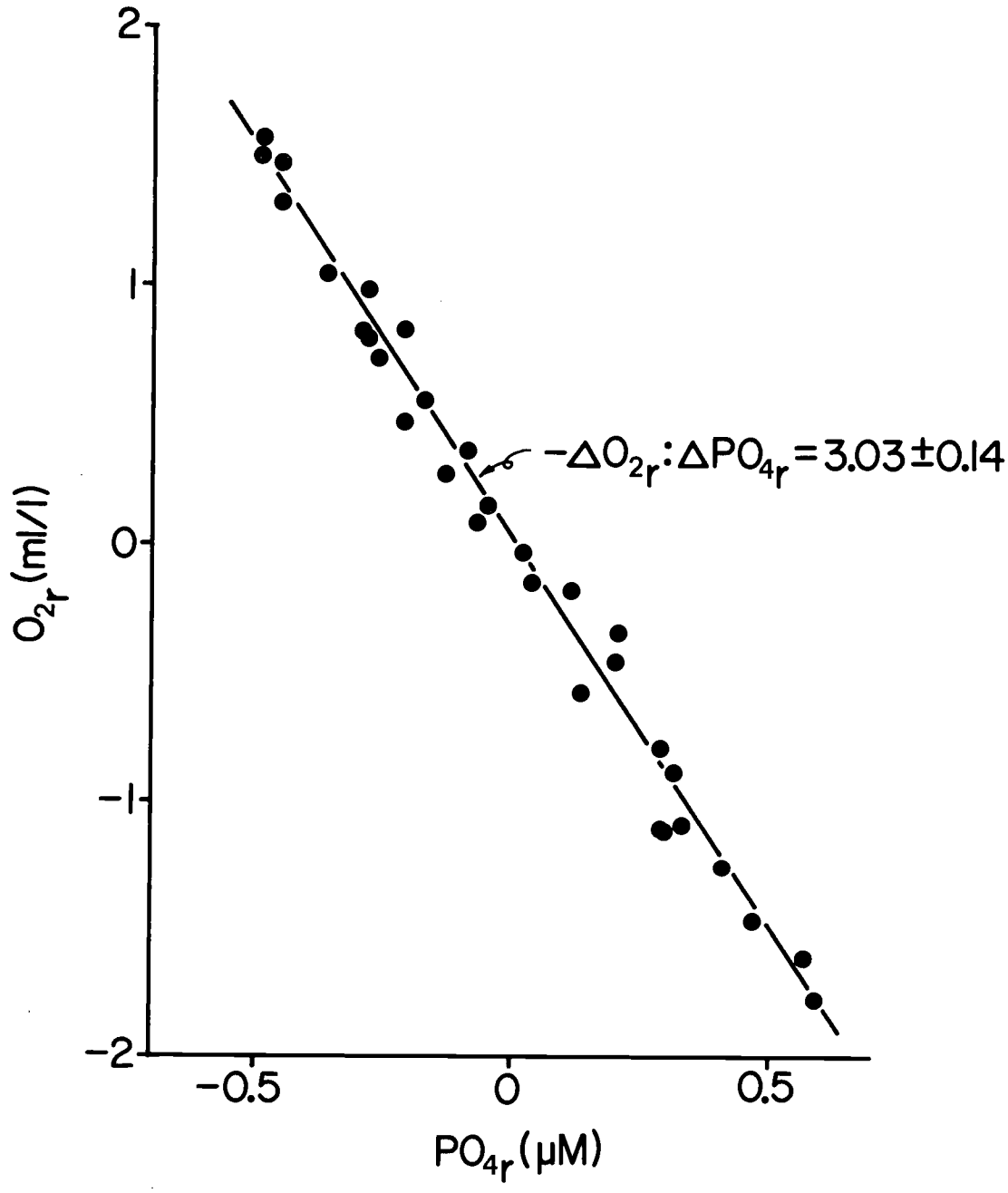

Figure 58. O_{2_r} versus PO_{4_r} diagram for station HAH22 (24° 30.6N, 161° 30.0'W).

coefficient of equation (44) is significantly different from zero indicates that biological oxidation is occurring, the reverse is not necessarily true. Because the $\theta^\circ C$ term may contain all the information about AOU due to high $\theta^\circ C$-AOU correlation, so that the regression of O_{2_r} on PO_{4_r} is not significant. These are geometric effects that may occur by chance. These types of effects are not due at all to the order in which the independent variables are added to the regression equation, but only to the correlations between the different variables. The order in which the independent variables are added to the regression equation is immaterial.

When PO_4 is added to the regression the adjustment is made for the $\theta^\circ C$ term (equation 65) so that in the final equation it only represents the conservative fractions of O_2 and PO_4. The O_{2_r}-PO_{4_r} diagram is useful only for calculating the ratio of the non-conservative fractions of O_2 and PO_4.

The complete regression equation for HAH22 (75 to 4550 m) is

$$O_2 = (11.33 \pm 0.45) - (0.31 \pm 0.02)\theta^\circ C + \\ - (3.03 \pm 0.14)PO_4 \qquad (68)$$

with a coefficient of determination $R^2 = 0.994$.

Figure 59 illustrates the comparison between field O_2 data, and the data calculated by using equation (68) and field PO_4 and $\theta^\circ C$ data from station HAH22. The standard error of the calculated values is almost constant. In all cases, from near the sea surface to near the

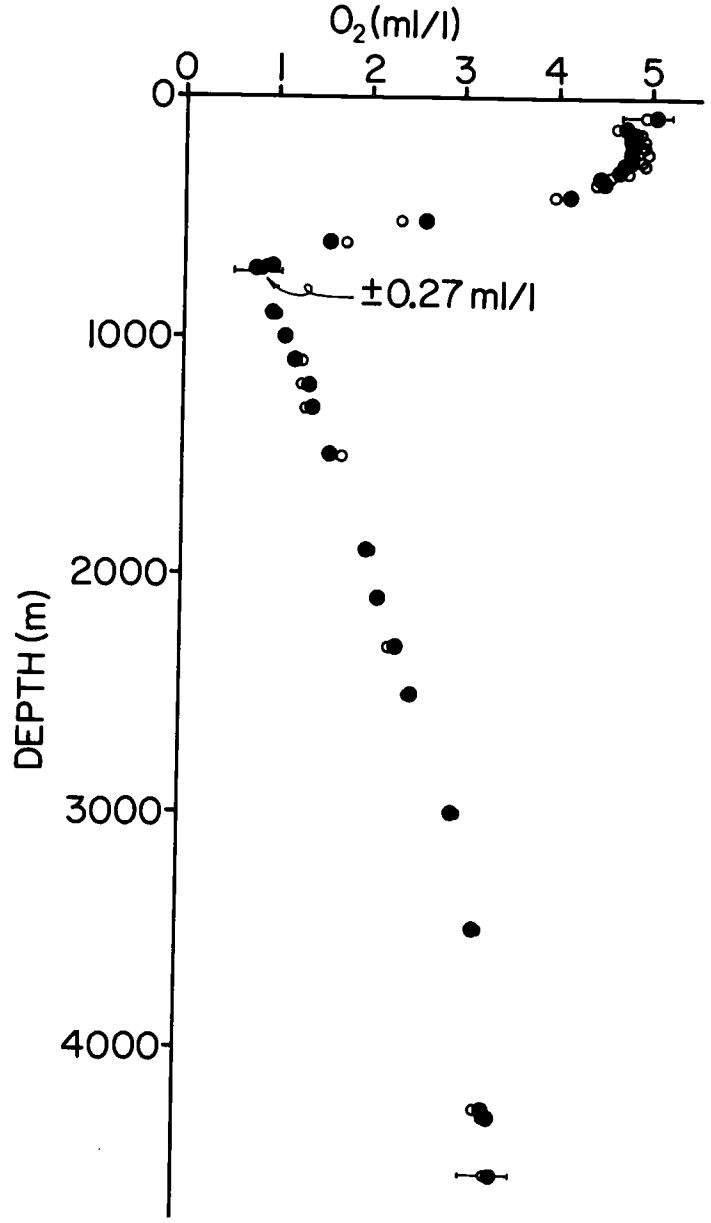

Figure 59. Oxygen profile for station HAH22. Comparison between measured data (closed circles) and data calculated by using equation (68), and PO_4 and θ°C measured data (open circles). The bars at the oxygen minimum zone, 75 m and 4550 m are the confidence intervals of the calculated values at 95% confidence level.

bottom, the confidence intervals, at the 95% confidence level, are the predicted points plus or minus 0.27 ml/l. This indicates that one of

the statistical requirements for the proper application of regression analysis, that the variance of the dependent variable should not be a function of the independent variables, is fulfilled.

Conclusions

In the Northeastern Pacific Ocean the O_2-PO_4 and O_2-NO_3 relationships for the region of the water column above the O_2 minimum zone vary systematically with latitude. A similar but less pronounced variation is found below the O_2 minimum zone. The slopes for these relationships in general increase with increasing latitude. In the entire water column, these slopes vary with depth. An effect on the slopes of the O_2-PO_4 and O_2-NO_3 relationships, similar to that observed when decreasing latitude, is observed when comparing winter versus summer data. The winter slopes are higher than the summer slopes.

The slope of the NO_3-PO_4 relationship for the region of the water column above the O_2 minimum zone also changes with latitude but in a much less pronounced way than the slopes for the O_2-PO_4 and O_2-NO_3 relationships. Below the O_2 minimum zone there is a pronounced variation of the NO_3-PO_4 relationship with latitude. The summer value for the NO_3-PO_4 slope is higher than the winter value.

Multiple regression analysis was applied to the oxygen, phosphate, nitrate, and potential temperature data from stations at different

geographic locations in the Pacific and Atlantic Oceans. Confidence intervals of 95% for the regression coefficients are consistent with the values predicted by the Redfield model for the ΔO_2:ΔPO_4 and ΔO_2:ΔNO_3 ratios for biological processes. Thus, the variation of the O_2-PO_4, O_2-NO_3 and NO_3-PO_4 slopes with depth, with latitude, and with time of the year is due to mixing between different water types with different preformed portions of oxygen, phosphate and nitrate.

Diagrams of the O_2 residuals after regression of O_2 on θ°C and PO_4, or on θ°C and NO_3, have proven to be useful to detect water types, some of which are not clearly shown by the classical T-S diagram. Qualitative studies on the proportions of water types at different stations can also be done by using the O_2 residuals versus θ°C diagram.

Once the field O_2, PO_4 and NO_3 data have been found consistent with Redfield's model, we can calculate quantities by using the model and rely on them with more certainty to describe the ocean. P.PO_4's were calculated by using Redfield's model and θ°C-P.PO_4 diagrams were constructed for different regions of the ocean. In the North Pacific Ocean the Subarctic Intermediate water is characterized by a P.PO_4 maximum. A deeper P.PO_4 minimum is also present. In the South Pacific Ocean the Antarctic Intermediate water is characterized by a P.PO_4 maximum which is eroded by mixing with surface water with low P.PO_4 values as the water moves northward. Near the

equator, in the Pacific Ocean, there is no minimum nor maximum in the θ°C-P.PO_4 diagram. In the Indian Ocean there is no minimum nor maximum in the θ°C-P.PO_4 diagram either. The P.PO_4 minimum present at intermediate depths in the northern North Pacific Ocean and Bering Sea is the product of having high P.PO_4 surface values in this oceanic region.

IV. OXYGEN-TOTAL INORGANIC CARBON DIOXIDE RELATIONSHIP IN THE PACIFIC OCEAN

Redfield (1934) proposed a model to explain the proportions of organic derivatives in sea water based on dissolved oxygen concentration (O_2), phosphate (PO_4), nitrate (NO_3) and total inorganic carbon dioxide (TCO_2) data from the Western Atlantic Ocean and on the elementary composition of plankton. The model is based on the assumption that, when biological oxidation occurs, the ratios of the consumption of dissolved oxygen to the production of nutrients and carbon dioxide are constant. So that, if we want to estimate the contribution of biological oxidation to the concentration of nutrients and total inorganic carbon dioxide, we need only calculate the amount of dissolved oxygen that has been utilized and multiply it by the respective constants associated with each of the nutrients and the inorganic carbon dioxide (Alvarez-Borrego, Guthrie, Culberson and Park, 1972).

There have been some modifications to the model since Redfield proposed it in 1934. Fleming (1941) assembled more extensive data for the elementary composition of plankton and proposed the ratios 106:16:1 for C:N:P, by atoms. Based on Fleming's (1941) values Redfield, Ketchum and Richards (1963) proposed that for each atom of phosphorus that is released by biological oxidation 276 atoms of dissolved oxygen are consumed from sea water. In this work we will

call the model Redfield's model. When O_2 and TCO_2 are expressed in mg-at/l and mM respectively, the ratio predicted by Redfield's model is $\Delta TCO_2:\Delta O_2 \doteq -106:276 \doteq -0.384$; and when O_2 is expressed in ml/l and TCO_2 is expressed in mM the predicted ratio is $\Delta TCO_2:\Delta O_2 \doteq -0.106:3.1 \doteq -0.0342$.

Postma (1964) and Craig (1969) questioned the validity of Redfield's model because they did not find a linear relationship between O_2 and TCO_2. But Culberson and Pytkowicz (1970) have shown that when changes in TCO_2 due to all the processes other than oxidation are compensated for, linear relationships between apparent oxygen utilization (AOU) (Redfield, 1942) and TCO_2 with essentially the slope predicted by Redfield's model are found. Culberson (1972) showed that the vertical and horizontal distribution of TCO_2 in the Pacific, Indian and South Atlantic Oceans conform to Redfield's model.

Culberson and Pytkowicz (1970) and Culberson (1972) used a direct approach to correct their AOU and TCO_2 data. Based on theoretical considerations they corrected the data so that only the changes due to biological processes were left. Their work was essentially a test of Redfield's model. The assumptions involved in their calculations are that the specific alkalinity at the source of the waters is constant, and that changes in total alkalinity (TA) are only due to changes of S‰ and precipitation or dissolution of carbonates.

Ben-Yaakov (1971, 1972) has introduced multiple linear

regression analysis to the study of the relationships between TCO_2, O_2, TA, T°C and S‰ in the ocean. He has shown that there is a linear relation between TCO_2, O_2, TA and T°C along vertical profiles in the Eastern Pacific. For his 1971 paper he used Culberson and Pytkowicz's (1970) data and found that the data are consistent with Redfield's model; but he suggested that two other processes, besides carbonate reaction, may be responsible for TA changes. For his 1972 paper he used data from a GEOSECS intercalibration station (Craig and Weiss, 1970; Takahashi, Weiss, Culberson, Edmond, Hammond, Wong, Li, and Bainbridge, 1970) and found the 95% confidence interval for the TA regression coefficient consistent with the assumption that, besides the S‰ effect, TA changes are only due to carbonate dissolution or precipitation. He indicated that possibly the inconsistency shown in his 1971 results are due to some systematic errors in the data. In his 1972 work he reports that the best estimate for the $\Delta TCO_2:\Delta O_2$ ratio, at the 95% confidence level is -0.042 ± 0.004 mM/ml, which is not consistent with Redfield's value of -0.0342. Thus, there is a discrepancy between the results of Culberson and Pytkowicz (1970) and Culberson (1972) and the results of Ben-Yaakov (1971), and between the results of Ben-Yaakov (1972) and Redfield's model.

Ben-Yaakov (1971, 1972) used the correlation coefficient and F ratio values (Draper and Smith, 1966) as the criteria to decide on

what the best results were. To test for the proper application of regression analysis to the field data he plotted the TCO_2 residuals, after regression on O_2, TA, and T°C, versus depth and versus TCO_2. According to him the TCO_2 residuals were small enough to assume that they result from only the random errors of the TA, pH, O_2 and T°C data, according to the reported precisions of these variables.

Alvarez-Borrego, Gordon, Jones, Park and Pytkowicz (1972) and Alvarez-Borrego, Guthrie, Culberson and Park (1972) applied multiple regression analysis to O_2, nutrients and potential temperature (θ°C) data to test Redfield's model. They found that the data are consistent with the model. Alvarez-Borrego, Guthrie, Culberson and Park (1972) developed a technique to separate the water column into suitable portions for the proper application of regression analysis.

The purpose of the present work is to solve the discrepancy between the theoretical and statistical approaches by introducing corrections to the data before the application of the statistical method. We apply the technique used by Alvarez-Borrego, Guthrie, Culberson and Park (1972) to separate the data from the whole water column into subsets for the proper application of regression analysis.

Sources of data

For this study we used the data that Ben-Yaakov (1971, 1972) used, that is, data from stations 70 and 127 of YALOC-69 (Culberson

and Pytkowicz, 1970) and data from the 1969 GEOSECS intercalibration station (Craig and Weiss, 1970; Takahashi, Weiss, Culberson, Edmond, Hammond, Wong, Li and Bainbridge, 1970). In addition to these, data from YALOC-66 cruise (Barstow, Gilbert, Park, Still and Wyatt, 1968) are used. TCO_2 data from YALOC-66 and YALOC-69 were calculated from pH and TA data, and TCO_2 data from the 1969 GEOSECS station were measured by gas chromatography. The location of the stations are shown in Figure 60.

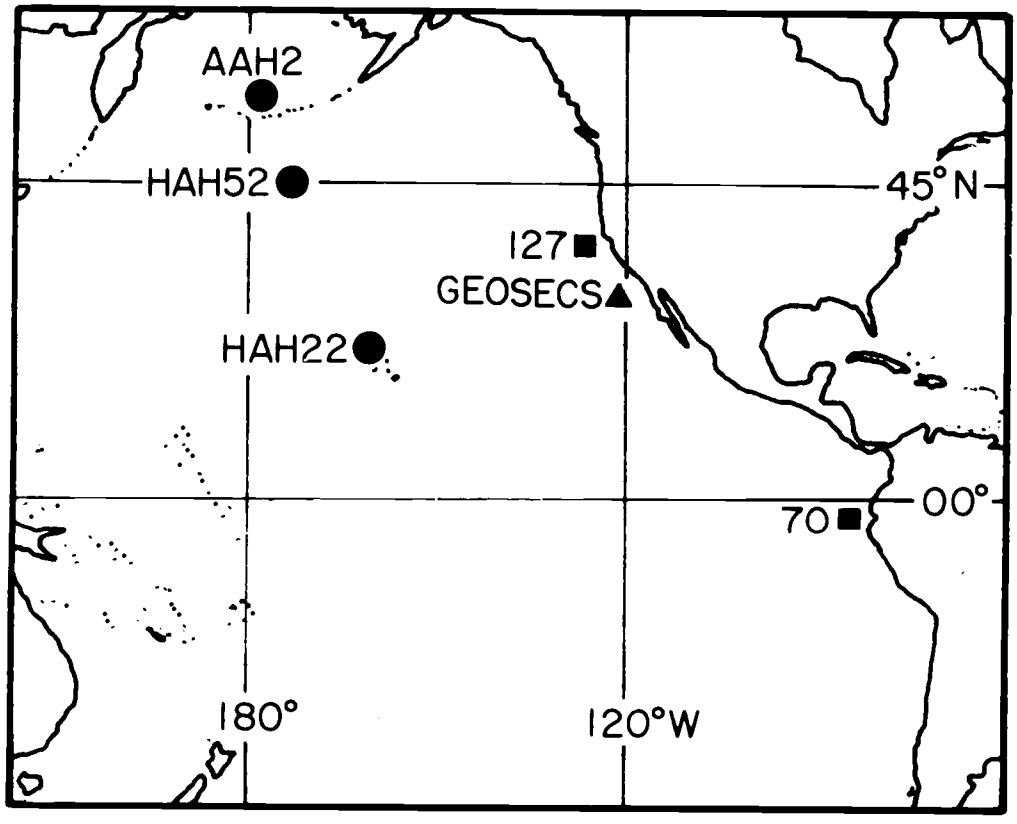

Figure 60. Location of the stations used in this study. HAH22: 24° 30.6'N, 161°30.0'W; HAH52: 45°52.8'N, 174°02.3'W; AAH2: 52°56.1'N, 177°55.0'W; 70: 04°00.0'S, 082° 00.0'W; 127: 38°00.2'N, 124°45.0'W; GEOSECS: 28° 29.0'N, 121°38.0'W.

Results and discussion

From Park (1965):

$$TCO_2 = P.TCO_2 + \Delta TCO_{2_{ox}} + \Delta TCO_{2_{CO_3^=}} \quad (69)$$

where $P.TCO_2$ is the preformed total inorganic carbon dioxide, $\Delta TCO_{2_{ox}}$ is the increment of total inorganic carbon dioxide due to biological processes, and $\Delta TCO_{2_{CO_3^=}}$ is the increment of total inorganic carbon dioxide due to carbonate dissolution or precipitation.

$$\Delta TCO_{2_{ox}} = a_R(AOU) = a_R(O'_2 - O_2) \quad (70)$$

$$\Delta TCO_{2_{CO_3^=}} = k(TA - P.TA) \quad (71)$$

where a_R is the $\Delta TCO_2{:}\Delta O_2$ ratio for biological processes, O'_2 is the oxygen concentration at saturation, k is the $\Delta TCO_2{:}\Delta TA$ ratio, and P.TA is the preformed total alkalinity. Substituting equations (70) and (71) in equation (69) we have

$$TCO_2 = P.TCO_2 + a_R(O'_2 - O_2) + k(TA - P.TA) \quad (72)$$

$$TCO_2 = (P.TCO_2 + a_R O'_2 - kP.TA) - a_R O_2 + kTA \quad (73)$$

If a_R and k are constants (according to the results obtained by Culberson and Pytkowicz, 1970; and Culberson, 1972, they are), the quantity $(P.TCO_2 + a_R O'_2 - kP.TA)$ is a conservative variable in the sense that it is not affected by biological or geological processes; it is only gained or lost at the boundaries. If we make a regression of

TCO_2 on O_2, TA, temperature and/or salinity, the temperature and/or salinity terms may represent the conservative fractions of total inorganic carbon dioxide, oxygen and total alkalinity, namely (P. TCO_2 + $a_R O'_2$ - kP. TA), so that the O_2 and TA terms represent only the non-conservative fractions. Ben-Yaakov (1971) indicated that, when dealing with a water mass which results from the mixing of n water types, at least n-1 conservative parameters are needed in the regression equation.

According to Postma (1964) two of the processes that affect TA and TCO_2 are changes in S‰ by evaporation or precipitation and formation or solution of particulate calcium carbonate. S‰ changes cause the P. TA and P. TCO_2 to change. Postma (1964), Culberson and Pytkowicz (1970) and Culberson (1972) applied corrections to their data to account for these effects by normalizing to a constant S‰ and constant alkalinity. They normalized the data to S‰ = 34.68 which is the value that corresponds to the deep Pacific waters. When normalizing to a constant alkalinity they used k = 0.5 based on the assumption that there are no other processes affecting TA besides those mentioned above. The factor 0.5 is to transform milliequivalents of TA to millimoles of TCO_2. Ben-Yaakov (1971) found the TA regression coefficient consistently higher than 0.5 (as high as 0.93) in most of the cases.

Ben-Yaakov (1971, 1972) used a regression equation of the type

$$TCO_2 = A_o + A_1 T°C + A_2 O_2 + A_3 TA \qquad (74)$$

where A_o, A_1, A_2 and A_3 are constant regression coefficients. At first it may seem that to properly apply equation (74) to the data it is necessary to choose a portion of the water column where mixing between no more than two water types is occurring, since there is only one conservative variable in the equation. But, by comparing equations (73) and (74) we can see that the only necessary and sufficient condition for the proper application of equation (74) is that the conservative quantity ($P.TCO_2 + a_R O'_2 - kP.TA$) be a linear function of T°C, that is

$$P.TCO_2 + a_R O'_2 - kP.TA = A_o + A_1 T°C \qquad (75)$$

according to equation (75) the T°C term of equation (74) has to be able to extract the changes in the preformed fractions of total inorganic carbon dioxide, oxygen and total alkalinity, otherwise the results of the regression analysis are not correct.

The variation of the O_2 and TA regression coefficients shown by Ben-Yaakov's (1971, 1972) results may be due to either of the two of the following reasons: a) equation (74) was not applied to the proper portion of the water column in all the cases; b) the changes of TCO_2 and TA due to S‰ changes were not properly extracted by the T°C term. According to his results, when S‰ is added to equation (74) the adjustment of the regression coefficients is not made towards

intervals consistent with the theoretical considerations. There is a significant correlation between all the variables of equation (74) and S‰ (Ben-Yaakov, 1971). There are different possibilities that may happen by chance, i.e.: the correlations may be such that the TA term of equation (74) represents the changes of TCO_2 due to both the S‰ changes and the carbonate reaction. In this case the regression coefficient would not be 0.5 but a higher one. When S‰ increases, TA and TCO_2 increase. If all the TA increase, due to S‰ increase, would consist of carbonate ions, the factor to transform ΔTA (milli-equivalents) to ΔTCO_2 (millimoles) would be 0.5. If all the TA increase would consist of bicarbonate ions, the factor to transform ΔTA to ΔTCO_2 would be 1.0. Since the borate alkalinity is small percentagewise ($\sim$4% of the TA) and since about 90% of the carbonate alkalinity consists of bicarbonate ions in the open ocean, the factor to transform ΔTA, due to changes of S‰, to ΔTCO_2 is between 0.5 and 1.0.

If the S‰ effect is causing the disagreement between the results obtained by Ben-Yaakov (1971, 1972) and those obtained by Culberson and Pytkowicz (1970) and Culberson (1972), the results obtained by applying regression analysis to data normalized to constant S‰ should be consistent with the results of Culberson and Pytkowicz (1970) and Culberson (1972).

To test the hypotheses that a_R is the value predicted by Redfield's

model and k is equal to 0.5 the data were normalized to a constant S‰ of 34.68, and the regression equation

$$TCO_{2_n} = a_o + a_1\theta^\circ C + a_2 O_{2_n} + a_3 TA_n + TCO_{2_{n_{res}}} \qquad (76)$$

was applied to the data; $TCO_{2_n} = TCO_2(34.68/S‰)$, $O_{2_n} = O_2(34.68/S‰)$, $TA_n = TA(34.68/S‰)$; a_o, a_1, a_2 and a_3 are constant regression coefficients, and $TCO_{2_{n_{res}}}$ are the residuals of TCO_{2_n} after regression on $\theta^\circ C$, O_{2_n} and TA_n. After normalization of the data equation (73) is transformed to

$$TCO_2(34.68/S‰) = (P.TCO_2 + a_R O'_2 - kP.TA)(34.68/S‰) + \\ - a_R O_2(34.68/S‰) + kTA(34.68/S‰) \qquad (77)$$

By comparing equation (76) and (77) we can see that the only necessary and sufficient condition for the proper application of equation (76) is that the conservative quantity $(P.TCO_2 + a_R O'_2 - kP.TA)(34.68/S‰)$ be a linear function of $\theta^\circ C$, that is

$$(P.TCO_2 + a_R O'_2 - kP.TA)(34.68/S‰) = a_o + a_1\theta^\circ C \qquad (78)$$

This is equivalent to saying that equation (76) must be applied to data from a portion of the water column where the diagram of $(P.TCO_2 + a_R O'_2 - kP.TA)(34.68/S‰)$ versus $\theta^\circ C$ is able to detect only two-water types mixing. We use potential temperature instead of "in situ" temperature to avoid the adiabatic heating effect of pressure.

A classical way to detect two-water-types mixing has been to look for straight portions of the temperature-salinity (T-S) diagram.

But, a straight T-S diagram is a necessary but not sufficient condition for two-water-types mixing (Alvarez-Borrego, Guthrie, Culberson and Park, 1972). The $(P.TCO_2 + a_R O'_2 - kP.TA)(34.68/S‰)$ versus $\theta°C$ or other diagrams may show water types that the T-S diagram does not show, and vice versa.

To separate the water column into portions for which equation (78) applies we use a method similar to the one Alvarez-Borrego, Guthrie, Culberson and Park (1972) used when they applied regression analysis to test Redfield's model for the oxygen-nutrients relationships.

If equation (76) is applied to the proper portion of the water column, a plot of $TCO2_{n_{res}}$ versus $\theta°C$ should be completely random, because $TCO2_{n_{res}}$ should result only from the random errors in the measurements of TCO_2, O_2, TA, S‰ and $\theta°C$. Thus, if we apply equation (76) to the whole water column and plot $TCO2_{n_{res}}$ versus $\theta°C$, the pattern shown by the diagram, if any, would give us an indication of how to separate the water column into suitable portions.

To illustrate this procedure let us examine a hypothetical example similar to the one used by Alvarez-Borrego, Guthrie, Culberson and Park (1972). Suppose we have data from the whole water column of a certain station, and suppose the $(P.TCO_2 + a_R O'_2 - kP.TA)(34.68/S‰)$ versus $\theta°C$ diagram is like the one shown in Figure 61a where at least three water types A, B and C are being detected. Since

$(P.TCO_2 + a_R O'_2 - kP.TA)(34.68/S‰)$ is not a linear function of $\theta°C$, the plot of $TCO_{2_{n_{res}}}$ versus $\theta°C$ would generate a diagram as shown in Figure 61b which would detect the three water types A, B and C. Thus, each minimum and maximum in the $TCO_{2_{n_{res}}}$ versus $\theta°C$ diagram represents a different water type.

This procedure was applied to station HAH22 of YALOC-66 (Barstow, Gilbert, Park, Still and Wyatt, 1968), to the two stations used by Culberson and Pytkowicz (1970) and Ben-Yaakov (1971) and to the station used by Ben-Yaakov (1972) (Figure 60). For station 70 of YALOC-69 (Culberson and Pytkowicz, 1970) the three deepest observations were not used (from 3706 to 3754 m depth), and for station 127 of the same cruise the two deepest observations were not

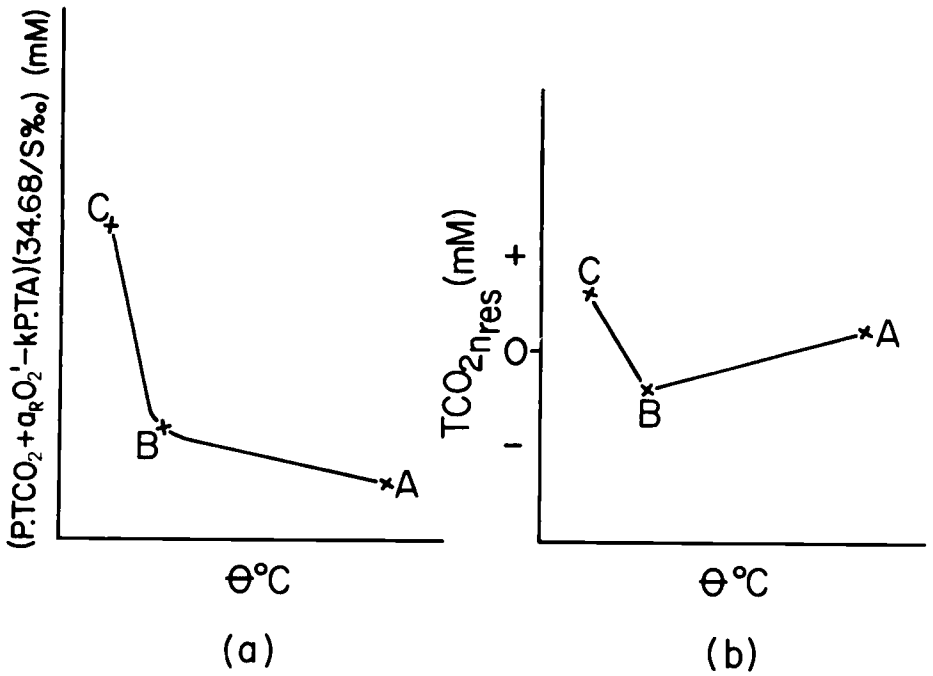

Figure 61. $(P.TCO_2 + a_R O'_2 - kP.TA)(34.68/S‰)$ versus $\theta°C$ diagram (a), and $TCO_{2_{n_{res}}}$ versus $\theta°C$ diagram (b), of a hypothetical station.

used (from 3913 to 3928 m depth). θ°C, S‰, O_2, TA and TCO_2 do not change significantly in those depth ranges.

Both regression equations, (74) and (76), were applied to the data to show that in some cases equation (74) gives a confidence interval for the TA regression coefficient inconsistent with the expected value of 0.5, and in other cases it gives a confidence interval for the O_2 regression coefficient inconsistent with Redfield's model while equation (76) gives confidence intervals consistent with the theoretical values. The regression analysis was performed by a computer program (SIPS) (Oregon State University, Department of Statistics, 1971). The results are shown in Table 3. Confidence levels of 95% are given for each of the coefficients of the resulting regression equations. In Table 3, for each station, equations are given for the whole water column first and then for the depth ranges chosen according to the $TCO2_{n_{res}}$ versus θ°C diagrams.

The $TCO2_{n_{res}}$ versus θ°C and the θ°C-S‰ diagrams for the whole water column of station HAH22 are shown in Figures 62a and b, respectively. A definite dependency of $TCO2_{n_{res}}$ on θ°C is shown in Figure 62a. Both diagrams (Figure 62a, b) show very distinctly four water types A, B, C and D, where C is the Subarctic Intermediate water. Equation (79) (Table 3) has confidence intervals for the O_2 and TA regression coefficients consistent with Redfield's number and 0.5, respectively. We consider this agreement fortuitous since,

Table 3. Regression equations expressing total inorganic carbon dioxide as a function of potential temperature, oxygen and total alkalinity. The confidence intervals are at the 95% confidence level.

STATION	TYPE OF DATA	DEPTH RANGE (METERS)	REGRESSION EQUATIONS (SHOWING 95% CONFIDENCE INTERVALS	R^2	n-p-1*	EQUATION NUMBER
HAH22 (YALOC-69) (24°30.6'N, 161°30.0'W) (near Hawaii)	Normalized to $S‰ = 34.66$	0-4545	$TCO2_n = (1.136 \pm 0.298) - (0.011 \pm 0.011)\theta°C - (0.0356 \pm 0.0034)O2_n + (0.567 \pm 0.118)TA_n$	0.997	32	79†
		74-414	$TCO2_n = (0.961 \pm 0.654) - (0.0151 \pm 0.0007)\theta°C - (0.0416 \pm 0.0122)O2_n + (0.669 \pm 0.257)TA_n$	0.999	7	80†
		414-4545	$TCO2_n = (1.005 \pm 0.575) - (0.009 \pm 0.004)\theta°C - (0.0339 \pm 0.0020)O2_n + (0.614 \pm 0.224)TA_n$	0.996	15	81†
	Not Normalized	74-414	$TCO2 = (0.843 \pm 0.552) - (0.0131 \pm 0.0014)\theta°C - (0.0421 \pm 0.0133)O2 + (0.706 \pm 0.208)TA$	0.999	7	82†
		414-4545	$TCO2 = (0.743 \pm 0.394) - (0.0090 \pm 0.0038)\theta°C - (0.0332 \pm 0.0019)O2 + (0.716 \pm 0.153)TA$	0.997	15	83†
70 (YALOC-69) (04°00.0'S, 082°00.0'W) (off Ecuador)	Normalized to $S‰ = 34.66$	0-3432	$TCO2_n = (0.511 \pm 0.710) - (0.0008 \pm 0.0028)\theta°C - (0.366 \pm 0.070)O2_n + (0.805 \pm 0.294)TA_n$	0.998	22	84‡
		0-90	$TCO2_n = (1.766 \pm 3.092) - (0.0053 \pm 0.0042)\theta°C - (0.376 \pm 0.112)O2_n + (0.23 \pm 1.68)TA_n$	0.998	4	85‡
		390-3432	$TCO2_n = (0.904 \pm 0.528) - (0.0091 \pm 0.0033)\theta°C - (0.333 \pm 0.077)O2_n + (0.641 \pm 0.220)TA_n$	0.991	11	86‡
	Not Normalized	0-90	$TCO2 = (1.749 \pm 2.044) - (0.0050 \pm 0.0034)\theta°C - (0.394 \pm 0.062)O2 + (0.25 \pm 0.87)TA$	0.999	4	87‡
		390-3432	$TCO2 = (0.729 \pm 0.396) - (0.0074 \pm 0.0024)\theta°C - (0.316 \pm 0.079)O2 + (0.709 \pm 0.176)TA$	0.992	11	88‡
127 (YALOC-69) (30°00.2'N, 124°45.0'W) (off California)	Normalized to $S‰ = 34.68$	0-3843	$TCO2_n = (1.556 \pm 0.370) - (0.0123 \pm 0.0028)\theta°C - (0.332 \pm 0.028)O2_n + (0.380 \pm 0.154)TA_n$	0.998	22	89‡
		197-3843	$TCO2_n = (0.888 \pm 0.924) - (0.0072 \pm 0.0065)\theta°C - (0.346 \pm 0.016)O2_n + (0.650 \pm 0.372)TA_n$	0.997	14	90‡
	Not Normalized	197-3843	$TCO2 = (0.939 \pm 0.638) - (0.0105 \pm 0.0077)\theta°C - (0.346 \pm 0.013)O2 + (0.631 \pm 0.252)TA$	0.999	14	91‡
GEOSECS 1969 (2°29'N, 121°30'W (off Baja California)	Normalized	0-4000	$TCO2_n = (1.570 \pm 0.398) - (0.0078 \pm 0.0024)\theta°C - (0.0307 \pm 0.0045)O2_n + (0.346 \pm 0.169)TA_n$	0.991	24	92§
	Not Normalized	0-4000	$TCO2 = (1.241 \pm 0.334) - (0.0082 \pm 0.0026)\theta°C - (0.0410 \pm 0.0042)O2 + (0.482 \pm 0.138)TA$	0.993	24	93§

*n-p-1 are the residual degrees of freedom, n is the number of observations and p is the number of independent variables already in the regression equation.

†O_2 and O_{2_n} expressed in ml/l, and TCO_2 and TCO_{2_n} in mM/l.

‡O_2 and O_{2_n} expressed in mg-at O_2/kg, and TCO_2 and TCO_{2_n} in mM/kg.

§O_2 and O_{2_n} expressed in ml/kg, and TCO_2 and TCO_{2_n} in mM/kg.

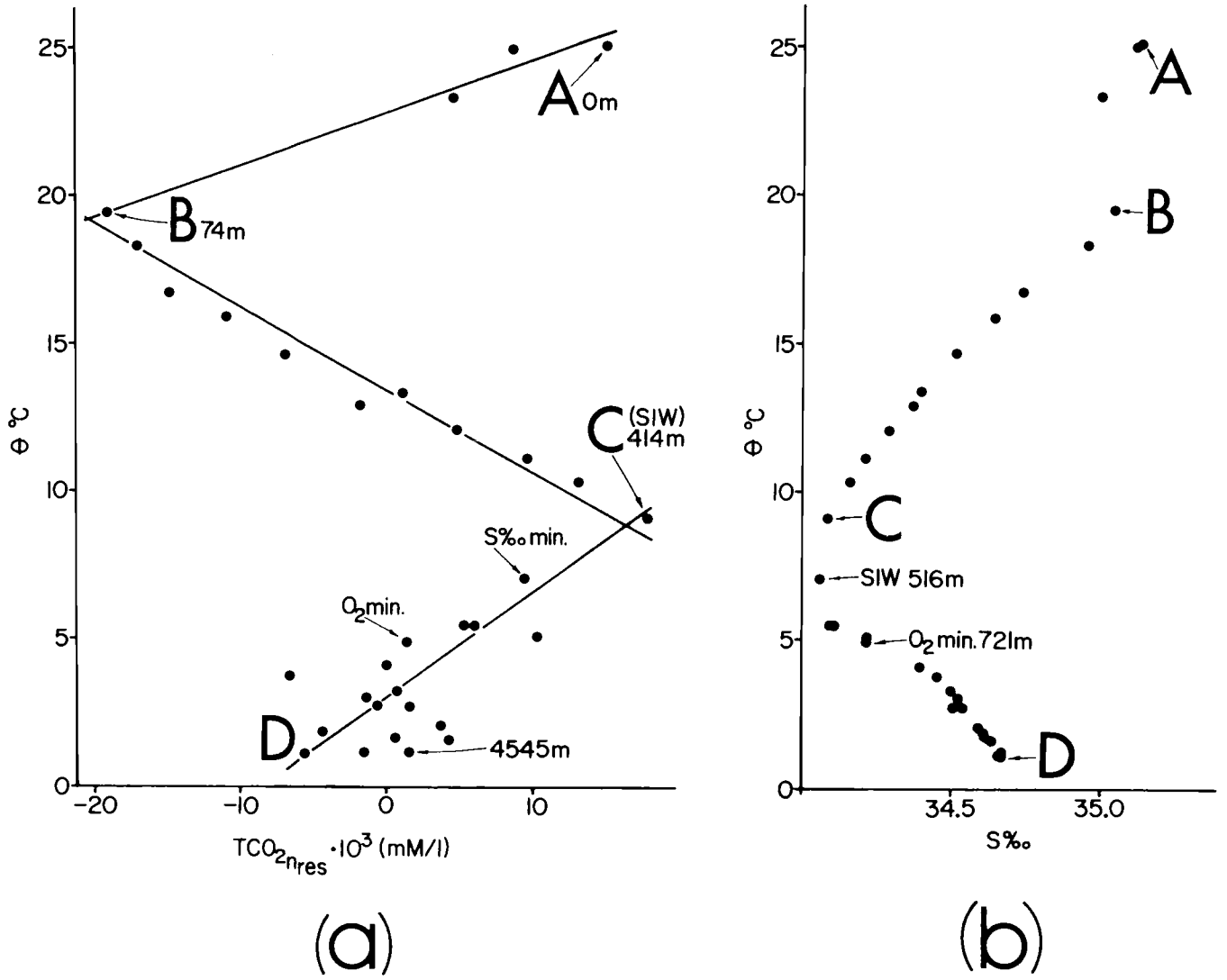

Figure 62. θ °C-$TCO_{2_{n_{res}}}$ diagram (a), and θ °C-S‰ diagram (b), for the whole water column of station HAH22. A, B, C and D denote water types. SIW means Subarctic Intermediate water.

according to Figure 62a, there is no oceanological nor statistical basis to justify the coefficient for θ°C as a valid one. According to Figure 62a equation (79) is not properly describing the data.

A separation of the data from HAH22 into two subsets was done; one from B to C and another from C to D; and equations (74) and (76) were applied to them. Between A and B (Figure 62a) there are only two data points; therefore, no regression was applied to that portion of the water column. Although not shown here, if we apply equation (74) to the whole water column of station HAH22 and plot $TCO_{2_{res}}$ versus θ°C, the resulting diagram is very similar to Figure 62a, with the same points as maxima and minima. A similar statement applies to the other stations.

Equations (80) and (82) (Table 3) have confidence intervals, for the oxygen and total alkalinity regression coefficients, consistent with the theoretical values. They show that with or without normalization of the data, from the depth range 74-414 m of HAH22, to constant S‰, we obtain essentially the same results. But, while equation (81) shows confidence intervals consistent with the theory, equation (83) has a confidence interval for the TA regression coefficient that is not consistent with the value 0.5. Thus, in this case normalization to a constant S‰ improved the results of the regression.

Figures 63a and b show the $TCO_{2_{n_{res}}}$ versus θ°C diagrams for the depth ranges 74-414 m and 414-4545 m of HAH22. These diagrams

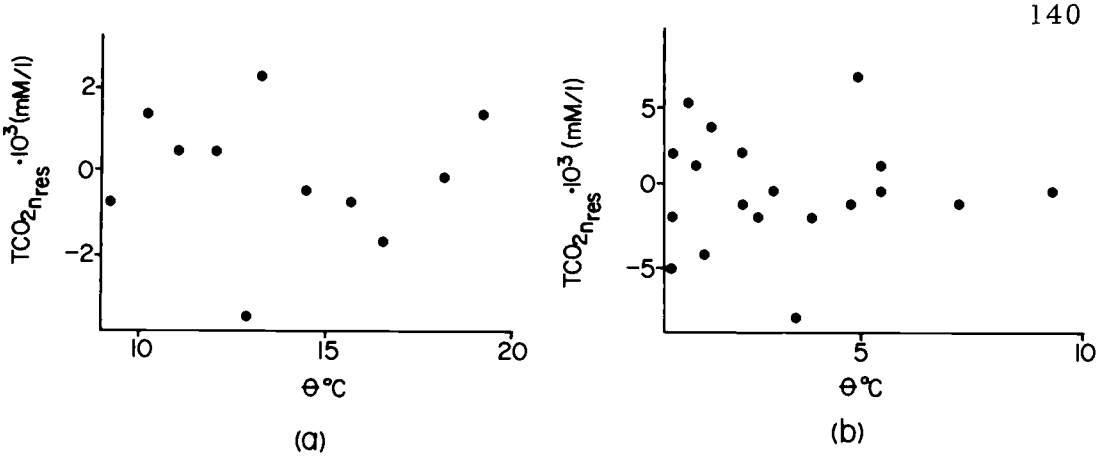

Figure 63. $TCO_{2_{nres}}$ versus θ°C diagrams for the portions of the water column between (a) 74 and 414 m, and (b) 414 and 4545 m of station HAH22.

do not show any particular trend. This indicates that $TCO_{2_{nres}}$ result from only the random errors in the measurements of TCO_2, O_2, TA, S‰ and θ°C and that equations (80) and (81) are properly describing the data.

The $TCO_{2_{nres}}$ versus θ°C and the θ°C-S‰ diagrams for the whole water column of station 70 of YALOC-69 are shown in Figures 64a and b. Figure 64a shows a definite dependency of $TCO_{2_{nres}}$ on θ°C. Both diagrams (Figures 64a, b) show the Antarctic Intermediate water very distinctly. C corresponds to the O_2 minimum. Equation (84) (Table 3) has a confidence interval for the O_{2_n} regression coefficient consistent with Redfield's model, and a confidence interval for the TA_n regression coefficient inconsistent with 0.5. We consider the agreement between equation (84) and Redfield's model fortuitous since according to Figure 64a equation (84) is not properly describing the data.

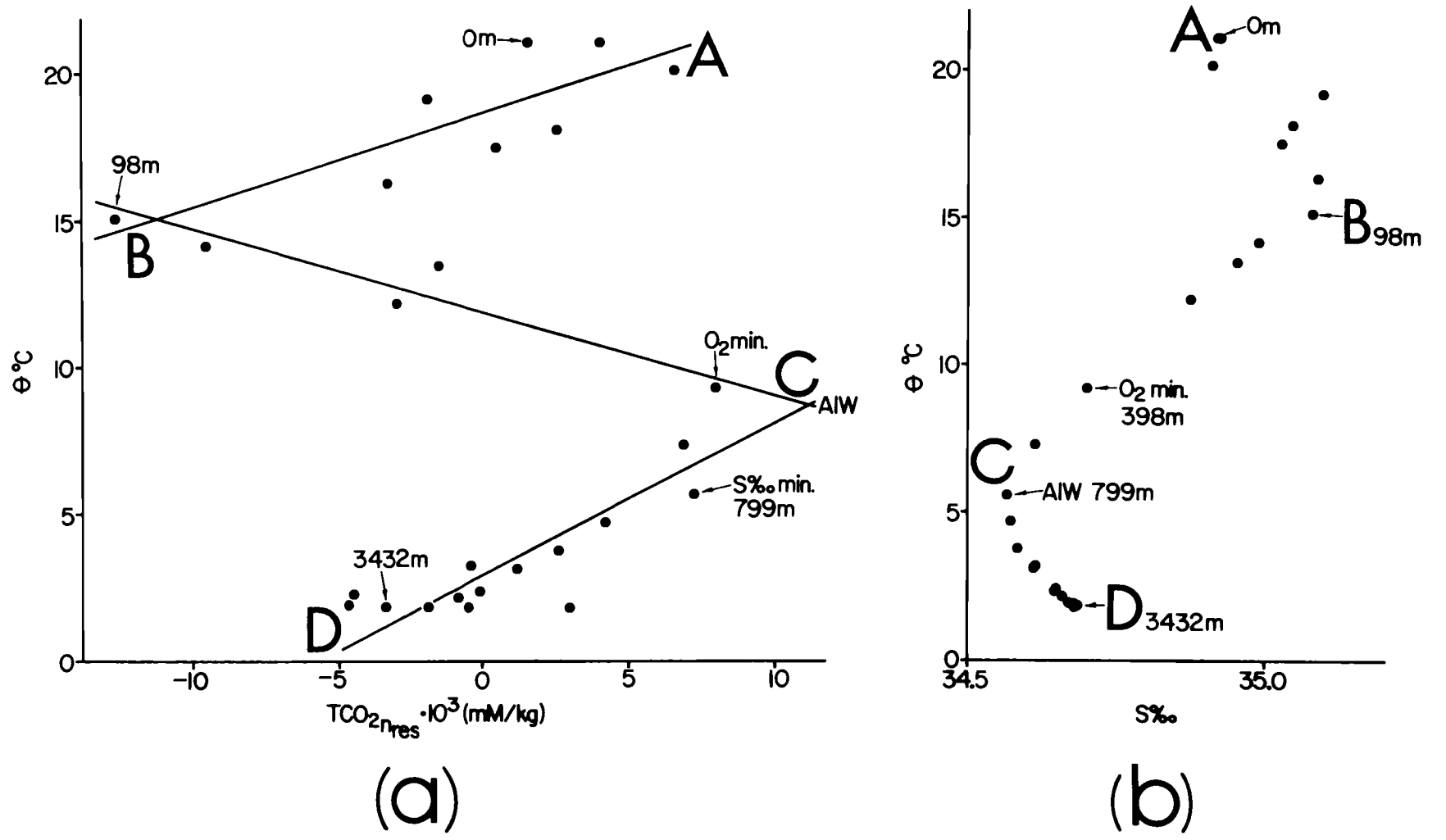

Figure 64. $\theta°C$-$TCO_{2_{n_{res}}}$ diagram (a), and $\theta°C$-S‰ diagram (b), for the whole water column of station 70. A, B, C and D denote water types. AIW means Antarctic Intermediate water.

A separation of the data from station 70 into two subsets was done, one from A to B and another from C to D (Figure 64a), and equations (74) and (76) were applied to them. Between B and C (Figure 64a) there are only three data points, therefore no regression was applied to that portion of the water column. Equations (85) and (87) (Table 3) show essentially the same results. The total alkalinity regression coefficients of equations (85) and (87) are not significantly different from zero. This indicates that possibly solution or precipitation of calcium carbonate does not significantly affect TCO_2 in the depth range 0-98 m. Pytkowicz (1972) (and previous authors cited therein) indicates that sea water is supersaturated with respect to calcite in the upper few hundred meters in the open ocean. Thus, no net dissolution of calcium carbonate is expected to occur in the upper few hundred meters. The confidence intervals for the oxygen regression coefficients of equations (85) and (87) (Table 3) are consistent with Redfield's model. For equation (85), without the TA_n term, the O_{2_n} regression coefficient is -0.365 ± 0.062, and for equation (87), without the TA term, the O_2 regression coefficient is -0.388 ± 0.052. These two intervals are consistent with Redfield's model. Culberson and Pytkowicz (1970) found agreement with Redfield's model only below 98 m at station 70. Possibly the disagreement found by them in the upper 98 m was due to their assumed constant initial specific alkalinity not applying to this depth range.

Equations (86) and (88) (Table 3) have confidence intervals for the oxygen regression coefficient consistent with Redfield's model. But, while equation (86) has a confidence interval for the TA_n regression coefficient consistent with 0.5, the one for equation (88) is not consistent with 0.5. Again, normalization of the data before application of regression analysis has improved the results. Figures 65a and b show the $TCO2_{n_{res}}$ versus θ°C diagrams for the depth ranges 0-98 m and 398-3432 m of station 70. According to Figures 65a and b equations (85) and (86) are properly describing the data.

Figures 66a and b show the $TCO2_{n_{res}}$ versus θ°C and the θ°C-S‰ diagrams, respectively, for the whole water column of station 127 of YALOC-69. Following the same criteria as with stations HAH22 and 70, the data from station 127 were divided into subsets. Between A and B, and between B and C (Figure 66a) there are only three data points. Thus, no regression was applied to these depth ranges. For

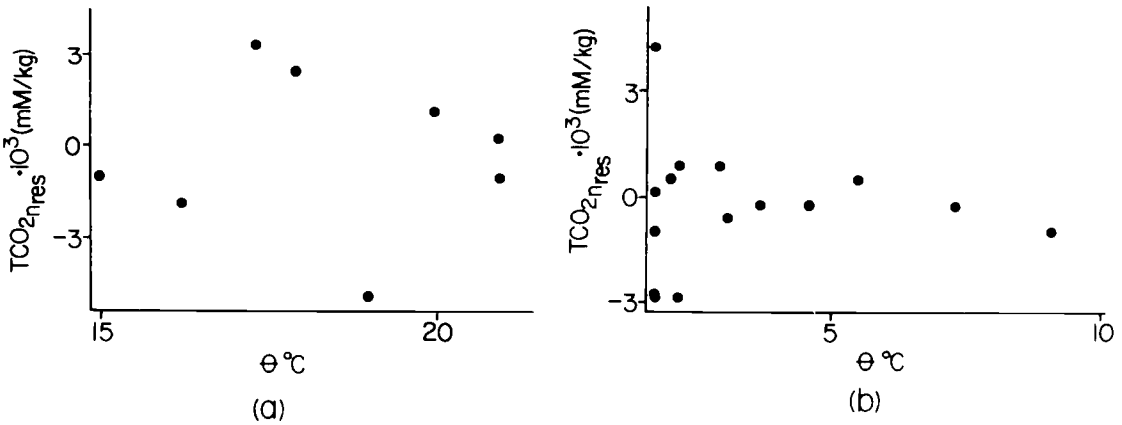

Figure 65. $TCO2_{n_{res}}$ versus θ°C diagrams for the portions of the water column between (a) 0 and 98 m, and (b) 398 and 3432 m of station 70.

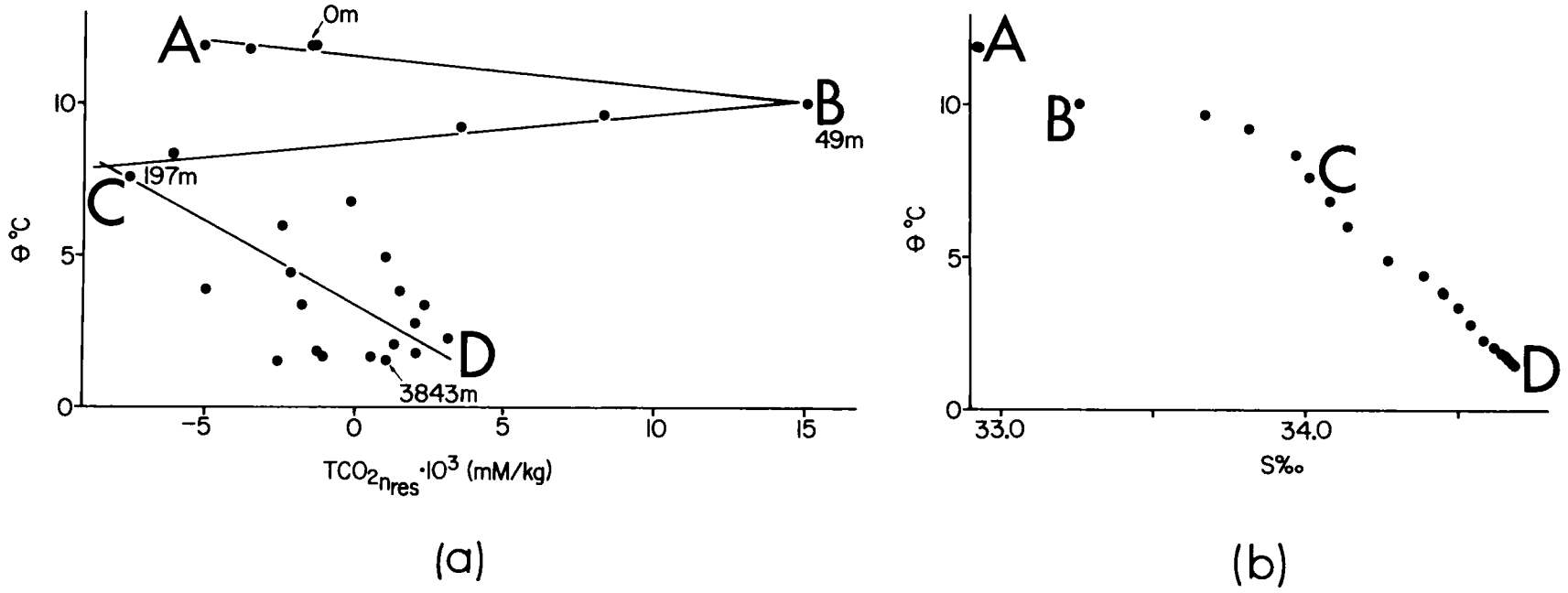

Figure 66. $\theta°C$-$TCO_{2_{n_{res}}}$ diagram (a), and $\theta°C$-S‰ diagram (b), for the whole water column of station 127. A, B, C and D denote water types.

the depth range 197 to 3843 m (C to D Figure 66a) the results are essentially the same with or without normalization of the data to constant S‰ [equations (90) and (91), Table 3]. The confidence intervals for the total alkalinity regression coefficients of equations (90) and (91) are consistent with 0.5. But the confidence intervals for the oxygen regression coefficients of these equations are not consistent with Redfield's model, they are a little too low. This is the only case in which we found disagreement between our results and Redfield's model. Culberson and Pytkowicz (1970) found agreement between their corrected data and Redfield's model below 400 m for station 127.

Figure 67 shows the $TCO2_{n_{res}}$ versus θ°C diagram for the depth range

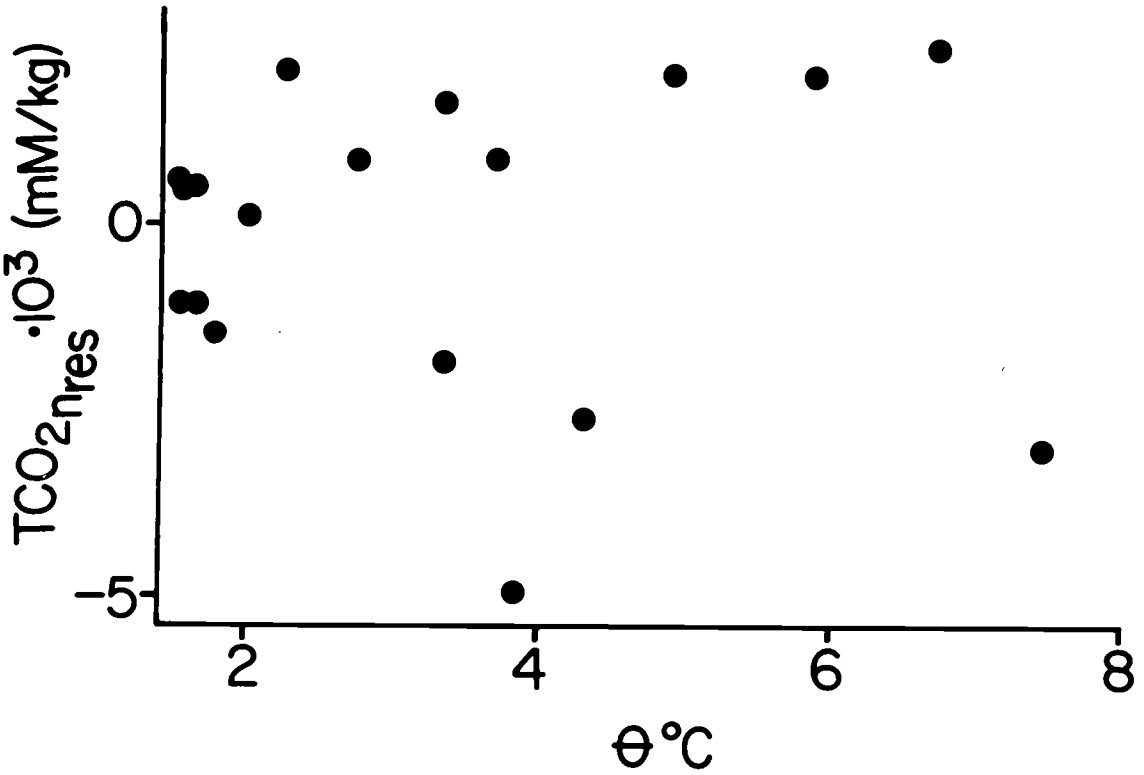

Figure 67. $TCO2_{n_{res}}$ versus θ°C diagram for the portion of the water column between 197 and 3843 m of station 127.

197-3843 m of station 127. This diagram does not show any particular trend. This indicates that equation (90) (Table 3) is properly describing the data.

The $TCO_{2_{n_{res}}}$ versus $\theta°C$ and $\theta°C$-S‰ diagrams for the whole water column of the 1969 GEOSECS station are shown in Figures 68a and b. Figure 68a does not show any particular trend. This indicates that equation (92) (Table 3) is properly describing the data from the whole water column. Equation (92) has confidence intervals for the O_{2_n} and TA_n regression coefficients consistent with Redfield's model and 0.5, respectively. Equation (93) (Table 3) has a confidence interval for the TA regression coefficient consistent with 0.5, but it has a confidence interval for the O_2 regression coefficient inconsistent with Redfield's model. Once again, the normalization improved the results of the regression. Ben-Yaakov (1972) applied regression analysis to data without normalization, from this station, and reported as his best estimate for the O_2 regression coefficient a confidence interval that is not consistent with Redfield's model.

The coefficients of determination (R^2) (Draper and Smith, 1966) are higher than 0.99 for all of our results (Table 3) This indicates that a very high fraction of the variability of TCO_{2_n} and TCO_2 has been explained by the regressions. In general, R^2's for the regression equations with normalized data are slightly lower than those for the regression equations without normalized data. This is due to the

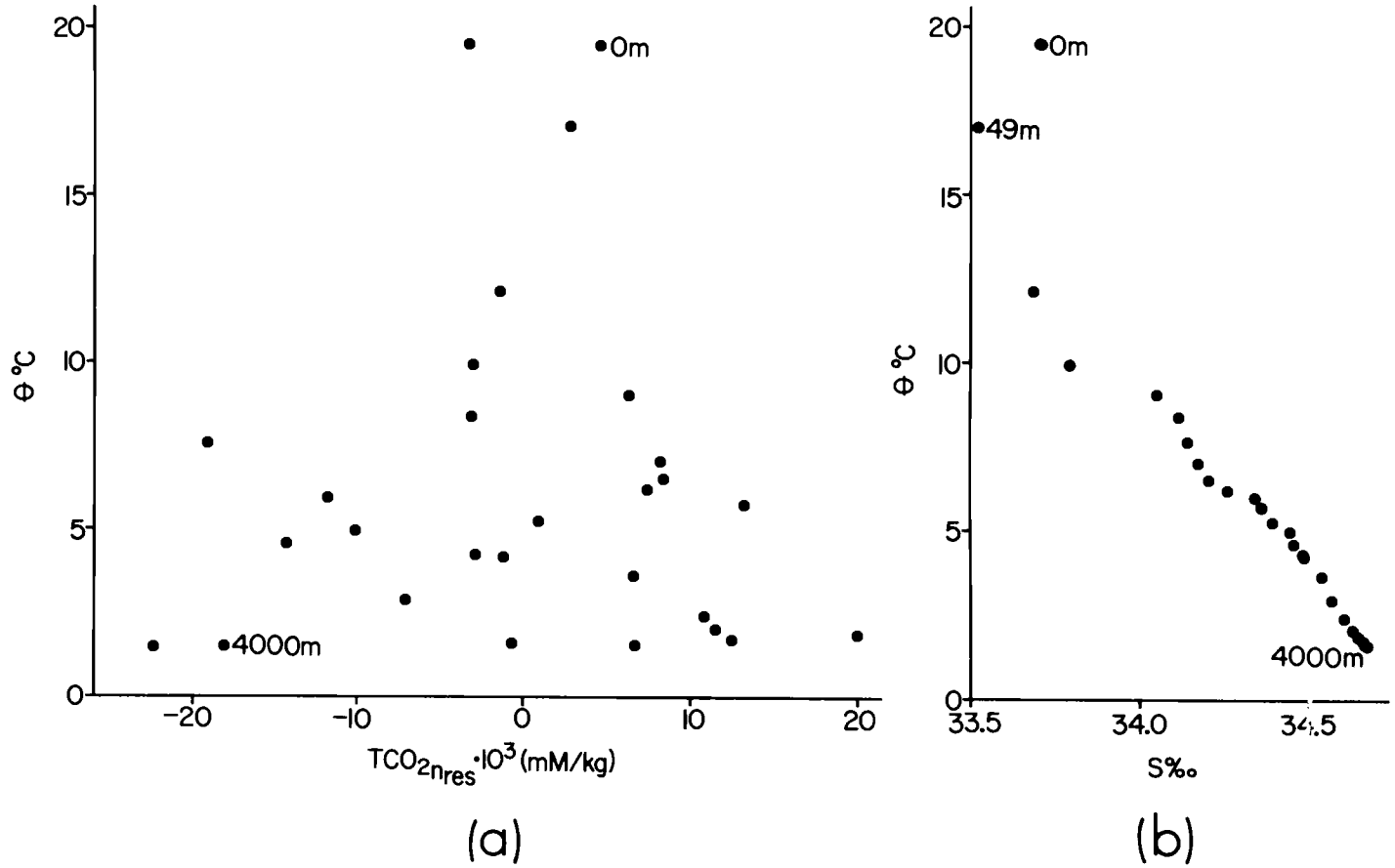

Figure 68. θ° C-$TCO_{2_{n_{res}}}$ diagram (a), and θ° C-S‰ diagram (b), for the whole water column of the 1969 GEOSECS station.

TCO_2 residuals resulting only from the random errors of TCO_2, O_2, TA and θ° C, while $TCO_{2_{nres}}$'s result also from the random errors of S‰.

Something important to consider is that when we properly apply equation (76) to a certain region of the water column, the fact that the O_{2_n} and TA_n regression coefficients are significantly different from zero does not provide any information as to where, geographically, the main bulk of the biological oxidation and the carbonate reaction, respectively, occurred. It only proves that at least part of the changes in TCO_2 are due to biological oxidation and carbonate reaction, but not that those changes occurred at the geographic location of the hydrographic station where the data are from. A statement similar to this was made by Alvarez-Borrego, Guthrie, Culberson and Park (1972) with regard to their results on the oxygen-nutrient relationships.

Diagrammatic illustration of the extraction of the mixing effect, the S‰ effect and the carbonate reaction effect

According to the results given above, data from the depth range 197-3843 m of station 127 of YALOC-69, and data from the whole water column of the 1969 GEOSECS station (Table 3, Figures 67 and 68a) can be properly described by regression equation (76). This gives us an opportunity to illustrate diagrammatically the extraction of the mixing, S‰ and carbonate reaction effects on the TCO_2 by

applying regression analysis to normalized data; so that only the biological effect is left and, in agreement with Redfield's model, a linear relationship between dissolved oxygen and total inorganic carbon dioxide is left.

When regressing $TCO2_n$ on O_{2_n}, TA_n and $\theta°C$, since O_{2_n}, TA_n and $\theta°C$ are correlated to a certain extent, the O_{2_n} term represents the regression of the residuals of $TCO2_n$, after regression on $\theta°C$ and TA_n, on the residuals of O_{2_n}, after regression on $\theta°C$ and TA_n. In other words, if we do the regression in a stepwise manner, adding $\theta°C$ and TA_n first we have

$$TCO2_n = c_o + c_1\theta°C + c_2TA_n + TCO2_{n_r} \tag{94}$$

and implicitly and simultaneously

$$O_{2_n} = d_o + d_1\theta°C + d_2TA_n + O_{2_{n_r}} \tag{95}$$

where c_o, c_1, c_2, d_o, d_1 and d_2 are constant regression coefficients and $TCO2_{n_r}$ and $O2_{n_r}$ are the $TCO2_n$ and O_{2_n} residuals after regression on $\theta°C$ and TA_n.

When we add O_{2_n} to regression equation (94), what we are doing is regressing $TCO2_{n_r}$ on $O_{2_{n_r}}$

$$TCO2_{n_r} = f_o + a_2O2_{n_r} + TCO2_{n_{res}} \tag{96}$$

where f_o and a_2 are constant regression coefficients and $TCO2_{n_{res}}$ is as defined for equation (76); substituting the values of $O_{2_{n_r}}$ from equation (95) into equation (96) we have

$$TCO2_{n_r} = (f_o - a_2 d_o) - a_2 d_1 \theta°C + a_2 O2_n - a_2 d_2 TA_n + TCO2_{n_{res}} \quad (97)$$

substituting equation (97) into equation (94)

$$TCO2_n = (c_o + f_o - a_2 d_o) + (c_1 - a_2 d_1)\theta°C + a_2 O2_n + \\ + (c_2 - a_2 d_2)TA_n + TCO2_{n_{res}} \quad (98)$$

$(c_o + f_o - a_2 d_o)$, $(c_1 - a_2 d_1)$ and $(c_2 - a_2 d_2)$ are constants, we can represent them by the symbols a_o, a_1 and a_3 respectively; equation (98) is the same as equation (76). The $O2_n$ regression coefficient of equation (76), a_2, is the slope of the $TCO2_{n_r}$ versus $O2_{n_r}$ diagram.

The TCO_2-O_2 and $TCO2_{n_r}$-$O2_{n_r}$ diagrams for the depth range 197-3843 m of station 127 of YALOC-69 are shown in Figures 69a and b. Figures 70a and b show the TCO_2-O_2 and $TCO2_{n_r}$-$O2_{n_r}$ diagrams for the whole water column (0-4000 m) of the 1969 GEOSECS station. Figures 69a and 70a show that the TCO_2-O_2 diagrams for these stations are not linear, they have a hook-like shape. Figures 69b and 70b show that after normalizing the data and regressing $TCO2_n$ and $O2_n$ on $\theta°C$ and TA_n, the hook-like shape disappeared. For station 127 the $TCO2_{n_r}$-$O2_{n_r}$ correlation coefficient is -0.997, and for the GEOSECS station it is -0.964. In Figures 69b and 70b the data points do not follow a sequence, with reference to depth, along the line. In other words, the points at one end are not necessarily the near surface points, and the points at the other end are not necessarily the deep points. The data points at the upper end of the $TCO2_{n_r}$-$O2_{n_r}$

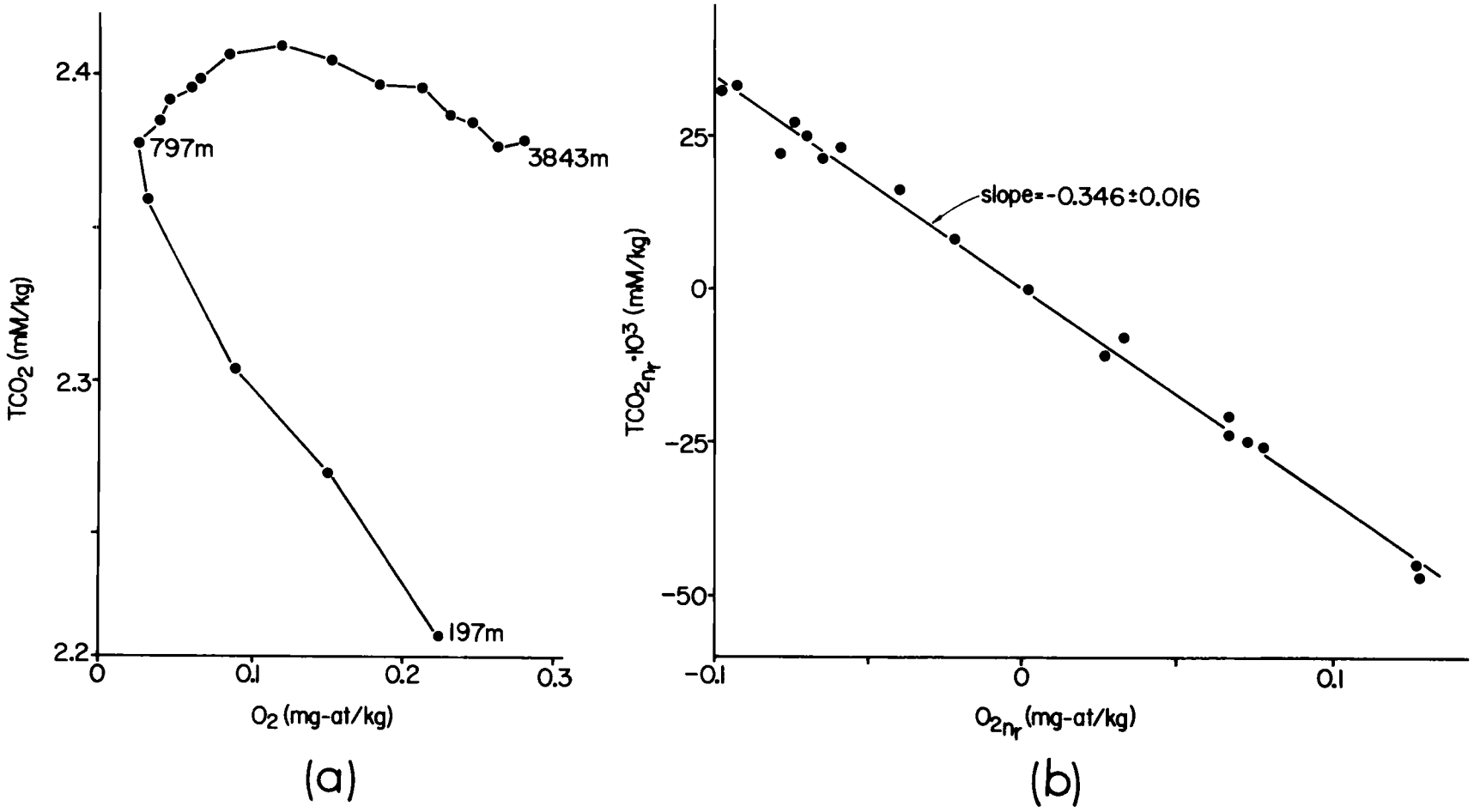

Figure 69. TCO_2-O_2 diagram (a), and $TCO_{2_{n_r}}$-$O_{2_{n_r}}$ diagram (b), for the portion of the water column between 197 and 3843 m of station 127.

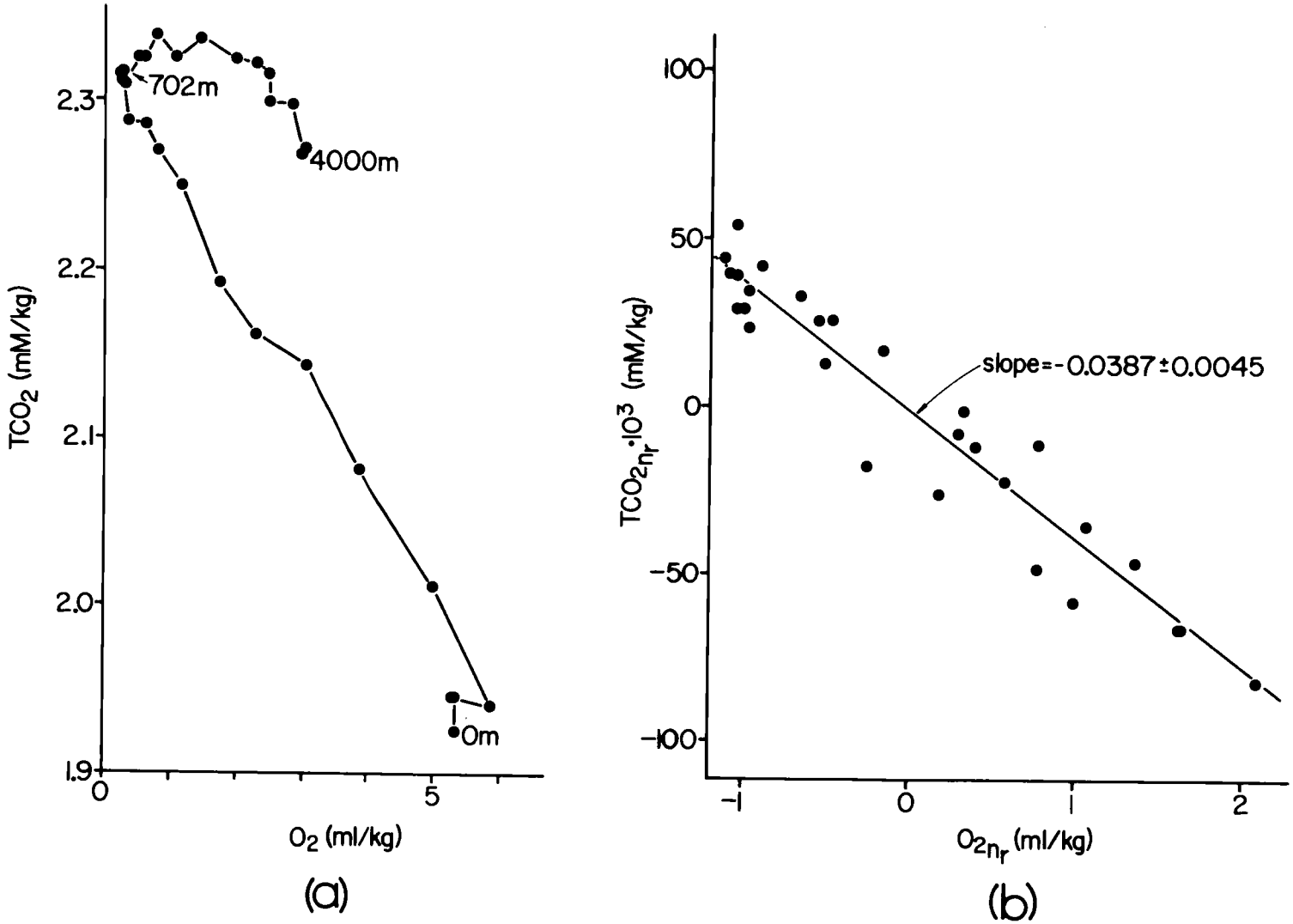

Figure 70. TCO_2-O_2 diagram (a), and $TCO_{2_{nr}}$-$O_{2_{nr}}$ diagram (b), for the whole water column of the 1969 GEOSECS station.

diagrams correspond to the O_2 minimum zone. $TCO_{2_{n_r}}$ and $O_{2_{n_r}}$ should not be regarded as the oxidative fractions of TCO_{2_n} and O_{2_n}. By definition the $TCO_{2_{n_r}}$'s and $O_{2_{n_r}}$'s add to zero, respectively. The $TCO_{2_{n_r}}$-$O_{2_{n_r}}$ diagram is useful only for calculating the ratio of the oxidative fractions of TCO_{2_n} and O_{2_n}.

TCO_2-O_2 relationship in the Northeastern Pacific Ocean and Southeastern Bering Sea

Alvarez-Borrego, Guthrie, Culberson and Park (1972) studied the O_2-nutrient relationships in the Northeastern Pacific Ocean and Southeastern Bering Sea. They found that the slopes of the O_2-PO_4 and O_2-NO_3 relationships for the region of the water column above the O_2 minimum zone vary systematically with latitude, and that in the entire water column they vary with depth. They concluded that these variations were due to mixing between different water types with different preformed portions of O_2, PO_4 and NO_3.

Using data from several stations of YALOC-66 (Barstow, Gilbert, Park, Still and Wyatt, 1968) (Figure 60) we have plotted TCO_2 versus O_2 (Figure 71). Figure 71 shows that the TCO_2-O_2 relationship for the region of the water column above the O_2 minimum zone varies systematically with latitude. The slope of this relationship is highest near Hawaii and lowest in the Bering Sea (Figure 71). In the entire water column the slope changes with depth. This

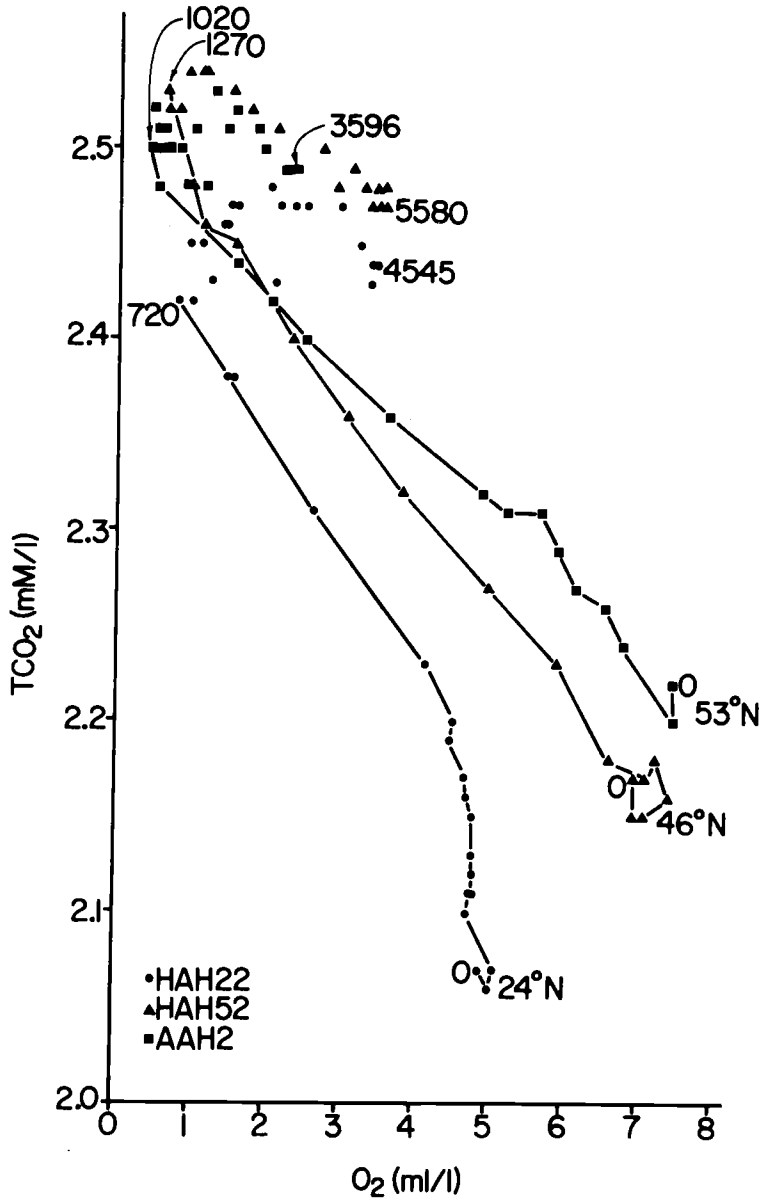

Figure 71. TCO_2-O_2 diagrams for the whole water column of stations HAH22, HAH52, and AAH2.

correlates very well with the results obtained by Alvarez-Borrego, Guthrie, Culberson and Park (1972) for the O_2-nutrient relationships. According to the results discussed above these variations of the TCO_2-O_2 relationship with latitude and with depth are due to

mixing between different water types with different preformed fractions of TCO_2 and O_2; and to the TA varying with depth as a result of S‰ changes and calcium carbonate reaction.

Conclusions

When applying multiple linear regression analysis to express total inorganic carbon dioxide as a function of oxygen, total alkalinity and potential temperature, better results are obtained if the data are first normalized to a constant S‰. If the normalization is not done, it is difficult to properly associate any physical meaning to the regression coefficients. Without the normalization sometimes the results are misleading due to the fact that total alkalinity or oxygen terms may represent not only the carbonate reaction or biological oxidation effects, respectively, but also the S‰ effect on the TCO_2.

Results obtained by applying multiple linear regression analysis to data normalized to constant S‰ are consistent with the hypothesis that TA changes are only due to S‰ changes and dissolution or precipitation of calcium carbonate. These results are also consistent, with only one exception, with Redfield's model.

In the Northeastern Pacific Ocean and Southeastern Bering Sea the total inorganic carbon dioxide-oxygen relationship vary with depth. For the region of the water column above the oxygen minimum zone it varies systematically with latitude. The slope of this relationship is

highest near Hawaii and lowest in the Bering Sea for the region above the oxygen minimum zone. These variations are due to mixing between different water types with different preformed portions of total inorganic carbon dioxide and oxygen, and to total alkalinity varying with depth as a function of S‰ and carbonate reaction.

V. GENERAL DISCUSSION AND SUGGESTIONS FOR FUTURE WORK

The application of multiple linear regression analysis, to study the relationship between different physico-chemical properties in the ocean, has proved to be very useful. The results, presented and discussed in the previous chapters, show that oxygen, nutrient and total inorganic carbon dioxide data from the Pacific Ocean are consistent with Redfield's model. Whenever applying regression analysis to the data we should not forget that, as a statistical method, it is just a tool that helps us to study the functional relations between the different oceanographic variables and to test some hypotheses concerning these relations. The results discussed in Chapter IV show us that, if we do not guide the application of regression analysis by taking into consideration well known relationships between the variables, the results can be misleading and we cannot properly associate any physical meaning to the regression coefficients.

In this work, regression analysis has been applied to data available in the literature. Possibly better results could be obtained with data from hydrographic stations with sampling designed to meet the necessities of regression analysis as we have applied it here. The sampling should be designed to serve two purposes: testing hypotheses concerning the relationships between the variables; and using plots of the residuals of the dependent variable (in our case O_2 or TCO_2)

versus θ°C to detect and trace water masses. Some of this was already discussed in Chapter III. A hydrocast designed to meet the necessities of this type of study should have the sampling bottles spaced according to the changes of θ°C, not according to depth, so that equal sampling density is obtained for the different θ°C ranges. As many samples as possible should be collected from the regions of the water column where the diagrams of the residuals of the dependent variable versus θ°C are relatively straight. Replicates should be taken at the points in the water column where cores of water masses have been detected, to check for consistency of results. To decide on this in advance historical data may be used. Historical data may not be as precise and as properly spaced as we need, but at least it helps giving some indications on the structure of the water column. In addition to this, if a computerized system is available aboard ship, T°C-S‰, O_2-S‰ and O_2-T°C instant plots, constructed with data from a salinity-temperature-depth-oxygen (STD with O_2 electrodes) probe, can be used to study the structure of the water column to help in the designing of the hydrochemical sampling. If any other physico-chemical property can be measured "in situ" and the data processed by a computer aboard, plots of them could also help. With data obtained from this type of sampling possibly we could not only test existent models, but also propose new ones.

Plots of $O_{2_{res}}$ versus θ°C, and $TCO_{2_{n_{res}}}$ versus θ°C could be

specially useful to detect water masses in those cases where the T°C-S‰ diagram shows a relative uniformity of the water column. Since P.TCO_2 is a function of θ°C and S‰, while preformed nutrients are not, the $O_{2_{res}}$ versus θ°C diagram is more useful for this purpose than the $TCO_{2_{n_{res}}}$ versus θ°C diagram. By comparing Figures 43 and 51d we can see that the $O_{2_{res}}$ versus θ°C diagram of station HAH30 of YALOC-66 accentuates much more the differentiation between the water types than the P.PO_4 versus θ°C diagram. Possibly in most of the cases, $O_{2_{res}}$ versus θ°C diagrams are better to clearly detect water types than preformed nutrients versus θ°C diagrams.

A very good opportunity to make a worldwide sampling appropriate for this type of study is presented now with the Geochemical Ocean Sections Study (GEOSECS) program. In Chapter III nutrient data from a GEOSECS intercalibration station (GOGO-1) were used. Unfortunately, the hydrochemical sampling of the GEOSECS program has been designed in such a way, up to now, that the sampling density of the higher θ°C's is very low compared to the sampling density of the lower θ°C's.

The TCO_{2_n} residual analysis for HAH22 station, presented in Chapter IV, show that pH, total alkalinity and O_2 data from this station are very precise. TCO_2 data from YALOC-66 were calculated from pH and TA data. The ranges for $TCO_{2_{n_{res}}}$ resulting from

equations (80) and (81) (Table 3) are smaller than ±0.008 mM/l (Figure 63a, b). If data from the rest of YALOC-66 cruise are as precise as those from HAH22, regression analysis can be applied to the data to explain the factors influencing the pH distribution in the Northeastern Pacific Ocean.

As biochemical oxidation occurs and CO_2 is released to the sea water pH decreases and in turn favors the dissolution of carbonate minerals. The effect of the dissolution of carbonate minerals is to increase pH (Park, 1968). Park (1968) expressed that in the open ocean it is difficult to separate the effects of carbonate dissolution and biochemical oxidation on the pH of sea water, for both go on concurrently. By using simplified mathematical approximations he constructed a model to predict the vertical distribution of apparent pH (the pH measured with glass electrodes at 25° C and 1 atmosphere pressure) in a water column in which variations of T° C and S‰ are relatively small. To relate AOU to pH through changes in TCO_2 he assumed Redfield's model to be correct. Results discussed in Chapter IV show that Redfield's model is correct. Those results, and others presented in previous chapters, show that by using regression analysis we can separate the effects of different factors on a certain chemical property. By using regression analysis on apparent pH, AOU, TA and θ° C data, a model may be constructed to predict the distribution of pH not only in a water column with small

variations of S‰ and θ° C but also in a more heterogeneous water column.

Whether or not calcium carbonate dissolves into sea water is determined mainly by the degree of calcium carbonate saturation of sea water (Lyahkin, 1968). Pytkowicz (1965) began attempting precise estimations of the degree of calcium carbonate in the ocean. To have a better understanding of the processes of dissolution and precipitation of carbonate minerals in the Northeastern Pacific Ocean, the degree of saturation for calcium carbonate can be estimated from pH and TA data from YALOC-66. Additional data from YALOC-70 (Wyatt, Tomlinson, Gilbert, Gordon and Barstow, 1971) could be used, after analyzing their quality. Lyahkin (1968) calculated the calcium carbonate saturation in the Pacific Ocean as a whole. For the Northeastern Pacific Ocean he used data from the 29th cruise of the research vessel VITYAZ (1958-1959). Hawley and Pytkowicz (1969) reported new solubility data at 2° C and high pressure, and calculated the degree of calcium carbonate saturation with respect to calcite for a section in the Pacific Ocean at 170° W. For the Central and Northern part of the Pacific they used data from the 26th (1958) and 29th (1958-1959) cruises of the VITYAZ. Ivanenkov (1966) (in: "Chemistry of the Pacific Ocean," ed. in chief: Bruyevich, 1966) when discussing the quality of the pH data from the Pacific Ocean mentioned that: "Part of the results of the 26th cruise (of the VITYAZ) were too high by 0.04 to 0.05 of a

pH unit, ... , and in the 29th voyage half of the data was either too low by 0.03 to 0.06 or too high by 0.03 to 0.06." Lyahkin (1968) indicates that he corrected the pH data making allowance for the criticisms of Ivanenkov (1966). Hawley and Pytkowicz (1969) compared the data from the 29th cruise of the VITYAZ with data from YALOC-66. According to them the two sets of data generally agree well. Li, Takahashi and Broecker (1969), as it was mentioned in Chapter II, calculated the degree of saturation of calcium carbonate with respect to calcite and aragonite by using TCO_2 and P_{CO_2} field data. They presented a single vertical profile representative of the whole Northern North Pacific Ocean. Culberson (1972) has shown that the disagreement between the results obtained by Lyahkin (1968) and Hawley and Pytkowicz (1969) and those obtained by Li, Takahashi and Broecker (1969) are due in part to Li, Takahashi and Broecker having used values for the change of partial molal volume for the solution of calcium carbonate at 22° C instead of at "in situ" temperature. According to Culberson (1972) the conclusions by Li, Takahashi and Broecker (1969) have been questioned for the reason mentioned above and for many of their TCO_2 measurements appearing to be systematically high due to bacterial respiration during storage of their water samples. Culberson (1972) calculated the calcite saturation for three stations in the Northeastern Pacific Ocean (off California). He also presented the depth of the 100% calcite saturation along 170° W from

30°N to 70°S.

Mehrbach, Pytkowicz, Culberson and Hawley (in preparation) have redetermined the apparent dissociation constants of carbonic acid in sea water (K'_1 and K'_2). Their values are different from those of Lyman's (1956). Lyman's (1956) values have been used up to now, for estimations of the calcium carbonate degree of saturation. The degree of saturation of calcium carbonate with respect to calcite and aragonite could be calculated and described in detail for the Northeastern Pacific Ocean using pH and TA data from YALOC-66 and YALOC-70, and Mehrbach, Pytkowicz, Culberson and Hawley's (in preparation) new values for K'_1 and K'_2.

BIBLIOGRAPHY

Alvarez-Borrego, S. 1970. Chemico-oceanographical parameters of the central North Pacific Ocean. M. S. Thesis. Corvallis, Oregon State University. 84 numb. leaves.

Alvarez-Borrego, S. and K. Park. 1971. AOU as indicator of water-flow direction in the central North Pacific. Journal of the Oceanographical Society of Japan 27: 142-151.

Alvarez-Borrego, S., L. I. Gordon, L. B. Jones, P. K. Park and R. M. Pytkowicz. 1972. Oxygen-carbon dioxide-nutrients relationships in the southeastern region of the Bering Sea. Journal of the Oceanographical Society of Japan 28: 71-93.

Alvarez-Borrego, S., D. Guthrie, C. H. Culberson and P. K. Park. 1972. Oxygen-nutrient relationships in the Pacific Ocean. Limnology and Oceanography, submitted.

Arsen'ev, V. S. 1967. The currents and water masses of the Bering Sea. Izdatel'stvo "nauka", Moscow. 135 p.

Barstow, D., W. Gilbert, K. Park, R. Still, and B. Wyatt. 1968. Hydrographic data from Oregon waters, 1966. Corvallis, Oregon State University, Department of Oceanography. Data Report No. 33. 109 p.

Ben-Yaakov, S. 1970. A method for calculating the in situ pH of seawater. Limnology and Oceanography 15: 326-328.

Ben-Yaakov, S. 1971. A multivariable regression analysis of the vertical distribution of TCO_2 in the eastern Pacific. Journal of Geophysical Research 76: 7417-7431.

Ben-Yaakov, S. 1972. On the CO_2-O_2 system in north eastern Pacific. Marine Chemistry, in press.

Ben-Yaakov, S. and I. R. Kaplan. 1971. Deep-sea in situ calcium carbonate saturometry. Journal of Geophysical Research 76: 722-731.

Berner, R. A. 1966. Diagenesis of carbonate sediments: Interaction of magnesium in seawater with mineral grains. Science 153: 188-191.

Brown, N. L. and B. V. Hamon. 1961. An inductive salinometer. Deep-Sea Research 8: 65-75.

Bruyevich, S. W. (ed.). 1966. The Pacific Ocean. Vol. 3. Chemistry of the Pacific Ocean, tr. by Irene Evans. Washington, U. S. Naval Oceanographic Office. 549 p. (Available as Defense Documentation Center No. AD-651-498)

Craig, H. 1969. Abyssal carbon and radiocarbon in the Pacific. Journal of Geophysical Research 74: 5491-5506.

Craig, H. 1971. The deep metabolism: Oxygen consumption in abyssal ocean water. Journal of Geophysical Research 76: 5078-5086.

Craig, H. and R. F. Weiss. 1970. The 1969 GEOSECS intercalibration station: Introduction, hydrographic features and total CO_2-O_2 relationships. Journal of Geophysical Research 75: 7641-7647.

Culberson, C. 1968. Pressure dependence of the apparent dissociation constants of carbonic and boric acid in seawater. M. S. Thesis. Corvallis, Oregon State University. 85 numb. leaves.

Culberson, C. 1972. Processes affecting the oceanic distribution of carbon dioxide. Ph. D. Thesis. Corvallis, Oregon State University. 170 numb. leaves.

Culberson, C. and R. M. Pytkowicz. 1968. Effect of pressure on carbonic acid, boric acid, and the pH in seawater. Limnology and Oceanography 13: 403-417.

Culberson, C. and R. M. Pytkowicz. 1970. Oxygen-total carbon dioxide correlation in the Eastern Pacific Ocean. Journal of the Oceanographical Society of Japan 26: 95-100.

Dodimead, A. J., F. Favorite, and T. Hirano. 1963. Salmon of the North Pacific Ocean. Part II. Review of Oceanography of the Subarctic Pacific Region. International North Pacific Fisheries Commission Bulletin No. 13. 195 p.

Draper, N. R. and S. Smith. 1966. Applied regression analysis. John Wiley, New York. 407 p.

Dugdale, R. C. and J. J. Goering. 1966. Dynamics of nitrogen cycle in the sea. Final report to the NSF, Institute of Marine Science Report R-66-2. 28 p.

Favorite, F. 1967. The Alaskan Stream. International North Pacific Fisheries Commission. Bulletin No. 21: 1-20.

Favorite, F. 1972. On flow into Bering Sea through the Aleutian island passes. International Symposium for Bering Sea study, 1972, University of Alaska-Hokkaido University. In press.

Fleming, R. H. 1941. The composition of plankton and units for reporting population and production. Proceedings of the Sixth Pacific Science Congress California, 1939. 3: 535-540.

Gilbert, W., W. Pawley and K. Park. 1968. Carpenter's oxygen solubility tables and nomograph for seawater as a function of temperature and salinity. Corvallis, Oregon State University, Department of Oceanography. Data Report No. 29. 139 p.

Gordon, L. I., K. Park, S. W. Hager and T. R. Parsons. 1971. Carbon dioxide partial pressures in North Pacific surface waters--time variations. Journal of the Oceanographical Society of Japan 27: 81-90.

Gordon, L. I., P. K. Park, J. J. Kelley and D. W. Hood. 1972. Carbon dioxide in the surface waters of the Bering Sea and Northwest Pacific Ocean, late summer. Marine Chemistry, submitted.

Hawley, J. and R. M. Pytkowicz. 1969. Solubility of calcium carbonate in seawater at high pressure and 2° C. Geochimica et Cosmochimica Acta 33:1557-1561.

Hirano, T. 1961. The oceanographic study on the Subarctic Region of the Northwest Pacific Ocean. Part IV. On the circulation of the Subarctic Water. Tokai Regional Fisheries Research Laboratories Bulletin No. 29: 11-39.

Horibe, Y. (editor). 1970. Preliminary report of the Hakuho Maru Cruise KH-68-4 (SOUTHERN CROSS cruise). Ocean Research Institute. University of Tokyo.

Ivanenkov, V. I. 1964. Hydrochemistry of the Bering Sea. Academy of Sciences of the USSR Izdatel'stvo Nauka, Moscow. 137 p.

Kelley, J. J. 1968. Carbon dioxide in the seawater under the Arctic ice. Nature 218: 862-864.

Kelley, J. J. and D. W. Hood. 1971a. Carbon dioxide in the surface water of the ice-covered Bering Sea. Nature 229: 37-39.

Kelley, J. J. and D. W. Hood. 1971b. Carbon dioxide in the Pacific Ocean and Bering Sea: Upwelling and mixing. Journal of Geophysical Research 76: 745-752.

Kelley, J. J., L. L. Longerich and D. W. Hood. 1971. Effect of upwelling, mixing and high primary productivity on CO_2 concentration in surface waters of the Bering Sea. Journal of Geophysical Research 36: 8687-8693.

Li, Y. H., T. Takahashi and W. S. Broecker. 1969. Degree of saturation of calcium carbonate in the oceans. Journal of Geophysical Research 74: 5507-5525.

Lyahkin, Y. I. 1968. Calcium carbonate saturation of Pacific water. Oceanology 8: 58-68.

Lyman, J. 1956. Buffer mechanism of seawater. Ph. D. Thesis. Los Angeles, University of California at Los Angeles. 196 numb. leaves.

MacIntyre, W. G. 1965. The temperature variation of the solubility product of calcium carbonate in sea water. Fisheries Research Board of Canada Manuscript Report Series No. 200. 153 p.

Mehrbach, C., R. M. Pytkowicz, C. H. Culberson and J. Hawley. 1972. Measurement of the apparent dissociation constant of carbonic acid in seawater at atmospheric pressure. Limnology and Oceanography, submitted.

Miyake, Y. and Y. Sugimura. 1969. Carbon dioxide in the surface water and the atmosphere in the Pacific, the Indian and the Antarctic Ocean areas. Records of Oceanographic Works in Japan 10: 23-28.

Mullin, J. B. and J. P. Riley. 1955. The spectrophotometric determination of nitrate in natural waters with particular reference to sea waters. Analytical Chimica Acta 12: 464-480.

National Oceanographic Data Center. Physical and chemical data of the 26th expedition of the Vityaz. 1957. NOAA. Department of Commerce. Washington, D. C.

Oregon State University, Department of Statistics. 1971. Statistics Instruction Programming System (SIPS). Preliminary User's Guide. Corvallis, Oregon. Unpublished manuscript. 25 p.

Packard, T. T., M. L. Healy and F. A. Richards. 1971. Vertical distribution of the activity of the respiratory electron transport system in marine plankton. Limnology and Oceanography 16: 60-70.

Park, K. 1965. Total carbon dioxide in sea water. Journal of the Oceanographical Society of Japan 21: 54-59.

Park, K. 1966a. Deep-sea pH. Science 154: 1540-1542.

Park, K. 1966b. Surface pH of the Northeastern Pacific Ocean. Journal of the Oceanographical Society of Korea 1:1-2.

Park, K. 1967a. Nutrient regeneration and preformed nutrients off Oregon. Limnology and Oceanography. 12: 353-357.

Park, K. 1967b. Chemical features of the Subarctic Boundary near 170°W. Journal of the Fisheries Research Board of Canada 24: 899-908.

Park, K. 1968. The processes contributing to the vertical distribution of apparent pH in the Northeastern Pacific Ocean. Journal of the Oceanological Society of Korea 3: 1-7.

Park, K., H. C. Curl, Jr. and W. A. Glooschenko. 1967. Large surface carbon dioxide anomalies in the North Pacific Ocean. Nature 215: 380-381.

Postma, H. 1964. The exchange of oxygen and carbon dioxide between the ocean and the atmosphere. Netherlands Journal of Sea Research 2.2: 258-283.

Pytkowicz, R. M. 1964. Oxygen exchange rates off the Oregon coast. Deep-Sea Research 11: 381-389.

Pytkowicz, R. M. 1968. Water masses and their properties at 160°W in the Southern ocean. Journal of the Oceanographical Society of Japan 24: 21-31.

Pytkowicz, R. M. 1971. On the apparent oxygen utilization and the preformed phosphate in the oceans. Limnology and Oceanography 16: 39-42.

Pytkowicz, R. M. 1972. Comments on a paper by S. Ben-Yaakov and I. R. Kaplan, "Deep sea in situ carbonate saturometry." Journal of Geophysical Research 77: 2733-2734.

Pytkowicz, R. M. and G. A. Fowler. 1967. Solubility of foraminifera in seawater at high pressures. Geochemical Journal 1: 169-182.

Pytkowicz, R. M. and D. R. Kester. 1966. Oxygen and phosphate as indicators for the deep intermediate waters in the Northeast Pacific Ocean. Deep-Sea Research 13: 373-379.

Rakestraw, N. W. 1936. The occurrence and significance of nitrite in the sea. Biological Bulletin 71: 133-167.

Redfield, A. C. 1934. On the proportions of organic derivatives in sea water and their relation to the composition of plankton. James Johnstone Memorial Volume, Liverpool, p. 176-192.

Redfield, A. C. 1942. The processes determining the concentration of oxygen, phosphate and other organic derivatives within the depths of the Atlantic Ocean. Papers in Physical Oceanography and Meteorology 9. 22 p.

Redfield, A. C., B. H. Ketchum and F. A. Richards. 1963. The influence of organisms on the composition of seawater, pp. 26-77 In: The Sea, M. N. Hill, ed., Interscience, 2.

Reid, L. J. 1965. Intermediate Waters of the Pacific Ocean. Baltimore, Johns Hopkins Press. 85 p.

Reid, L. J. 1966. Zetes expedition. Transactions, American Geophysical Union 47: 555-561.

Riley, G. 1951. Oxygen, phosphate and nitrate in the Atlantic Ocean. Bingham Oceanographic College Bulletin 13.

Scripps Institution of Oceanography. 1966. Boreas expedition. Data report: Physical and chemical data. University of California at San Diego, Scripps Institution of Oceanography Reference 66-24. 164 p.

Scripps Institution of Oceanography, Woods Hole Oceanographic Institution, and Massachusetts Institute of Technology. 1969. SCORPIO expedition. Data report: Physical and chemical data. Scripps Institution of Oceanography Reference 69-15, and Woods Hole Oceanographic Institution Reference 69-56. 89 p.

Spencer, D. W. 1970. GEOSECS intercalibration and test cruise. Technical report. Woods Hole Oceanographic Institution Reference 70-63. Unpublished manuscript.

Strickland, J. D. H. and T. R. Parsons. 1965. A manual of sea water analysis. Ottawa, Fisheries Research Board of Canada. Bulletin No. 125. 203 p.

Sugiura, Y. and H. Yoshimura. 1964. Distribution and mutual relation of dissolved oxygen and phosphate in the Oyashio and the northern part of the Kuroshio regions. Journal of the Oceanographical Society of Japan 20: 14-23.

Sverdrup, H. U., M. W. Johnson and R. H. Fleming. 1942. The oceans, their physics, chemistry, and general biology. N. W. Prent-Hall. 1087 p.

Takahashi, T., R. F. Weiss, C. H. Culberson, J. M. Edmond, D. E. Hammond, C. S. Wong, Y. H. Li and A. Bainbridge. 1970. A carbonate chemistry profile at the 1969 GEOSECS intercalibration station in the eastern Pacific Ocean. Journal of Geophysical Research 75: 7648-7666.

Uda, M. 1935. The origin, movement and distribution of dicothermal water in the northeastern sea region of Japan. Umi to Sora 15: 445-452.

Uda, M. 1963. Oceanography of the Subarctic Pacific Ocean. Journal of the Fisheries Research Board of Canada 20: 79-119.

Von Brand, T. and N. W. Rakestraw. 1941. Decomposition and regeneration of nitrogenous organic matter in sea water. IV. Biological Bulletin 81: 63-69.

Wattenberg, H. 1936. Kohlensäure und Kalziumkenbonat in Meere. Fortschr. Mineral. 20: 168-195.

Weyl, P. K. 1967. The solution behavior of carbonate materials in seawater. Studies in Tropical Oceanography Miami 5: 178-228.

Woods Hole Oceanographic Institution. 1964. Final cruise report Anton Bruun Cruise 2. Oceanographic Data. U. S. Program in Biology, IIOE.